Thermal exposure from burning leaks on LNG hoses: experimental results

Johan Sjöström, Petra Andersson

SP Technical Research Institute of Sweden

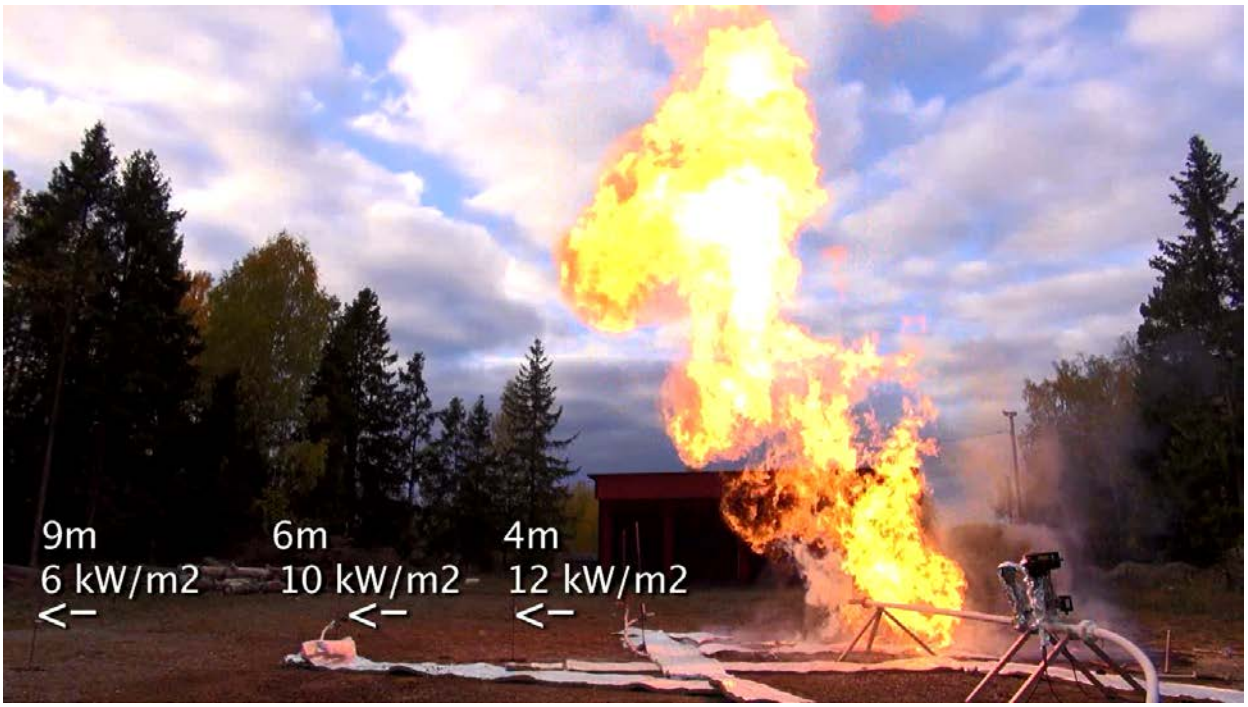

Fire Technology

SP Report 2013:61

Thermal exposure from burning leaks on LNG hoses: experimental results

Johan Sjöström, Petra Andersson

Abstract

This report summarises a series of tests on thermal impact to the surrounding from damaged Liquefied Natural Gas (LNG) hoses pressurized to approximately 10 bar. The results of temperatures of insulated surfaces, incident heat flux and flame dimensions are reported. For the design scenarios of 1" and 2" hoses (test 4 and 7) the distance to an incident radiant heat flux of 15 kW/m^2 is 2 and 4 m, respectively. The equivalent distance to 5 kW/m^2 is 3 and 9 m, respectively.

Key words: LNG, fire, risk, plate thermometer, radiation, thermal impact

SP Sveriges Tekniska Forskningsinstitut
SP Technical Research Institute of Sweden

SP Report 2013:61
ISBN 978-91-87461-47-7
ISSN 0284-5172
Borås 2013

Contents

Preface

There is a lack of guidance of how to design filling stations involving liquefied natural gas (LNG) with respect to the fire safety. The safety of both people and nearby structures are not investigated in relation to the use of LNG in public areas. The Swedish gas industry has issued a number of different guidelines for the use of natural gas in filling stations and LNG in industrial facilities but not for LNG filling stations. The regulatory responsibility is with the Swedish Civil Contingencies Agency (MSB). To aid the development of guidelines, the Swedish Gas Association (Energigas Sverige), together with their members conducted an experimental series of leaking LNG pipes and hoses in October 2013. SP Technical Research Institute of Sweden were consulted to perform measurement and documentation of thermal impact to the surrounding.

A number of people took part in the experimental work and planning including

Mattias Hanson	Enerigas Sverige
Torgny Eriksson	AGA
Anders Melin	Fordonsgas
Anders Trönell	E.ON
Håkan Carlsson	Wiro
Michael Lindström	AGA
Johan Sjöström	SP
Michael Rahm	SP
Henrik Fredriksson	SP
Emil Norberg	SP

This report summarizes the results of tests. Associated with this report are the video recordings of the tests and for better understanding these are available on request.

Summary

This study describes a series of tests of leaking LNG pipes and hoses subject to a pilot flame. The leaks were of varying sizes from 1 mm^2 holes to slots of 5 by 45 mm in 1" and 2" pipes/hoses. The study shows that jet flames are not easily formed when a stainless steel braid was covers the opening. For the design scenarios of 1" and 2" hoses (test 4 and 7) the distance to incident radiant heat flux of 15 kW/m^2 is 2 and 4 m, respectively. The equivalent distance to 5 kW/m^2 is 3 and 9 m, respectively. These levels are subject to a 10 bar hose pressure. Additionally, small changes in pressure has minor effect on thermal impact if an undamaged stainless steel braid is covering the opening. Without a covering braid the pressure is a more important factor for the spatial range of thermal impact.

A summary of the tests in terms of incident heat flux at different distances is given below. For a more nuanced description the reader is referred to chapter 4.

Opening (mm)	**Covering braid (Y/N)**	**P (bar)**	**Horizontal continuous flame width [1] (m)**	**Horizontal maximum flame width (m)**	**Flame height (m)**	**Horizontal $\dot{q}''_{inc}$ outside flame [2] ($\dot{q}''_{inc}$/distance) (kW/m^2 / m)**
2x25	Y	9-6	1	3	3-4	(27 / 1m) 22 / 2m 12 / 3m
2x25	N	9-10	5	6	7-9	12 / 2.5m 17 / 4m 12 / 6m 11 / 9m
1x10	Y	9.5	2	3	2-2.5	(45 / 1m) 26 / 2m 11 / 3m
1x10	N	12-7.5	3.5	6	1-2	14 / 6m 3.5/ 9m
1x1	Y	9-15	<0.5	0.8	0.5-1	8 / 1m 3 / 2m 1.5 / 3m
1x1	N	10		not self-sustained		5 / 1m 1 / 2m Piloted!
1/3 of circumf.	Y	10	2	2.5	1-2	12 / 2m 6.5 / 3m
1x5	Y	9-11	1	1.5	1	9 / 2m 3 / 3m
1x1	Y	12-13	< 0.5	0.5	0.5	2 / 1m 0.5 / 2m
1/3 of circumf.	Y	10	3	4	8-10	18 / 2.5m 12 / 4m 10 / 6m 6 / 9m
5x45	Y	5-9	7	8	10-12	27 / 9m
5x45	Y	5	6	7	7-10	13 / 9m
5x45	N	9-7	11	12	9-12	Flame > 9m
12.6 mm^2	N	10	~4 (piloted)	-	1-2	-
63.6 mm^2	N	10	~8	-	4-5	-
113 mm^2	N	10	~15	-	-	-

[1] Continuous flame for more than 10 seconds.
[2] highest floating average over a ten second period. Very short peaks are thus ignored. The values within parenthesis are for PT partially engulfed in flames.
[3] This was a shorter test with higher pressure, which ended due to instrument malfunction.

1 Introduction

LNG (Liquefied Natural Gas) is condensed natural gas containing mostly methane but also a small portion of ethane and traces of longer hydrocarbons. When condensing natural gas by cooling it to below -160 °C the density increases by a factor 600, which enables more efficient transportation, especially from places without distribution pipelines. LNG is thus mostly used as a transportation mean, the liquid is re-gassified before use. However, the use of LNG stored directly in the fuel tank of a ship or heavy vehicles is increasing.

Natural gas is a flammable gas igniting at concentrations of typically 5 – 15 % by volume in air. Thus, fire safety is of uttermost importance for the production, transportation, storage and use of LNG. In Sweden, the regulations for flammable and explosive goods are provided by the Swedish contingency agency (MSB). Requirements and advice are given by SÄIFS 2000:4 [1], in which it is prescribed that the minimum distance from the hose connection for a tank truck to a building is in general 25 m (not within an industrial plant) and half of this if the building fulfils EI60 fire resistance requirements. No requirements are given relating distances from dispenser. The Swedish gas industry has written clarifications of how to comply with the requirements when building filling stations for gas driven vehicles [2]. However, this guidance only treats high pressure gas processes but not LNG. Similar guidance is written for LNG use at industrial areas inaccessible for the public [3]. Thus, there is a lack of guidance for safety distances for LNG filling stations

The literature on fire hazards from LNG has predominantly focused on spills leading to large pool fires, either on water or land. The experimental work done on pool fires is summarized in Raj [4]. It is stated that for large (several tens of metres) pool fires the burning behaviour is similar to higher hydrocarbon fuels (kerosene, crude oil etc.) which burn with a sooty flame reducing radiant impact to the surrounding.

There are different models for simulating LNG pool fires. LNGFIREIII [5] is approved by the US department of transportation as a tool for risk assessments. For simulating fires from spills of pressurized pipes a number of studies have been made on natural gas pipes [6-8] but nothing focused on LNG leakage in particular. Scandpower has issued a publication on simulations using the PHAST software [9] were the radiant heat flux from three different holes of pressurized LNG pipes was calculated. Among the results is an 11 m distance to 32 kW/m^2 for a 25 mm^2 hole on a 15 bar pipe [10].

To obtain experimental results on leaks relevant for LNG filling stations which can be used as background data in development of guidance on LNG filling stations, tests on damaged pipes and hoses with different opening sizes have been performed in this work. The tests are meant to mimic situations of leakage from hose from dispenser as well as from tanker truck providing LNG to the station. The damage scenario defined by the Swedish contingency agency is wear from the inside on the convoluted hose resulting in an opening with a length corresponding to 1/3 of the hose circumference. The most common place for damages on LNG hoses is close to the connection on the upper part of the corrugation. This work does not include hypothetical worst case scenarios that potentially could be more hazardous.

Temperatures and incident radiant heat fluxes were measured at different distances from the leakage for the different tests and the flames. The tests were also documented using video and IR cameras.

2 Different types of heat exposures

The heat exposure of a solid surface from nearby flames is essentially a mixture of three processes, absorbed radiation, emitted radiation and convective heat transfer.

A flame emits radiation which hits nearby surfaces. A point source radiates in a spherically symmetric manner and the incident radiant heat flux, $\dot{q}''_{inc}$, to a surface a distance *r* away decreases as, $\dot{q}''_{inc} \sim 1/r^2$. A solid flame has a more complex radiation field and the incident flux is determined by the radiant intensity and the configuration factor (view factor) between the flame and surface. Far from the flame the radiation appears to originate from a point source. The portion of the incident radiant heat flux that is not reflected is absorbed by the surface. This portion is determined by the surface emissivity, ε, which is assumed it to be wavelength independent for simplicity. ε of many materials varies between 0.6 and 0.8 but very high values can also be found (human skin ~0.97) as well as very low (aluminium ~0.05-0.1).

The surface also emits radiant heat. The heat flux is given by $\dot{q}''_{emi} = \varepsilon\sigma T_s^4$, where $\sigma = 5.67 \cdot 10^{-8}$ W/m^{2}K^4 and T_s is the surface temperature [K]. Thus, the emitted radiant heat from the surface is a very strong function of the temperature, increasing 15 times between T_s = 20 and 300 °C and 122 times between 20 and 700 °C.

The convective heat transfer is the heat transfer between the surface and the adjacent gas phase. It is usually simplified as $\dot{q}''_{con} = h(T_g - T_s)$, where T_g is the adjacent gas temperature and *h* the convective heat transfer coefficient. *h* is difficult to determine and depends on velocity of the gas and surface temperature. A large object usually has a lower *h* than a smaller and empirical correlation is usually used to calculate convective heat transfer. A surface being heated by radiation but placed in ambient air is thus convectively cooled by the surrounding air but as soon as the flames reach the surface it is convectively heated by the flames and/or hot gases.

Thus, the total heat flux at a surface is given by $\dot{q}''_{tot} = \dot{q}''_{abs} - \dot{q}''_{emi} + \dot{q}''_{con} = \varepsilon\dot{q}''_{inc} - \varepsilon\sigma T_s^4 + h(T_g - T_s)$. The total heat flux to a surface therefore changes dramatically during most fire scenarios as the surface temperature changes. The heat flux levels that usually are prescribed in codes and regulation refer to incident heat flux outside the flames. Thus, this flux level is only relevant for objects outside the flames and irrelevant for objects engulfed in the flames.

In addition, the temperature of the surface of the exposed object is highly dependent on the material properties (specific heat, density and thermal conductivity) as well as the materials physical configuration (e.g. very thick or thin).

2.1 Hazard related to incident radiant heat

As discussed above, the hazard of an incident radiant heat flux depends on the surface emissivity of the particular object/structure of interest as well as the convective heat transfer associated with it. For guidance the Swedish National Board of Housing, Building and Planning defines 15 kW/m^2 during 30 minutes as the acceptable exposure towards nearby structures [11]. This is based upon the limit where a wooden structure can undergo piloted ignition (in presence of a pilot flame/spark) after prolonged exposure.

Some observed effects of different incident radiant heat fluxes are given in Ref. [12] and tabulated below.

Table 2.1 Effects of thermal radiation (from [12] and references therein).

Radiant heat flux (kW/m^2)	Observed effect
0.67	Summer sunshine in UK
1	Maximum for indefinite skin exposure
6.4	Pain after 8 s exposure
10.4	Pain after 3 s exposure
12.5	Volatiles from wood may be ignited after prolonged exposure
16	Blistering of skin after 5 s
29	Wood may ignite spontaneously after prolonged exposure
52	Fibreboard ignites spontaneously in 5 s

3 Experimental

In order to measure/verify the incident radiation and heat exposure from accidental releases of LNG a test series was set-up to mimic damages on the hose from the dispenser as well as from a tanker truck providing LNG to the filling station. Pipes and hoses of 1" (25.4 mm) and 2" (50.2 mm) inner diameter, respectively, represent the two cases. The relevant damage scenario defined by the Swedish contingency agency is wear from the inside on the convoluted hose resulting in an opening with a length corresponding to 1/3 of the hose circumference [13]. This leak is then assumed to ignite by a pilot flame. 1" and 2" hoses with the tube cut accordingly were used. These were covered by an undamaged stainless steel flexible braid since the damage is not thought to result from an external force. In addition, 1" and 2" pipes are used, both with and without stainless steel braid, to investigate the effect of the braid on the thermal impact.

3.1 Experimental set-up

The experimental setup was a pipe with pressurized LNG connected to a hose or short pipe with a prefabricated hole or slot in it. The pressure was provided by a pump and was not due to heating of the LNG. The pipe was placed horizontally about 0.5 m above the ground. The hole/slot was mostly placed such that the leak was horizontal but for some of the tests the leak was directed at an angle from the horizontal plane.

LNG was provided by a tanker truck, providing LNG to either a 1´´ or 2´´ pipe, 3.3 m long (with inner diameter of 25 and 50 mm, respectively). The other end of the pipe was connected to different types of pipes or hoses.

Figure 3.1 Photo of part of the setup.

The thermal impact to the surrounding was measured using Plate Thermometer (PT) pairs together with Heat Flux meters (HFM) (see figure 3.1), and thermocouples (TC). Two different types of setups were used to capture the relevant ranges of heat exposures in the tests with very varying severity. Setup 1 had a narrow range with PT and TC measurements at 1, 2 and 3 m in a direction perpendicular to the pipe direction as well as

measurements 1 m off centre. HFM measurements were conducted at 1 and 2 m distance from the leak as well as off centre. Setup 2 had a wider range with PT/TC measurements at 2.5, 4, 6 and 9 meters from the leak as well as 3 m off centre, see figure 3.2.

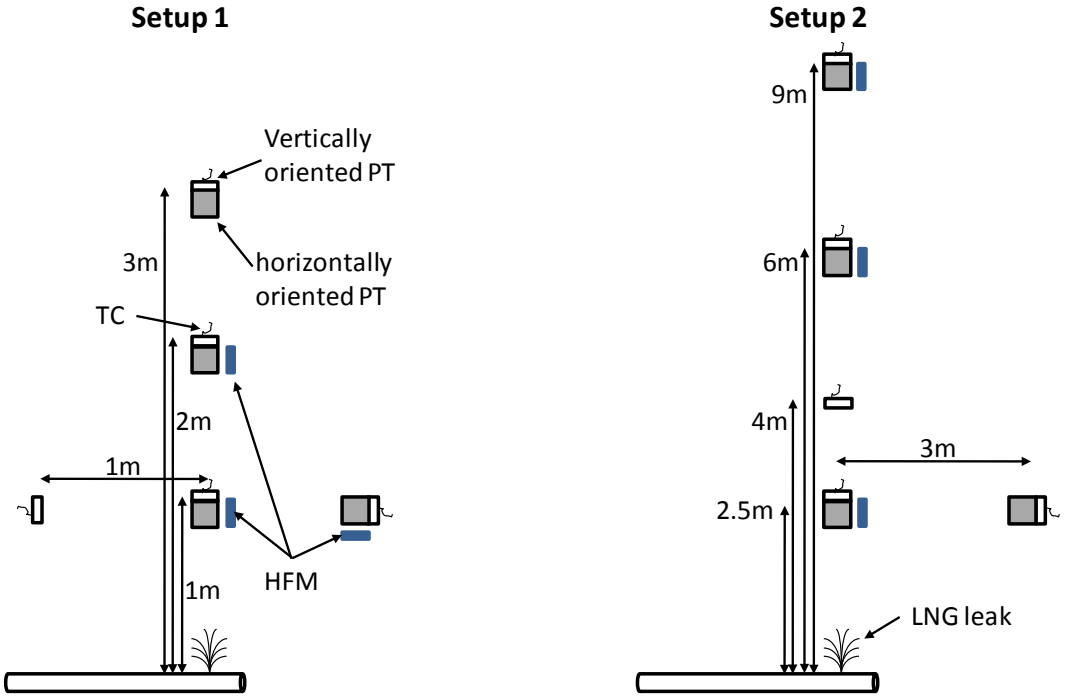

Figure 3.2. The two setups used to measure thermal impact. The two setups are not to scale between each other. The IR and video cameras were moved between all the tests.

3.2 Instrumentation

3.2.1 Plate Thermometers

To assess the thermal impact from the burning leaks plate thermometers (PT) are used [14]. These have previously been successfully used in many different fire scenarios such as large scale pool fires, scaling experiments of industrial fires, radiant heating tests and burning goods [15, 16]. In total nine PT were used in the tests.

The PT consists of an exposed surface of 0.4 mm thick Inconel600 alloy, 100 by 100 mm. It is insulated with 300 mm of ceramic wool insulation and supported on the backside with a stainless steel plate. The Inconel600 and stainless steel plates are connected via four thin strips of Inconel in the corner [15]. A 1 mm shielded type K thermocouple is attached to the inside of the exposed surface.

In steady state, the PT records a temperature close to the adiabatic surface temperature, the highest temperature a large surface, with equal surface emissivity and same orientation, can achieve if it is exposed to the same fire exposure and convective heat transfer coefficient. In addition, it can be used to calculate the incident radiant heat flux, $\dot{q}''_{inc}$, normal to the surface orientation, through the relation [14]:

$$\dot{q}_{inc}^{''} = \sigma T_{PT}^4 + \frac{(h + K_{PT})(T_{PT} - T_g) + C_{PT}\frac{dT_{PT}}{dt}}{\varepsilon_{PT}} \quad (3.1)$$

where h is the convective heat transfer coefficient, T_{PT} and T_g are temperatures of PT and ambient air, respectively, ε_{PT} is surface emissivity of the exposed surface and σ is Stefan-Boltzmann's constant. K_{PT} and C_{PT} are correction parameters for heat loss and storage, respectively, in the PT. These are determined through calibration and comparison against water cooled heat flux meters (HFM), in turn calibrated according to ISO 14934-2. For these type of PT, calibration yields $K_{PT} = 4$ W/m^2 and $C_{PT} = 3000$ J/m^{2}K.

The convective heat transfer coefficient is varied from natural convection (no wind, h = 10 W/m^{2}K) and wind speeds of 7 m/s (h = 30 W/m^{2}K) for investigating the sensitivity in Appendix 8.3. This gives a span of results which clearly incorporates the margin of error in the tests [15]. For the results presented in Chapter 3, the convective heat transfer coefficient is set to h = 15 W/m^{2}K for all measurements where the PT was not engulfed in flames. The correlation with HFM measurements (see Appendix 6.2.2) shows that this assumption is fair in these test conditions.

The PT can be combined two by two in vertical (V) orientation (facing the fire) and horizontal (H) orientation (facing upwards). This configuration enables the calculation of maximum incident radiation to an object of optimum orientation towards the fire through

$$\dot{q}_{max}^{''} = \sqrt{\dot{q}_H^{''2} + \dot{q}_V^{''2}} \quad (3.2)$$

where H and V represent horizontal and vertical orientation, respectively. Note that this way of calculating the heat flux to an optimally oriented surface is only valid for point source radiators. For a distributed flame the maximum heat flux will be somewhat lower. In chapter 3 the heat flux to a vertical surface is given. The flux to optimally oriented surfaces is only given in the appendix.

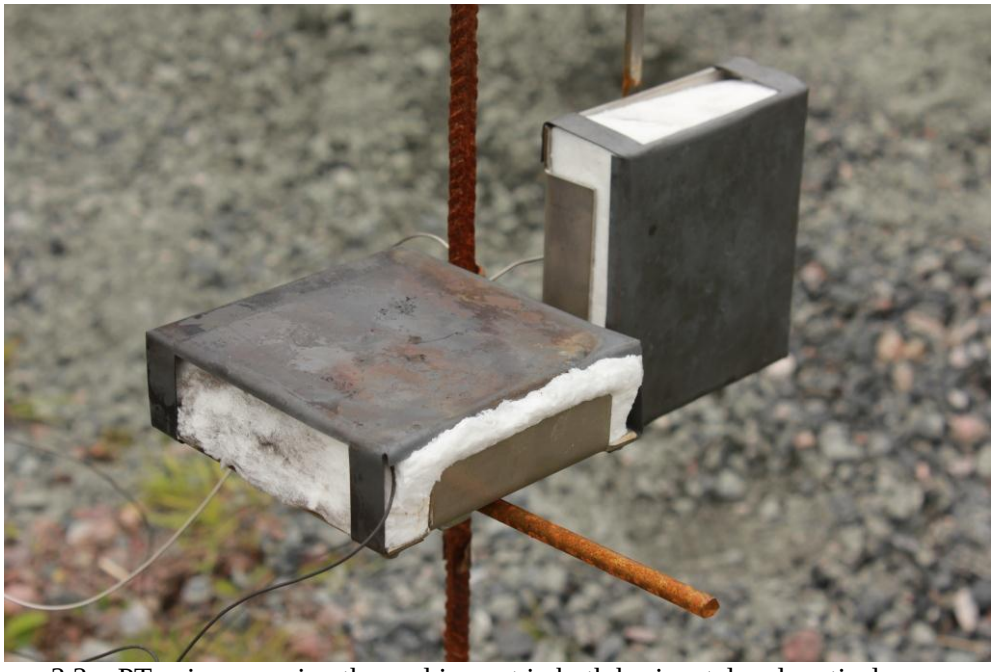

Figure 3.3. PT pair measuring thermal impact in both horizontal and vertical direction.

3.2.2 Other temperature measurements

Behind each vertically oriented PT a welded type K thermocouple (TC) of 0.25 mm in diameter was placed to register the gas temperature. I total five naked TC were used.

Additionally, a PT100 probe was inserted into the pipe to register the LNG temperature.

3.2.3 Heat flux meters

Three water cooled heat flux meters (HFM) were used in the tests (Medtherm models 64-5-18, 64-2-18). These were calibrated according to ISO 14934-2 at SP. HFMs are widely recognised in the fire community to accurately measure the incident heat flux to a surface if placed in a gas atmosphere of ambient temperature.

The heat flux meters used for these tests were ruggedized by mounting them in steel tubes and wrapping insulation around the electrical connection and water tubes to protect them from cool LNG or hot gases in the fire testing environment.

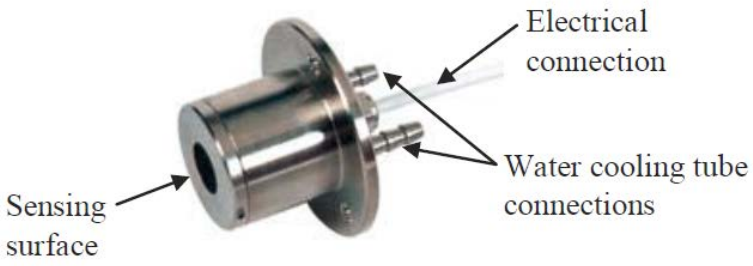

Figure 3.4. A typical HFM used in the test.

A HFM measures the heat flux to a surface kept at a constant temperature (usually 20°C). If the meter is placed in an environment with a gas temperature equal to the HFM temperature the convective heat transfer to the surrounding will be very low. Since the emitted radiation from the measuring surface is constant the signal from the HFM will be a measure of the incident radiant heat flux. If, on the other hand, the HFM is placed such that it is affected by flames or hot gases, there can be significant convective heat transfer to the adjacent gas. Thus there will be an absorbed radiant heat flux plus a convective heat flux. The emitted radiant heat flux will still be low. The HFM then measures the total heat flux to a cooled surface which has the same convective heat transfer coefficient (and emissivity) as the HFM itself. Any non-cooled surface will of course be heated by the thermal impact and therefore experience a lower convective heat transfer and a larger emitted radiation, which both will lower the total heat flux through the surface.

3.2.4 Video recording

Each test was documented by at least one video camera.

3.2.5 IR camera recording

IR temperature recordings were conducted using two different IR cameras. One FLIR T335 registering temperatures from -20 to 120 ˚C and one FLIR A320 measuring from 80 to >1000 ˚C

3.3 Tests

The tests were conducted at the training site of Räddningstjänsten Enköping-Håbo in Bålsta east of Stockholm, Sweden. The weather was ideal with very low winds (varying between 1 and 2.5 m/s). The wind direction was north to south, varying 30° to the east and west during the day. The leak direction for the outlet of methane was from north-east to south west. No precipitation fell during the day or the day before.

A total of 15 tests were conducted. A summary of the 12 tests simulating leaking hoses is provided in Table 3.1.

Table 3.1. Summary of the tests conducted with measurements of thermal impact from damaged hoses/pipes.

Test	**Pipe dim.**	**Pipe or hose**	**Hole size (mm)**	**Covered by braid**	**PT/TC/HFM setup.**
1a	1"	p	2x25	Y	1
1b	1"	p	2x25	N	2
2a	1"	p	1x10	Y	1
2b	1"	p	1x10	N	2
3a	1"	p	1x1	Y	1
3b	1"	p	1x1	N	1
4	1"	h	~1 mm thick. 1/3 of circumference (~30 mm)	Y	1
5	1"	h	1x5	Y	1
6	1"	h	1x1	Y	1
7	2"	h	~1 mm thick. 1/3 of circumference (~60 mm)	Y	2
8a	2"	p	5x45	Y	2
8b	2"	p	5x45	N	2

In addition, three tests were conducted with thinner pipes with an open end. Thus, not a failure along the side of the pipe was simulated but just an open end. All these tests were conducted with a pipe pressure of 10 bar. During these tests no measurements on thermal impact was conducted, only video and IR recording.

Table 3.2. Dimensions of the pipes in test 9-11.

Test	Pipe length (mm)	Pipe inner diameter (mm)
9	220	4
10	320	9
11	350	12

For the different tests pipes or hoses with different types of holes/slots were connected to the far end of the pipe. An example of a 5x45 mm slot in a 2" pipe is shown in figure 3.5. Figure 3.6 shows a hose partially inserted in a stainless steel braid. The temperature and static pressure were measured just upstream of the pipe in tests 1 - 8b.

The pressure in the hoses is usually around 10 bar. A constant pressure could not be maintained throughout all the tests collectively but the pressure varies between 5 and 12 bar. Many tests were conducted when the pipe/hose was filled with LNG. However, a few of the tests started when methane was ejected through the opening already in the gas phase. In these cases the tests lasted long enough for liquid to reach all the way to the opening. Temperature and pressure was continuously measured 3.3 m from the opening throughout the tests.

For most of the tests the methane stream was not ignited until the pipe was cooled enough to let liquid methane through the slot. Ignition was conducted with a pilot flame (a burning rag on long stick).

Figure 3.5. A 2" pipe without braid. A 5 by 45 mm slot is cut crosswise. The photo is taken after the test when gas still remained in the pipe.

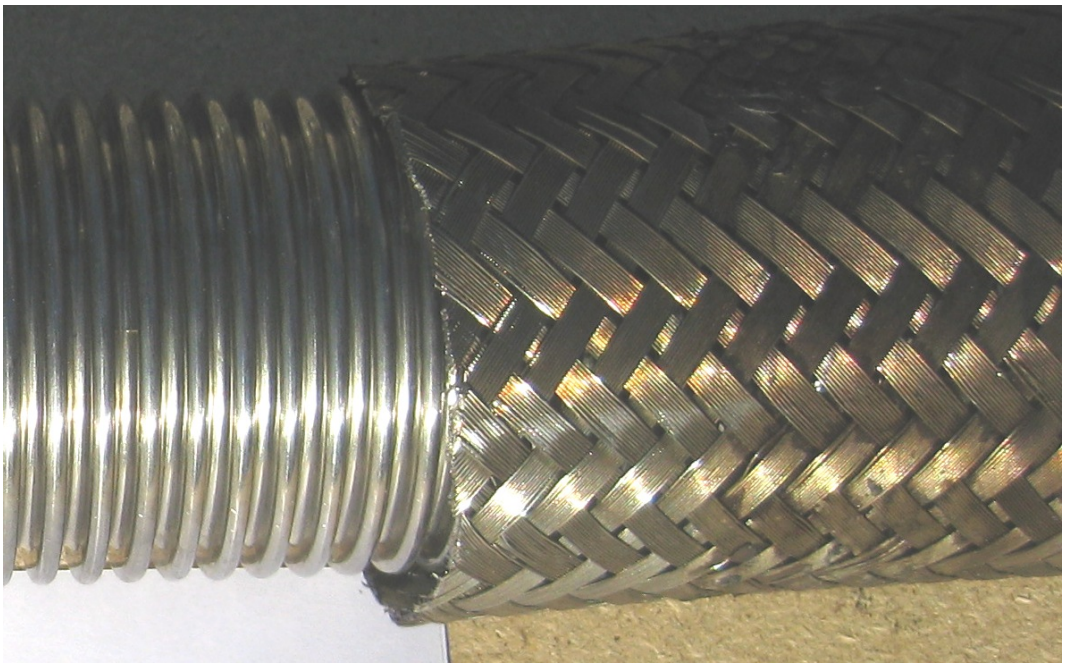

Figure 3.6. A 2" pipe partially inserted in a stainless steel braid.

4 Results

Below the different tests are described in detail, main results are described below and a full set of the results is provided in the appendices. At the end of the chapter, table 4.1 summarizes all the tests. Associated with these tests are the video recordings of the flames. They serve as informative on the transient behaviour of flame width and height and also indicated some radiant heat flux levels, but are not displayed here.

4.1 Test 1a - 1" pipe, 2x25 mm slot, with braid

Test 1a was a 1" pipe of inner diameter 25 mm and 2 mm thickness with a 2 by 25 mm long slot cut crosswise, similar to figure 3.5 but with other dimensions. The pipe was covered by a stainless steel braid. Thermal impact was measured with setup 1.

The test resulted in flames ejecting from the side of the pipe where the slot was cut. The flame had a height around 3-4 m and a width between 1-2 m. Some typical photos are shown in figure 4.1. The thermal impact is the same on both vertical and horizontal PT at 1 m distance from the leak. Further away from the flame the incident radiation is mostly in horizontal direction, affecting mostly the vertically oriented PT.

The pressure during the test started at 9 bar and decreased steadily to about 6 bar at the end of the, just over 2 minute long, experiment. Correspondingly, the heat exposure is largest in the beginning and decreases slowly. In the beginning of the test no liquid is seen ejected from the pipe. However, during the late part liquid is clearly noticed, see figure 4.1 (right).

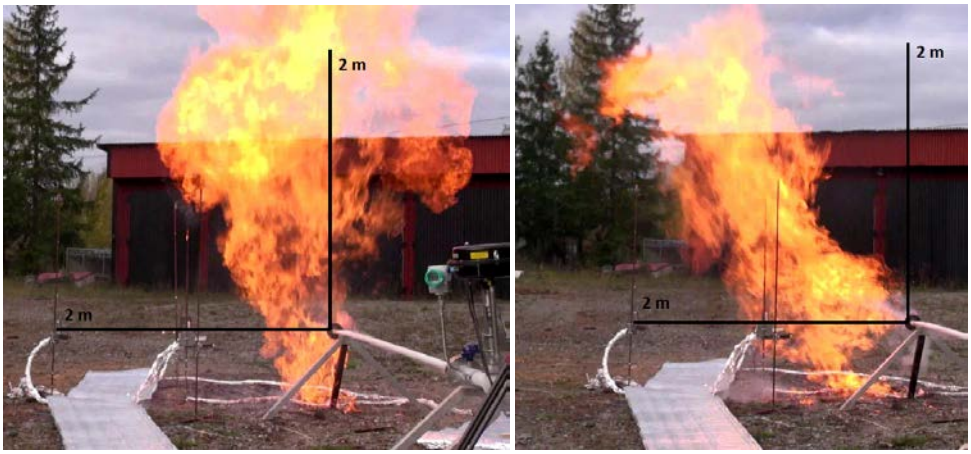

Figure 4.1. Photos from test 1a (1" pipe with 2x25 mm slot, covered by a braid). The left figure is from the early stages of the test and the right from the very late stage. Fluid from the leak is visible in the right photo.

The small TC at 1 m distance occasionally picked up hot gases from the flames (see appendix 8.1) but during the large part of the test the PT was convectively cooled. The incident heat flux in horizontal direction is shown in figure 4.2.

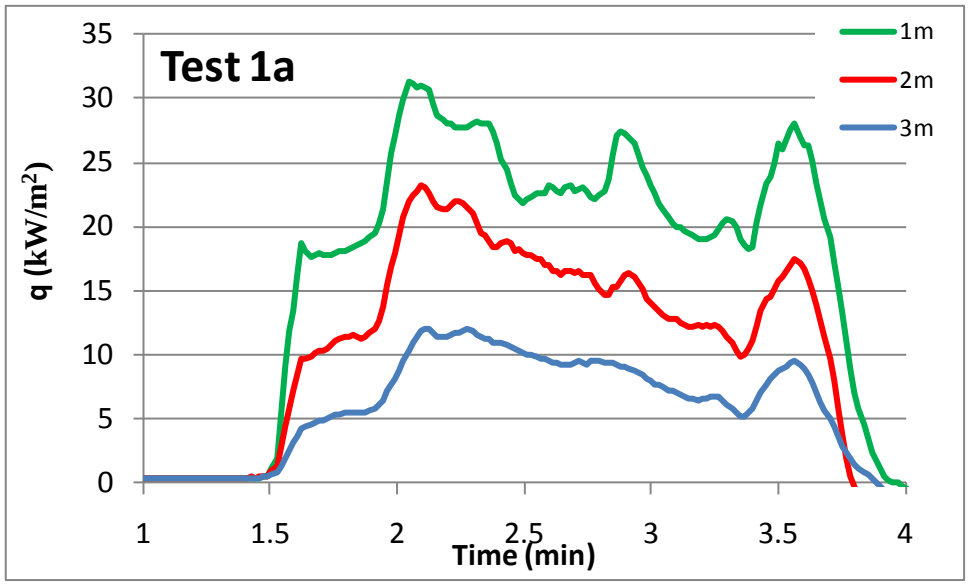

Figure 4.2. Horizontal radiant heat flux (to a vertically oriented surface) at different distances from the leak in test 1a.

4.2 Test 1b - 1" pipe, 2x25 mm slot, no braid

Test 1b was identical to test 1a but the braid was removed. The methane stream was strong enough to blow out the ignition rag several times. Setup 2 was used for PT, TC and HFM measurements.

The pipe was cut in such a way that the flame ejected at 35 °C angle upwards. The flame was about 9 m long but went at a height above all PTs and HFMs, including the one at 2.5 m, see figure 4.3. The flame was almost constant in intensity over the more than 4 minutes that the test lasted with only a temporary decrease after one minute. The pressure was constant at 9.5 bar throughout the test.

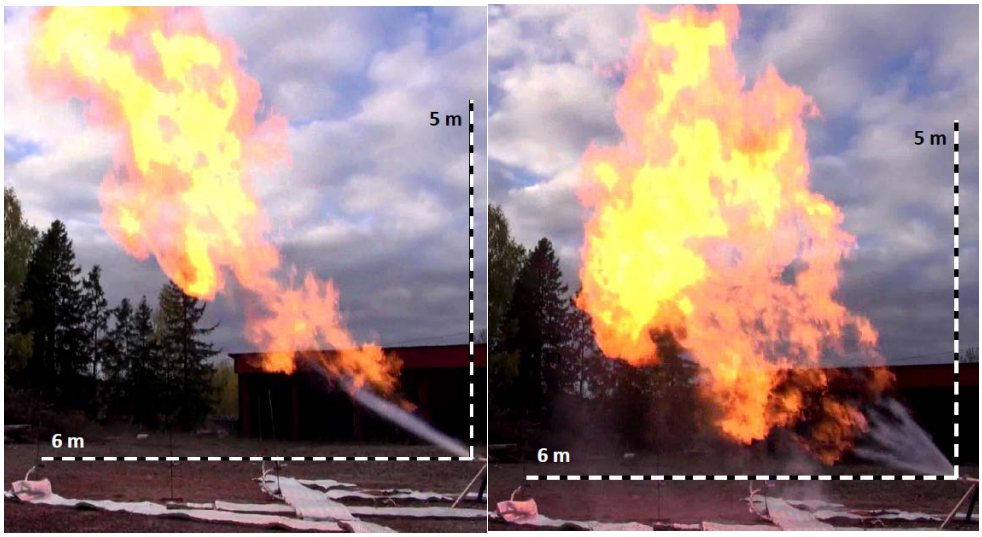

Figure 4.3. Two typical photos from test 1b (1" pipe with 2x25 mm slot, no braid).

The horizontal incident radiant heat flux (to a vertical surface) at the different distances is shown in figure 4.4. It can be noticed that the largest horizontal heat flux is at 4 m whereas the flux is almost identical at 2.5 and 6 m distance.

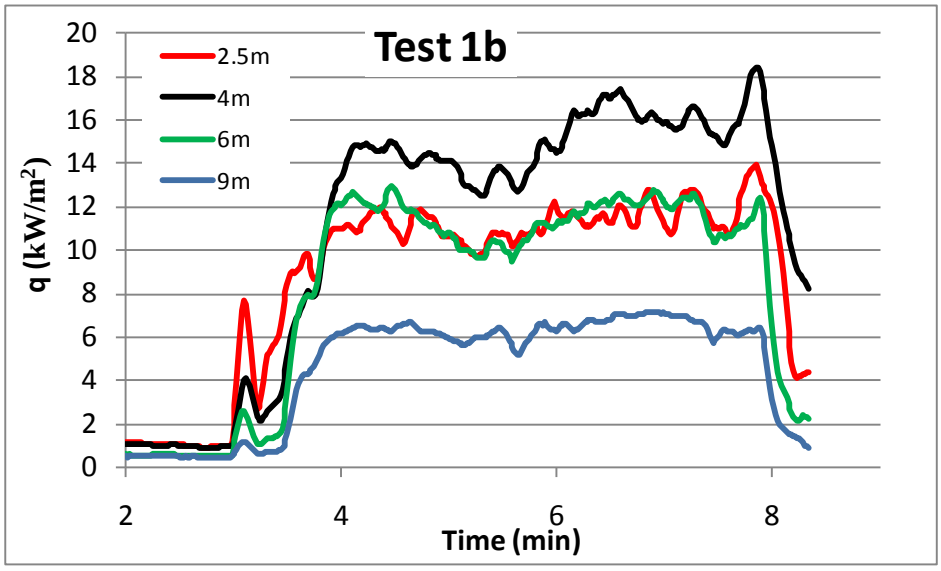

Figure 4.4. Horizontal radiant heat flux (to a vertically oriented surface) at different distances from the leak in test 1b.

In this test, substantial radiant heat flux was also measured in the vertical direction (to a horizontally oriented surface). Figure 4.5 shows incident heat flux to the horizontally oriented surfaces. It can be seen that at 2.5 and 6 m the vertical heat flux is far from similar.

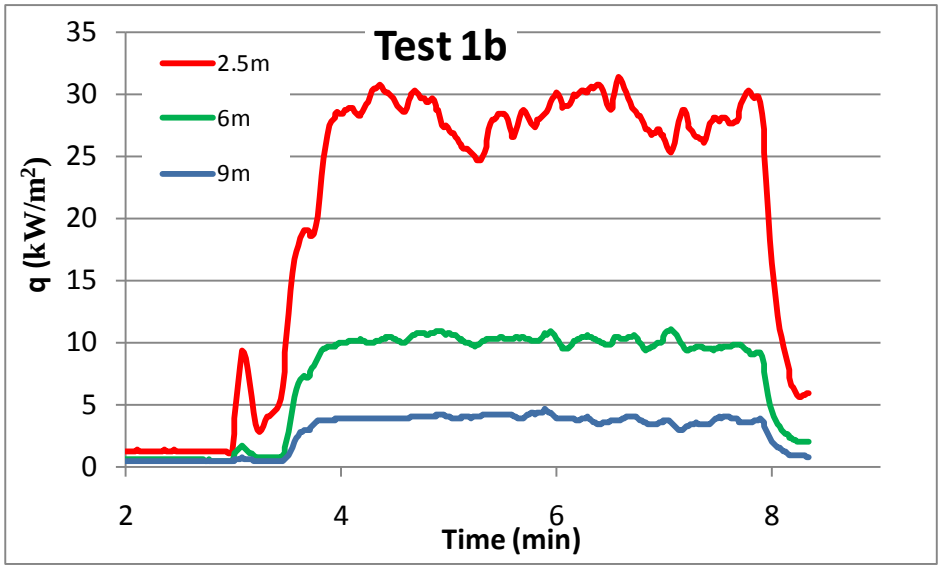

Figure 4.5. Incident radiant heat to horizontally oriented surfaces, at different distances along the leak direction in test 1b.

4.3 Test 2a - 1" pipe, 1x10 mm slot, with braid

Test 2a was a 1" pipe (25 mm Ø and 2 mm thickness) with a 1 by 10 mm long slot cut crosswise. The pipe was covered by a stainless steel braid. Thermal impact was measured with setup 1.

The release was easily ignited and continued burning steadily during 50 s. The pressure was held around 9.5 bar throughout the test. The flame was roughly 1 m high and

extended in the leak direction approximately 0.7 m. It appeared as that in the beginning of the test only methane gas was released from the braid covered pipe. After 50 s the behaviour changed. Liquid methane was clearly noticed from the leak and in most directions orthogonal to the pipe direction. Liquid was also dripping from the braid, soaking the insulation placed below the pipe such that the insulation continued burning after the test was completed. The flame height grew to roughly 2 m and extended just over the first measuring station at 1 m in the leak direction. The flame continued to grow slowly and started leaning over the leak direction with a flame length up to 3 meters. The PT at 2 and 3 m distance was not directly in the flame even though the flame extended further above these directions, see figure 4.6. At 2 m distance the radiant heat flux was primarily in the horizontal direction, see appendix 8.2. Figure 4.7 shows the incident radiant heat to vertical surfaces at 2 and 3 meters.

It should be noticed that the heat flux increased stepwise during the test and that additional increase cannot be excluded. However, comparing with test 1a, which is the same configuration with a larger opening gives us a hint. The final limit in test 2a at 3 m is about the same as the more stable level from test 1a. The reason that test 1a gave a similar heat flux compared to 2a is the lower pressure of test 1a.

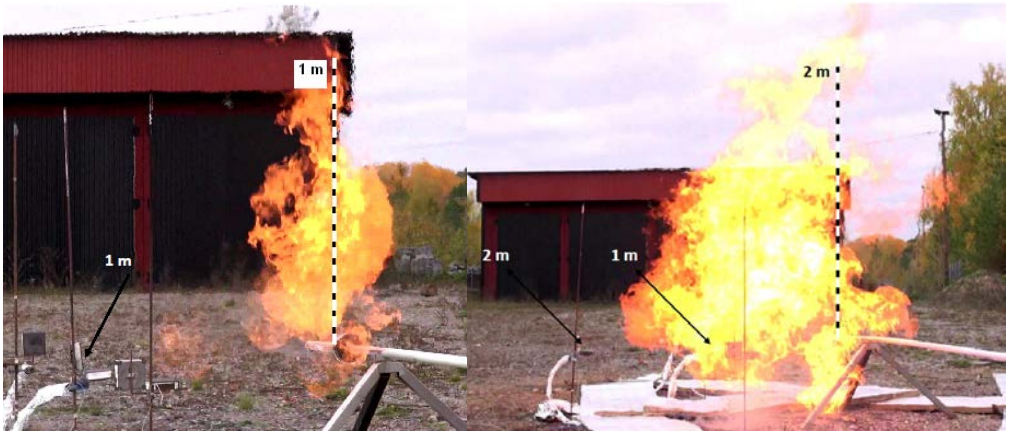

Figure 4.6. Photos from test 2a (1" pipe with 1x10 mm slot, covered by a braid).

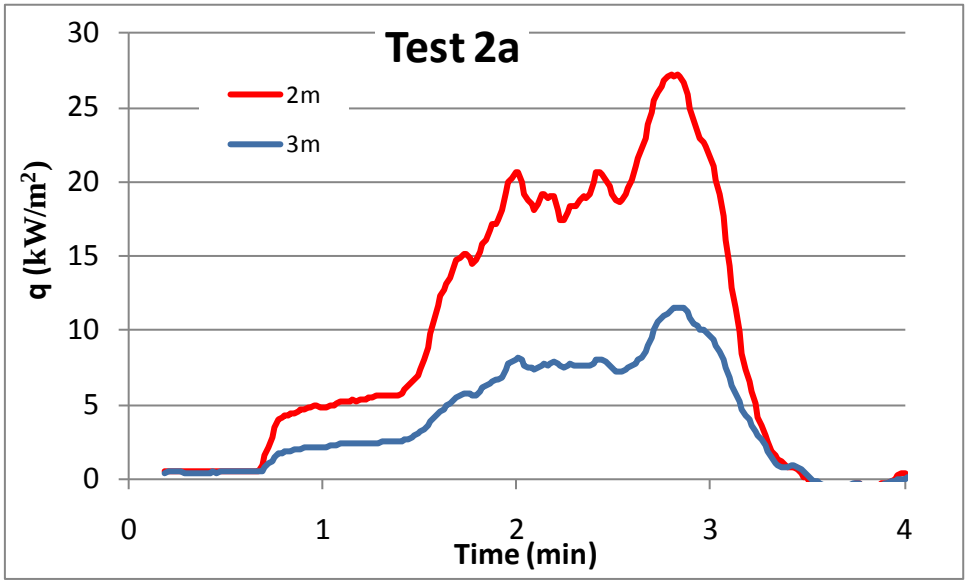

Figure 4.7. Incident radiant heat flux in horizontal direction (to a vertical surface) at 2 and 3 m distance from the main direction.

4.4 Test 2b - 1" pipe, 1x10 mm slot, no braid

Test 2b was identical to test 2a but the braid was removed. Thermal impact was measured with setup 2.

The release was first ignited two times followed by self-extinguishment after a few seconds. The third ignition resulted in a self-sustained flame. The pressure increased rapidly to 12 bar at the main ignition and then dropped quickly to 8.5 bar during the following 30 s. During the remaining 1.5 minutes the pressure slowly decreased to 7 bar, see appendix 8.1.

The flame length varied between 4-6 m during the first 30 second and 3-3.5 meters during the remaining 1.5 minutes of the test, see figure 4.8. The TC at 4 m distance reached a temperature of 150 °C during the first part of the test but remained below 25 °C during the rest of the test. Thus, incident radiant heat flux is a relevant parameter to study at distances ≥ 4 m in the leak direction.

Figure 4.8. Photos from test 2b (1" pipe with 1x10 mm slot, no braid). Upper photo: a large flame pulse from the first part of the test with a pressure close to 12 bar. Lower photo: Typical behaviour for the main part of the test, with a lower pressure in the pipe (around 8 bar).

The maximum heat flux was almost totally horizontal, see appendix 8.1. Figure 4.9 shows the incident radiant heat flux during the test at 4, 6 and 9 meters distance.

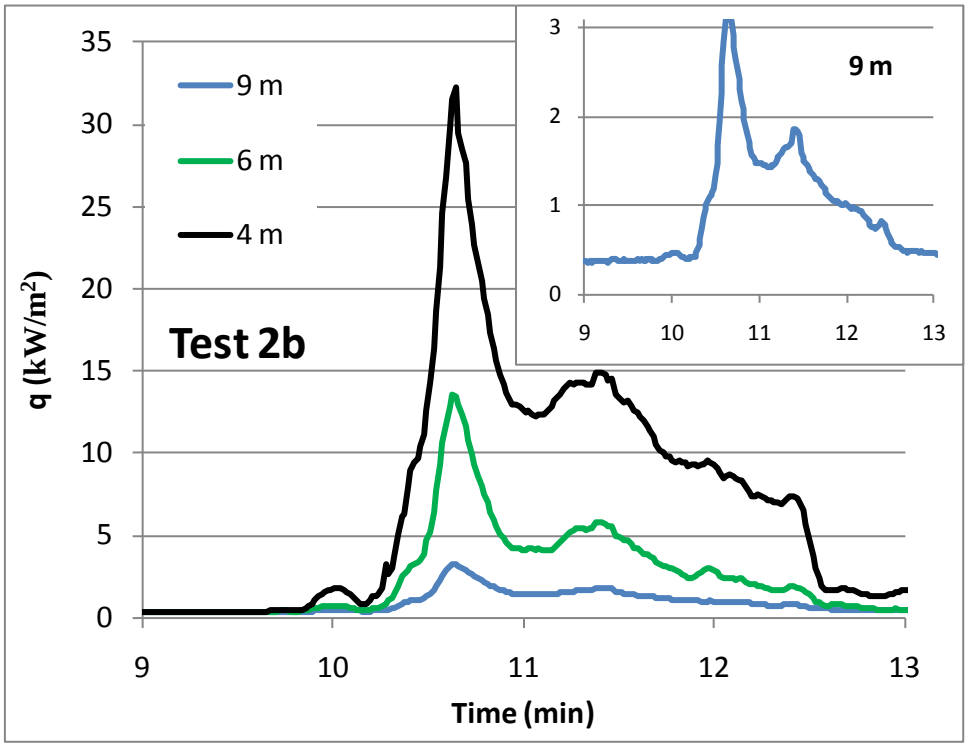

Figure 4.9. Incident horizontal radiant heat during test 2b at 4, 6 and 9 meters in the main direction. The inset shows the data for 9 m in magnification.

The very transient behaviour of the incident heat flux can be better understood in relation to the maximum temperatures at the vertical PT. The full transient behaviour is shown in the appendix. The maximum PT temperatures as a function of distance is shown in figure 4.10.

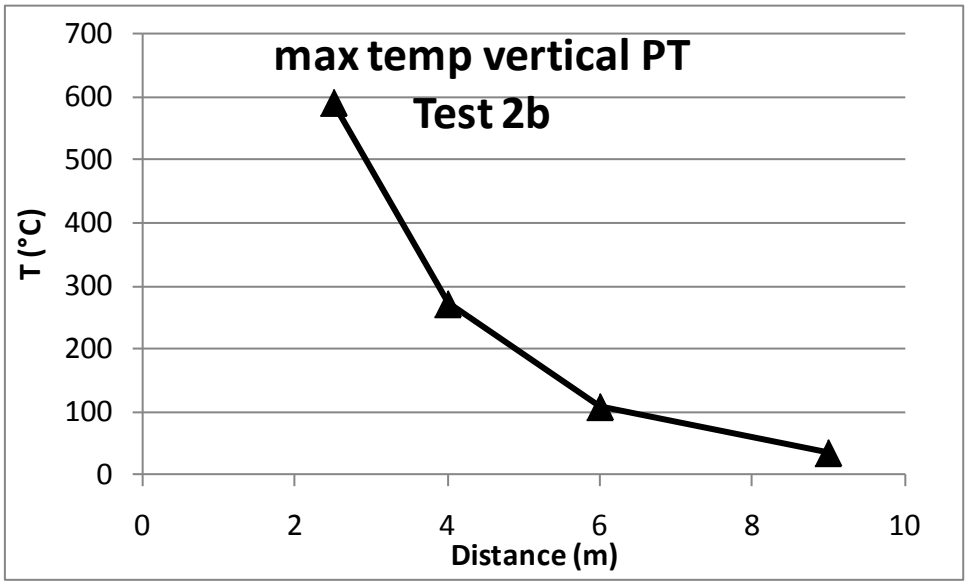

Figure 4.10. Maximum temperature on the vertical PT in test 2b.

4.5 Test 3a - 1" pipe, 1 mm^2 hole, with braid

Test 3a was a 1" pipe (25 mm Ø and 2 mm thickness) with a 1 mm^2 hole drilled into it. The pipe was covered by a stainless steel braid and setup 1 was used.

The gas was easily ignited and continued almost 5 minutes. The flame was localised around the pipe, not particularly directed towards any position. The pressure varied between 9-10 bar with a sudden increase after almost 3 minutes, reaching 15 bar and relaxing to 11 bar at the end of the test. This pressure change had very little impact on the response of the PT or HFM as well as the size of the flame which had a continuous width of less than 0.5 m and reached 0.8 m at its maximum. The flame height was 0.5 -1 m, see figure 4.11. Figure 4.12 shows the incident radiant heat flux for 1, 2 and 3 m along the main direction from the pipe.

Figure 4.11. Photo from test 3a (1" pipe with 1 mm^2 hole, covered by a braid).

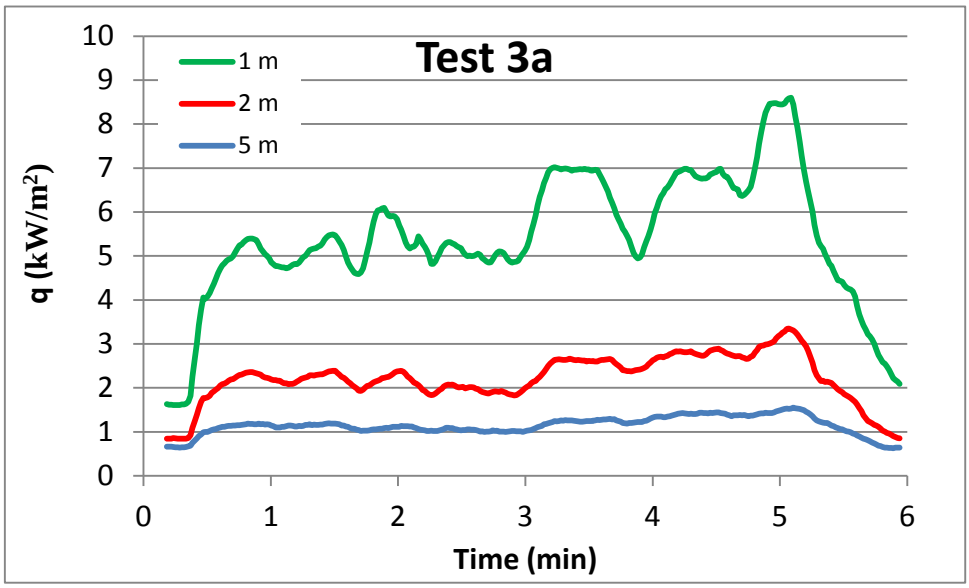

Figure 4.12. Incident radiant heat flux during test 3a.

4.6 Test 3b - 1" pipe, 1 mm^2 hole, no braid

Test 3b was identical to test 3a but the braid was removed. The methane stream repeatedly blew out the ignition rag and after trying from several different positions a self-sustained flame could not be accomplished as soon as the pilot flame was removed. Setup 1 was used for thermal impact.

A small jet flame was produced when the pilot flame was put into the methane stream but only if the pilot was less than 0.5 m from the leak, see figure 4.13. At further distances no additional flame except the pilot can be noticed visually

Figure 4.13. The pilot aided flame from test 3b (1" pipe with 1 mm^2 hole, no braid). The flame was never self-sustained without the presence of the pilot.

4.7 Test 4 - 1" hose cut 1/3 of circumference

A flexible convoluted 1" DN25 hose of 0.2 mm thick stainless steel with an inner diameter of 25.4 mm and an outer diameter 33.7 mm was used in Test 4. The hose is shown in Figure 4.14. A slot of 1/3 of the circumference was cut, see figure 4.14, and a stainless steel braid covered the hose (the braid itself was not damaged). The opening was cut such that the centre of the slot was pointing horizontally perpendicular to the hose. The end of the hose was supported such that it continued horizontally. PT, TC and HFM measurements were conducted with setup 1.

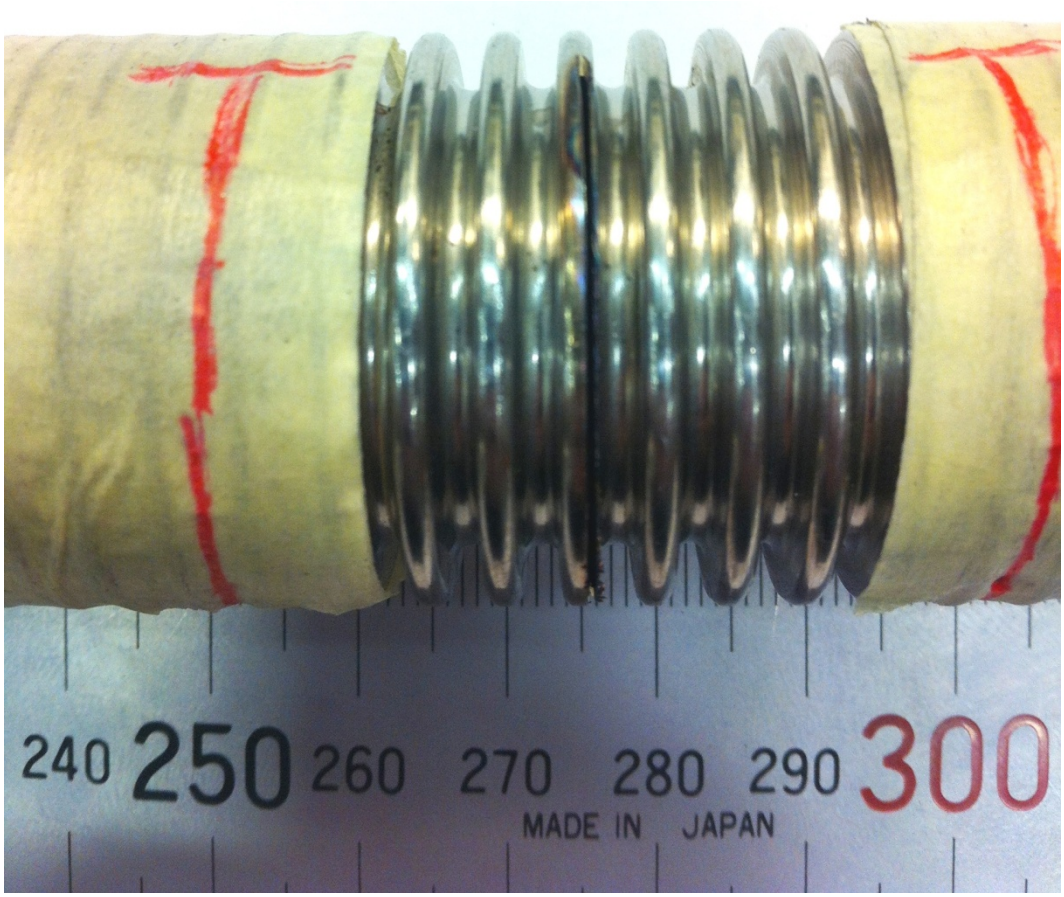

Figure 4.14. The hose with slot used in test 4. During test a non-damaged stainless steel braid covered the hose.

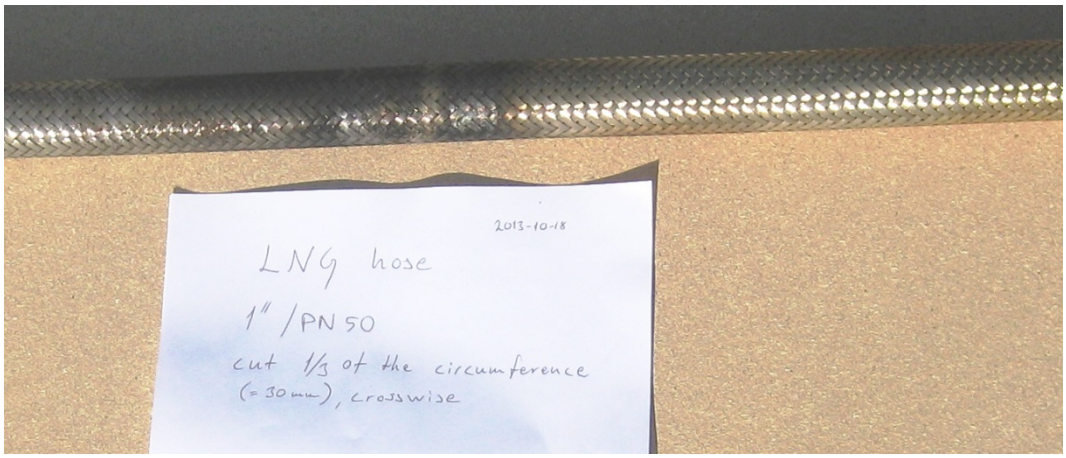

Figure 4.15. The same hose with the stainless steel braid on after the fire tests.

Test 4 lasted for two minutes. Flames were ejected from the hose in both the main direction and the opposite (horizontally, the other way), see figure 4.16. During the first 30 minutes the flames extended 1- 2 m in both directions and rose 0.5-1 m high. Thereafter the flames grew stepwise, as previously seen in e.g. test 2a. During the later stages of the test the flames grew higher (2-3 m) but not much wider in the horizontal directions.

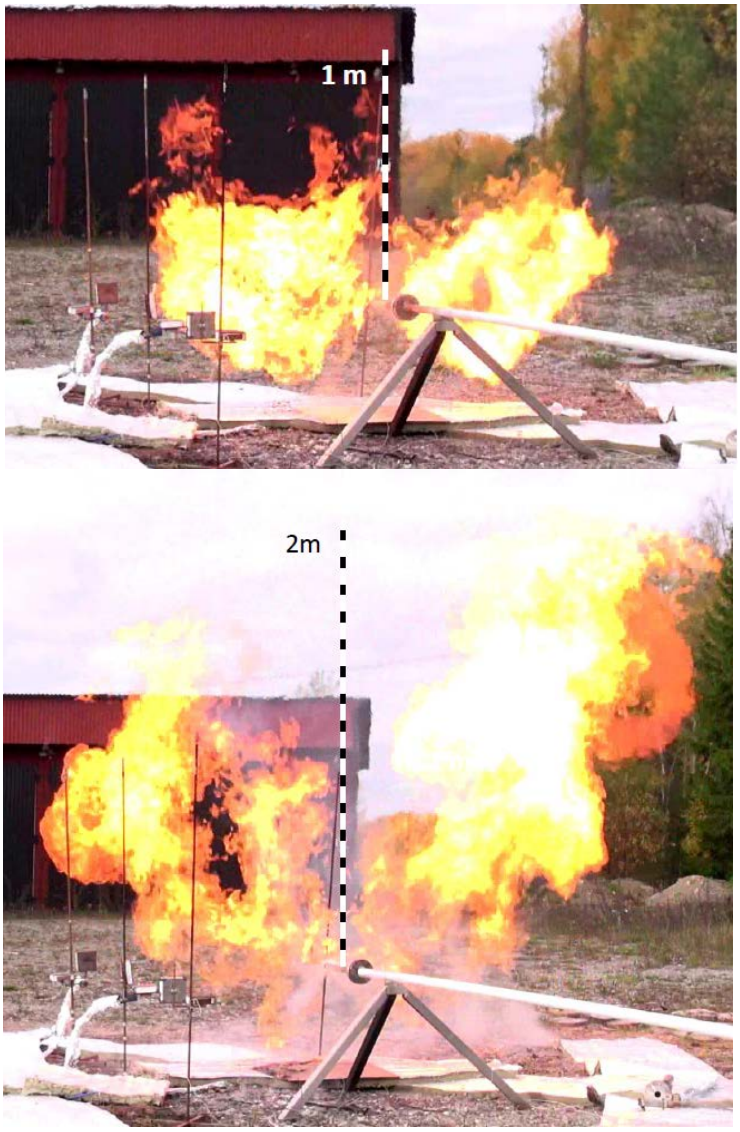

Figure 4.16. Photos from the early (upper) and late (lower) stage of test 4.

The horizontal incident radiant heat flux at 2 and 3 meters distance is given in figure 4.17.

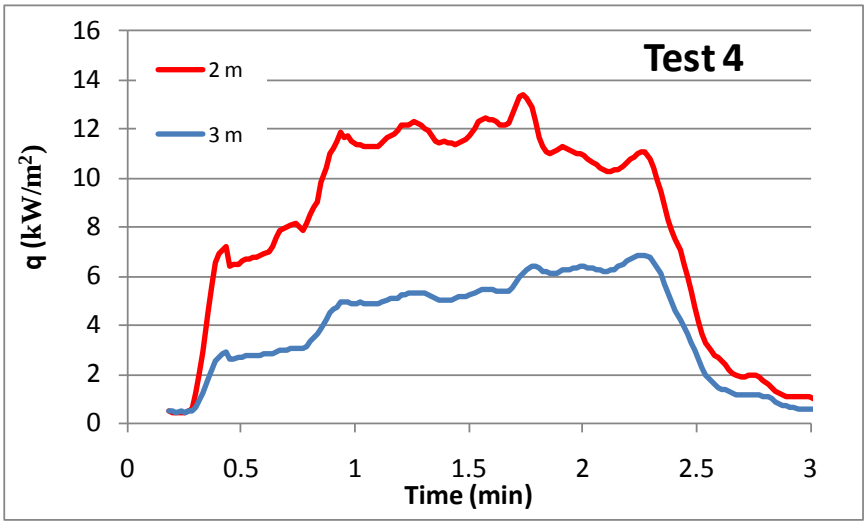

Figure 4.17. Incident radiant heat flux at 2 and 3 m distance in the main direction for test 4 (1" hose with a slot 1/3 of the circumference).

The maximum temperatures of the vertical PT are shown in figure 4.18. At 1 and 2 m the temperature was either stabilised or had already reached its maximum at the end of the test. The temperature at 2 m distance was below 250 °C. At 3 m the temperature was still increasing.

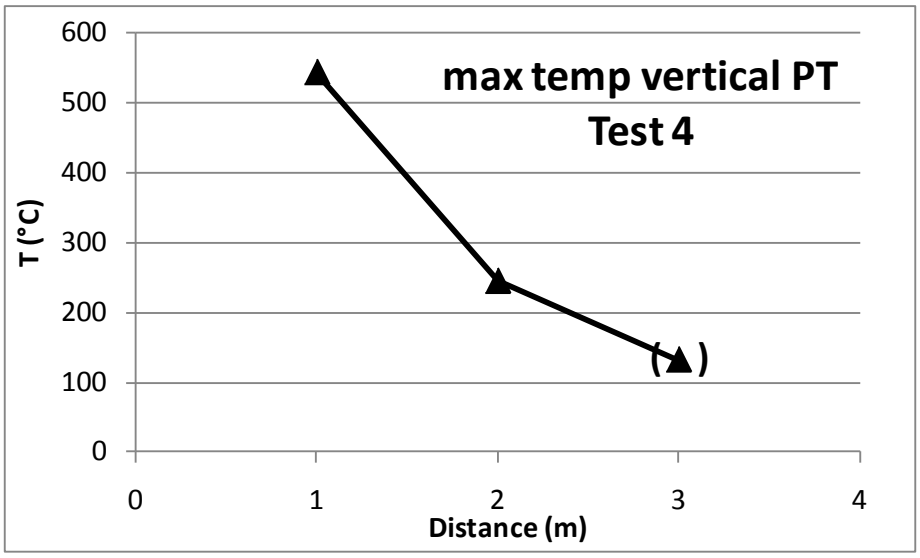

Figure 4.18. Maximum temperature of the vertical PT as a function of distance for test 4 (1" hose with a slot 1/3 of the circumference). At 3 m distance the temperature had not yet reached its maximum when the test was finished.

From observations of the test it appeared that the hose had broken around the complete circumference since, during the later stage of the test, LNG was pushed out of the braid in essentially a circular manner, in all directions perpendicular to the hose direction. However, examining the hoses afterwards showed that the hose had not opened more than what was originally cut. Below is a figure of the same hose after removal of the braid. Note the similarity to the initial cut shown in figure 4.14

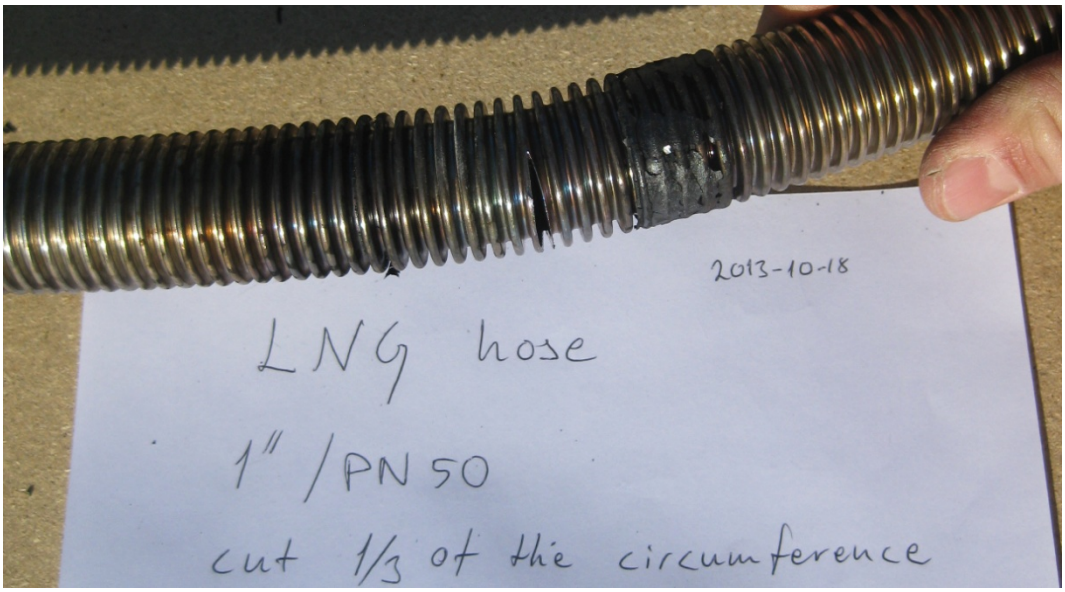

Figure 4.19. Photo of the hose, stripped from its braid, after test 4 (1" hose with a slot 1/3 of the circumference).

Test 5 - 1" hose cut 5 mm

Test 5 was conducted on the same type of hose as test 4 but the slot was 1x5 mm in dimensions. It also produced two flames from the hose. One pointing in the main direction but approximately 45° downwards and one in the straight opposite direction, see figure 4.20. The flame impinged the ground under the PT pair at 1 m distance. After 1.5 minutes the flames increased and more or less covered the PT at 1 m but never reaching the measurements at 2 m. The naked TC at 2 m distance did not increase in temperature at all. The pressure was held steady at 10 bar during the entire test. Almost no impact was found on the PT measuring radiation from above and the maximum radiant heat flux was in the horizontal direction. Figure 4.21 shows the incident heat flux at 2 and 3 m.

Figure 4.20. Photos from test 5 (1" hose with 1x5 mm slot, covered by a braid).

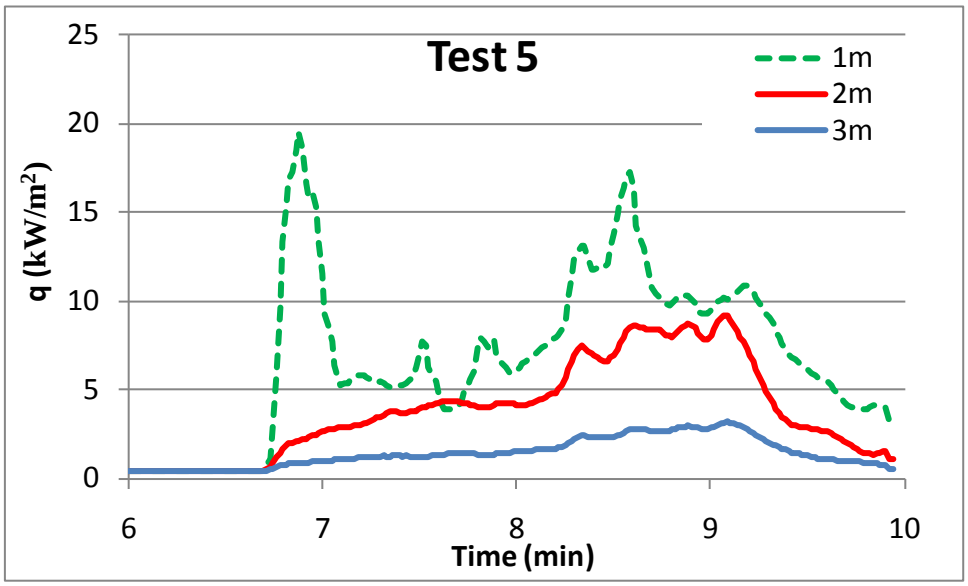

Figure 4.21. Horizontal incident radiant heat flux at different distances in the main direction for test 5. The 1 m distance is partially engulfed in the flame.

4.8 Test 6 - 1" hose, 1 mm^2 hole

Test 6 was also conducted on the same type of hose as test 4 but instead of a slot the damage was a 1mm^2 hole.

A small (< 0.5 m) flame rose from the hose during all the duration of the test (3.5 minutes), see figure 4.22. The pressure varied between 12 and 13 bar throughout the test. The incident heat flux at 1 m distance was less than 2.5 kW/m^2, harmless for people and structures.

Figure 4.22. Photo from test 6 (1" hose with 1 mm^2 hole).

4.9 Test 7 - 2" hose cut 1/3 of circumference

A flexible convoluted 2" DN50 hose of 0.25 mm stainless steel with an inner and outer diameters of 50.2 and 62.5 mm, respectively, was used in Test 7. A slot of 1/3 of the circumference was cut (see Appendix 8.5 for a photo post-testing), and a stainless steel braid covered the hose. As with tests 4-6, the braid itself was not damaged. The opening was cut such that the leak direction was perpendicular to the hose. The end of the hose was supported by a pin such that it continued horizontally. PT, TC and HFM measurements were conducted with setup 2.

The test lasted for about three minutes. Methane was spraying out from the braid in all directions perpendicular to the hose elongation direction, but was predominantly directed towards the PT. However, the flame was mostly buoyancy dominant and rose to the sky, see figure 4.23. Pressure was constant at 10 bar during the test. Figure 4.24 shows the incident radiant heat flux to a horizontally oriented surface.

The maximum temperature for the vertically oriented PT is shown in figure 4.25. Note that all temperatures had saturated during the test, see appendix 8.1.

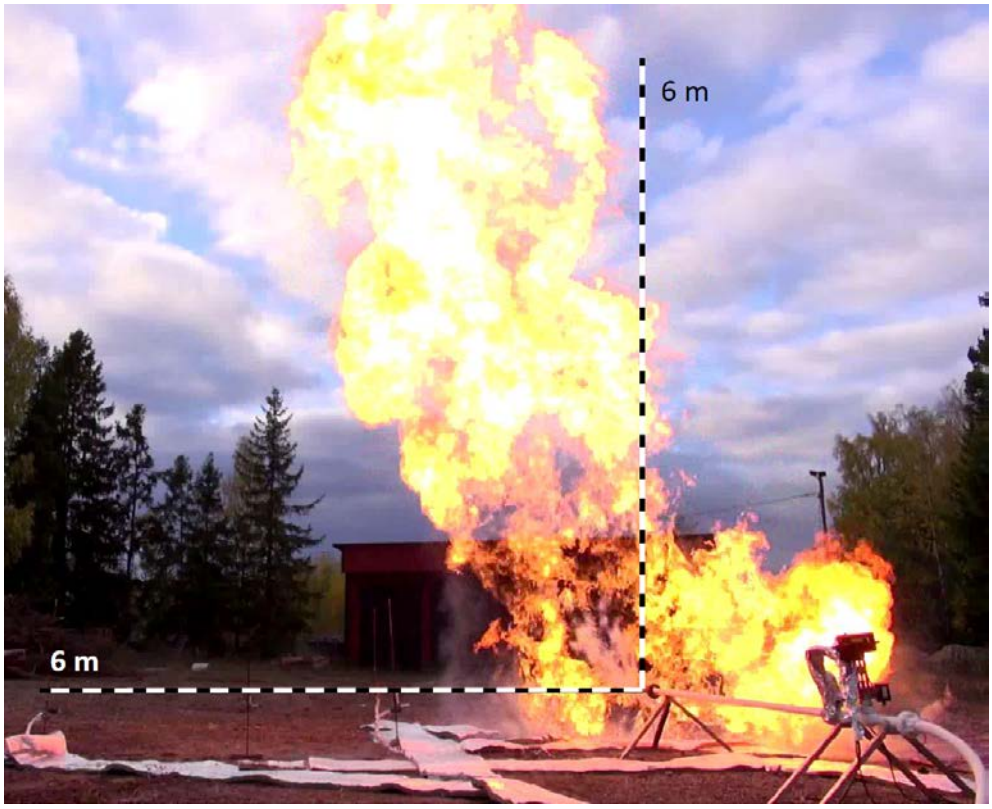

Figure 4.23. Photo of test 7 (2" pipe with 1 mm slot cut 1/3 of circumference and covered with a braid).

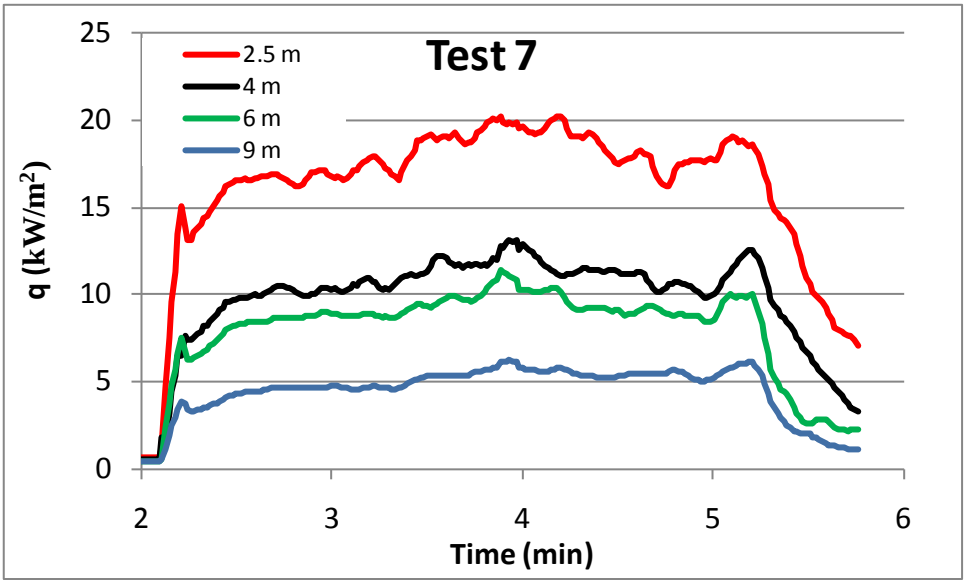

Figure 4.24. Incident radiant heat flux to a horizontally oriented surface at different distances in the main direction for test 7.

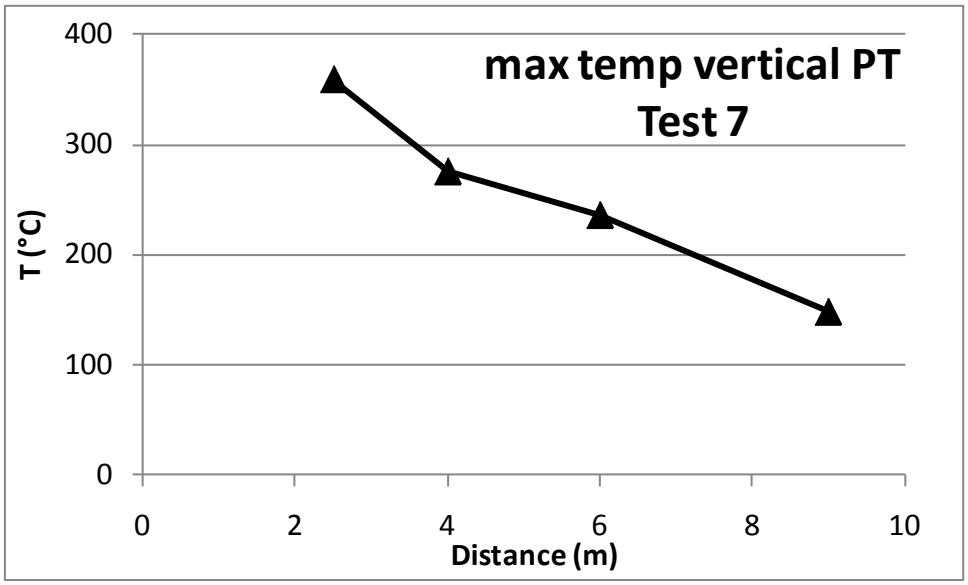

Figure 4.25. Maximum temperature for the vertical PT during test 7.

4.10 Test 8a - 2" pipe, 5x45 mm slot, with braid

In test 8a a 2" pipe with 2 mm thickness was used. A 5 by 45 mm slot was cut crossways such that the centre of the slot was pointing horizontally. A stainless steel braid covered the pipe. Setup 2 was used for the thermal impact measurements.

The test had to be run twice. In the first attempt the ignition was delayed for 13 seconds which resulted in a larger flame initially for a few seconds. During this time the TC at 9 m distance reached almost 700 °C. Later, the flame stabilized with a width just more than 6 m. The pressure during this test was between 5-7 bar. This attempt was however interrupted after 1 minute due to failure of the pump to maintain pressure.

The second attempt was ignited directly and no large volume of gas was accumulated. The pressure was somewhat smaller for this test, around 5 bar, and the flame reached 4-5 m horizontally and between 7 and 12 meters high, see figure 4.26.

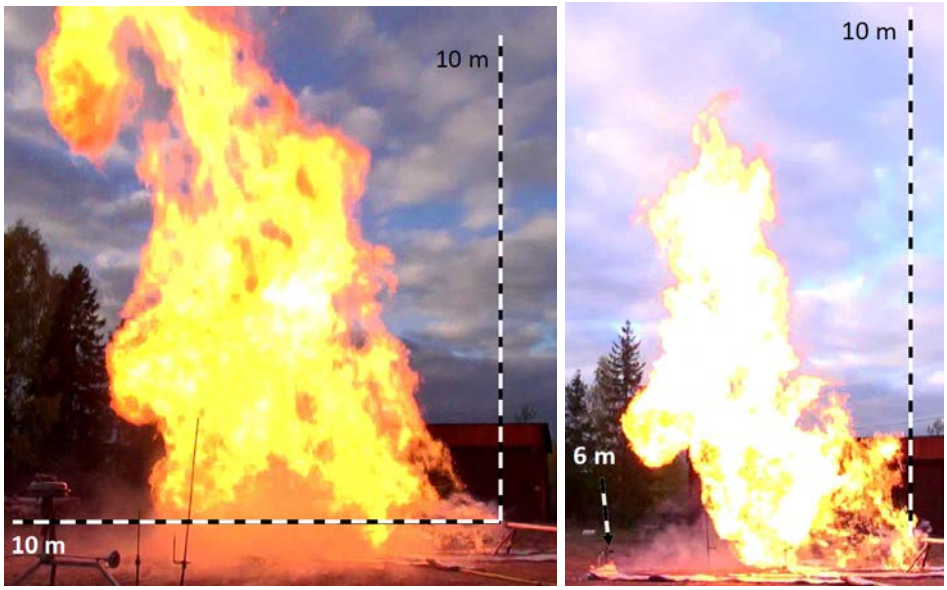

Figure 4.26. Photos from the first (left) and second (right) attempt of test 8a (2" pipe with 5x45 mm slot and covered with a braid).

The incident heat flux to a vertical surface at 9 m distance is shown in figure 4.27, comparing the two attempts, with different pressure in the pipe.

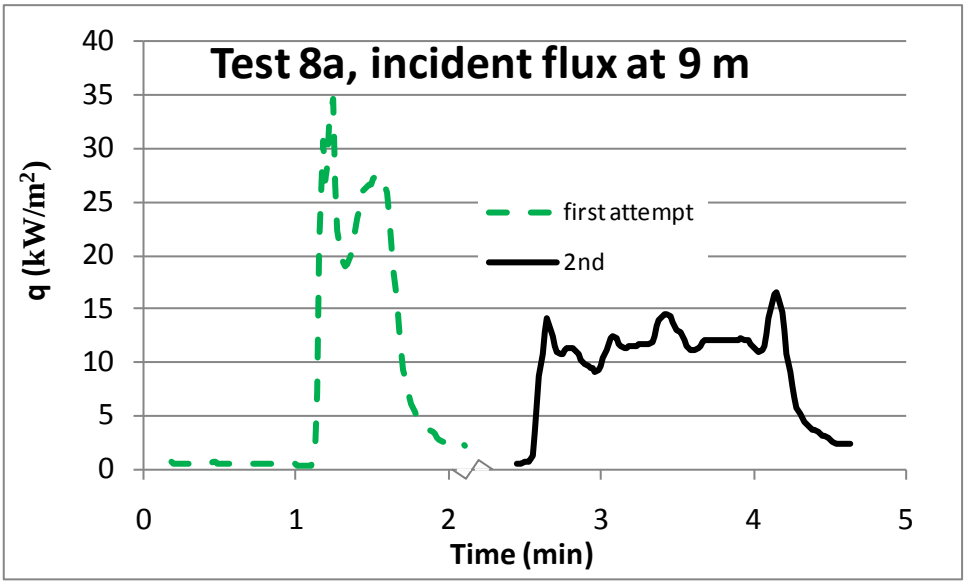

Figure 4.27. Incident radiant heat flux to a vertical surface at 9 m distance in the main direction for test 8a. The two curves represent the two attempts. The first with a pipe pressure varying between 5-7.5 bar and the second with 5 bar. The time duration between the tests was longer than indicated in the graph.

More detailed information on the incident radiation for the 2nd attempt, both in vertical and horizontal direction can be found in figure 4.28.

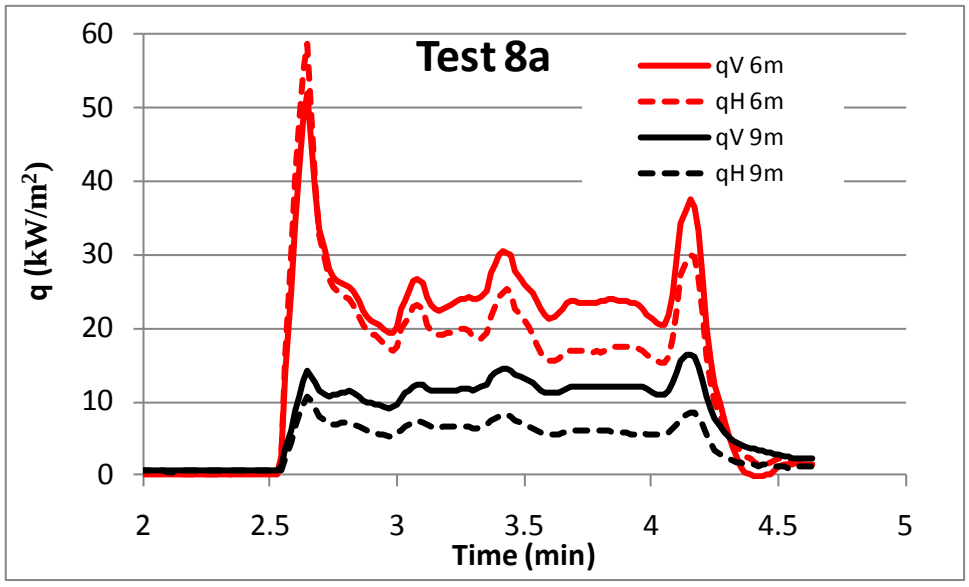

Figure 4.28. Incident radiant heat flux at 6 and 9 m distance in the main direction for test 8a (second attempt). V indicates incident heat flux to a vertical surface (from the leak) and H to a horizontal surface (from above).

4.11 Test 8b - 2" pipe, 5x45 mm slot, no braid

The same pipe and configuration was used in test 8b as in test 8a. The difference was the removal of the braid.

The test lasted just under a minute. The flames reached between 9 and 13 m horizontally in the leak direction and rose 12 meters high, see figure 4.29. The pressure was around 7 bar.

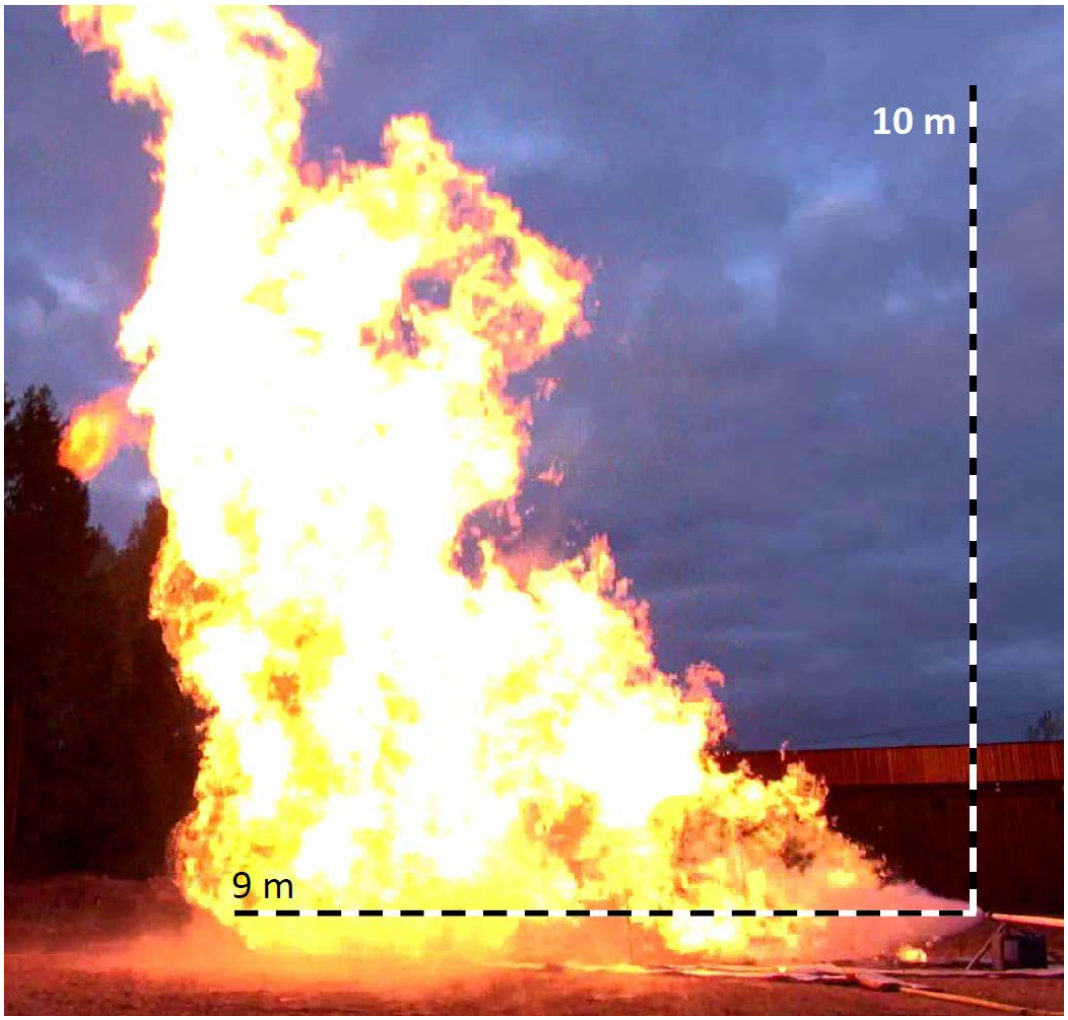

Figure 3.24. Photo (2" pipe with 5x45 mm slot, no braid)

The response of the PT at 2.5 m is different from the others at further distance. The initial heating is much lower and there is a temporarily decrease of the temperature during the test. This is most probably due to cooling of non-combusted LNG impinging on the surface. At further distance the PT temperatures are much higher. Figure 4.30 shows the temperature development of the vertically oriented PT in the main direction.

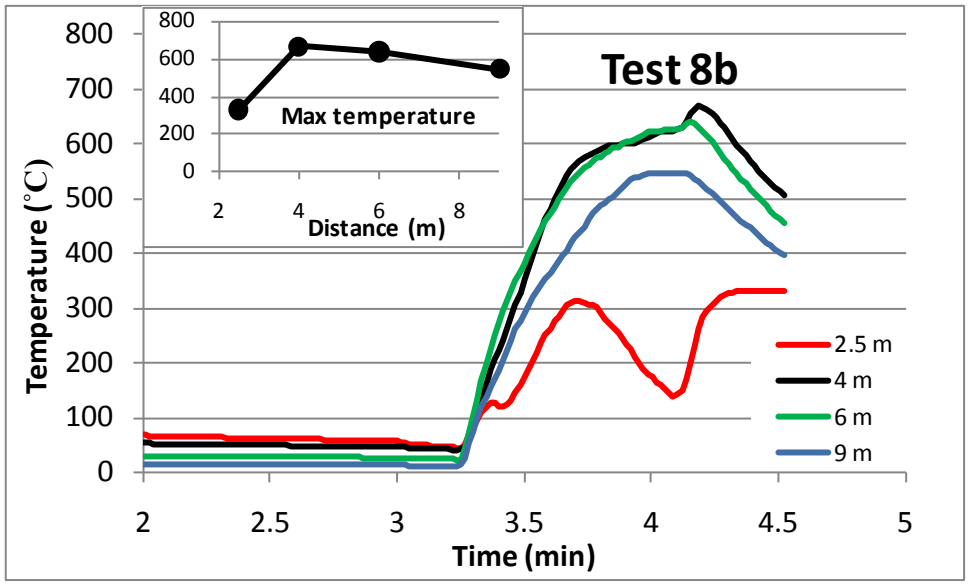

Figure 4.30. Temperature of the vertically oriented PT in the main direction during test 8b. The inset shows the maximum temperatures reached during the test.

4.12 Test 9 - pipe (Ø=4 mm) with open end

No self-sustained flame could be produced in this test. A substantial horizontal jet flame, just over 4 m in length was formed when assisted by the pilot flame, see figure 4.31. Naturally, as methane had been leaking for some time the flame was initially larger during the first second after each ignition.

Figure 4.31. Snapshot of the piloted jet flame from test 9. As soon as the pilot flame was removed the jet flame was put out .

4.13 Test 10 - pipe (Ø=9 mm) with open end

Test 10 ignited and continued burning with a constant jet flame, about 8 meters in length, see figure 4.32. No flames existed within 2-3 m from the open pipe.

Figure 4.32. Temperature of the vertically oriented PT in the main direction during test 8b. The inset shows the maximum temperatures reached during the test.

4.14 Test 11 - pipe (Ø=12 mm) with open end

Test 11 was easily ignited and first a constant jet flame of 10-11 m length was formed (with a maximum height of 4-5 m). This burned during 15 s until a sudden increase in flame intensity was observed. The flames reached at this second stage about 15 m from the open pipe and an unknown height.

Figure 4.33. The jet flame from the first stage of test 11.

Figure 4.34. Snapshot from the second stage of test 11.

4.15 IR camera results

Recording diffusion of cold gas from the tests with IR imaging turned out to be a difficult task. The high optical depth coefficient of the gas makes it almost transparent to the background if the gas cloud is small. An example of this is the thin (but strong) flow in test 3b (1 mm^2 hole in a 1" pipe, no braid). The flow only burned in the presence of the pilot flame. Figure 4.35 shows two snapshot from the test separated only 0.5 s in time. Without the ignition no cold gas flow could be detected with the IR camera. The only surfaces with a temperature below 0 °C (marked green in the snapshot) is the LNG pipe, the sky and the aluminium in the insulation which reflects the cold sky. During this test a constant flow from the pipe was observed and we can be certain that cold methane was present.

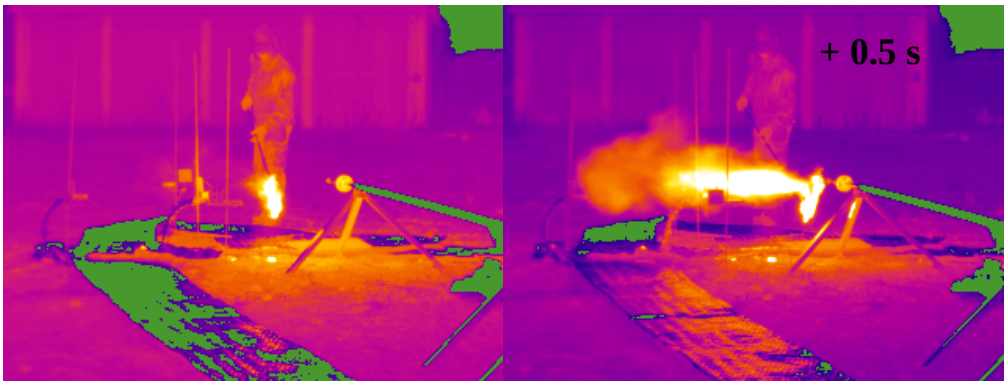

Figure 4.35. IR image trying to record cold gas in test 3b. Everything with a black body radiation < 0°C is indicated as green.

For situations where the gas assembly was larger it could be detected more easily. These were also situations where the gas was more easily ignited. Figure 4.36 shows two snapshots from the first attempt of test 8a. One is just when the gas is released. A small but marked cloud (indicated in blue for temperatures below 0°C) can be noticed directly. 13 seconds later ignition occurs and a big cloud could be noticed with almost the exact same shape as the visible could at the same instance.

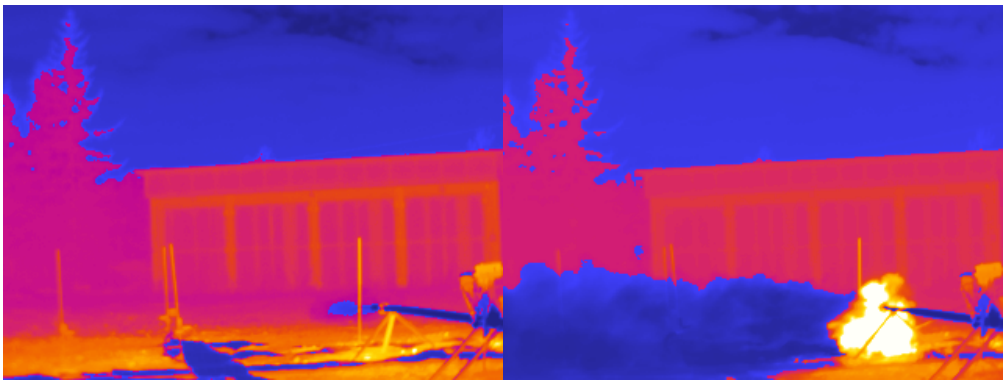

Figure 4.36. IR image recording cold gas in test 8a. Everything with a black body radiation < 0°C is indicated as blue.

The difference between test 3b and 8a is not just the amount of gas released, gas could be identified even initially in test 8a. Instead, the main difference is the velocity of the leaking gas. There is a very high flux from test 3b compared to test 8a even though the flow is probably bigger in the latter test. This can have severe effects on the optical absorption depth and therefore also on the emissivity of the gas.

The flame temperature is also very difficult to determine. Since flame emissivity is unknown for smaller flames the actual flame temperature is best determined for the larger flames. Figure 4.37-4.40 show the recorded black body temperature from the larger flames (test 1b, 2b, 7, 8a and 8b).

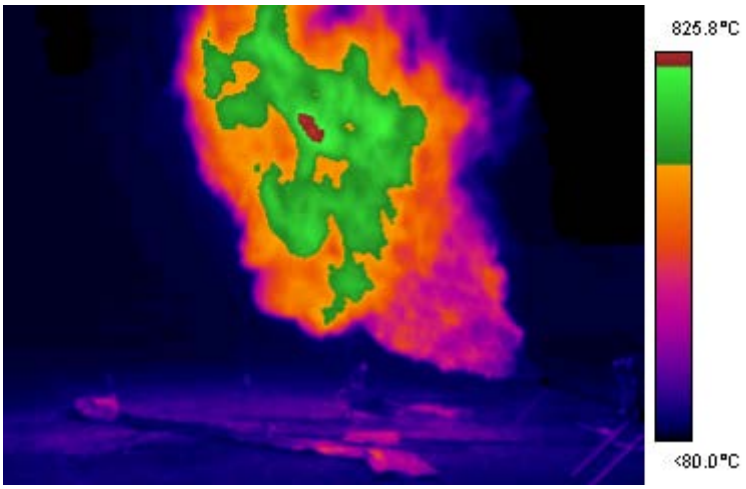

Figure 4.37. IR image recording hot gas in test 1b. The green regions indicate black body radiation temperatures between 600 and 800 °C. The dark red region represents temperatures above 800 °C.

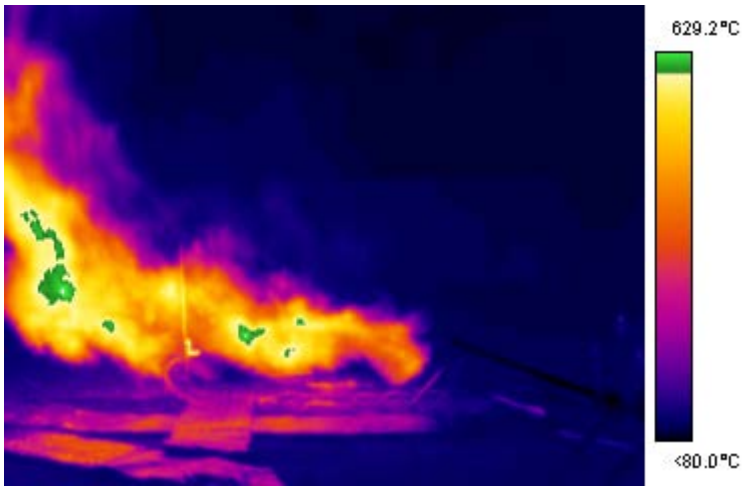

Figure 4.38. IR image recording hot gas in test 2b. The green regions indicate black body radiation temperatures above 600 °C.

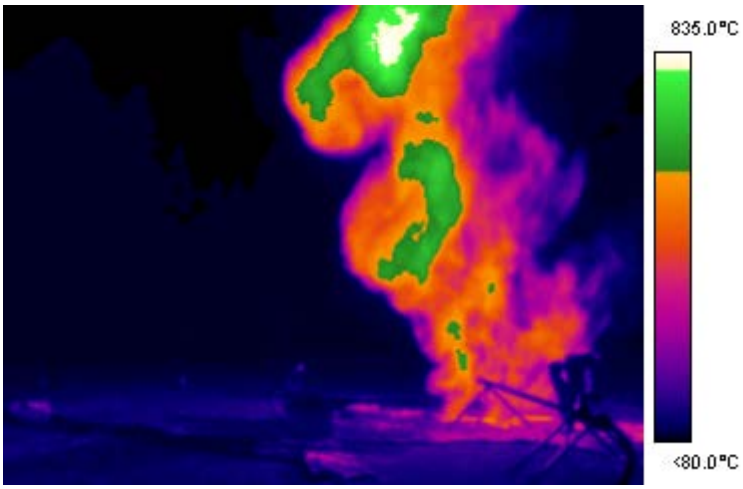

Figure 4.39. IR image recording hot gas in test 7. The green regions indicate black body radiation temperatures between 600 and 800 °C. The white region represents temperatures above 800 °C.

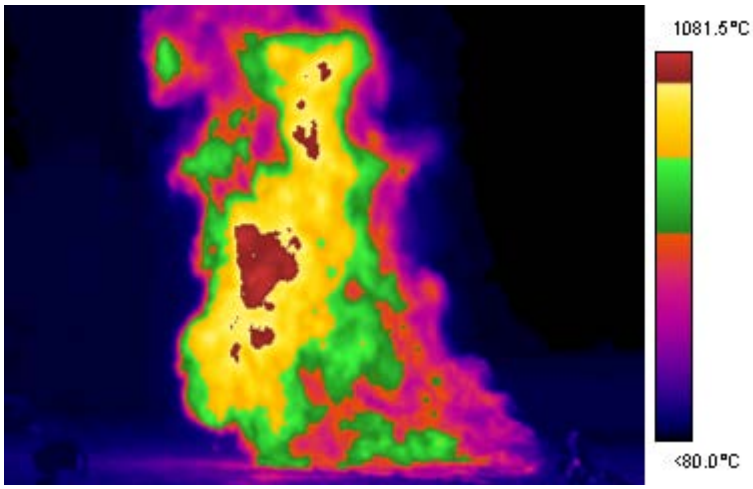

Figure 4.40. IR image recording for cold gas in test 8b. The green regions indicate black body radiation temperatures between 600 and 800 °C. The yellow regions represent temperatures between 800 and 1000 °C. The dark red region represents temperatures above 1000 °C.

4.16 Summary of the tests

Table 4.1 shows a summary of the experimental results for the different tests. The table describes the horizontal continuous flame width which is the maximum horizontal distance to which the flame is continuous for more than 10 seconds during a test. Note that this width can be above the height of the PT such that the PT can still measure incident radiant heat flux outside the flame even though its distance to the leak is closer than the horizontal continuous flame width. The horizontal maximum flame width is also indicated which describes the maximum width to which flames extend, even for very short durations. The horizontal incident radiant heat flux indicated in the table is maximum values reached for ten seconds or more. For a more complete view of the incident fluxes throughout the tests, study the diagrams for each individual test.

Table 4.1. Overview of results from the tests.

Test	**P (bar)**	**Horizontal continuous flame width [1] (m)**	**Horizontal maximum flame width (m)**	**Flame height (m)**	**Horizontal $\dot{q}''_{inc}$ outside flame [2] ($\dot{q}''_{inc}$/distance) (kW/m^2 / m)**
1a	9-6	1	3	3-4	(27 / 1m) 22 / 2m 12 / 3m
1b	9-10	5	6	7-9	12 / 2.5m 17 / 4m 12 / 6m 11 / 9m
2a	9.5	2	3	2-2.5	(45 / 1m) 26 / 2m 11 / 3m
2b	12-7.5	3.5	6	1-2	14 / 6m 3.5/ 9m
3a	9-15	<0.5	0.8	0.5-1	8 / 1m 3 / 2m 1.5 / 3m
3b	10		not self-sustained		5 / 1m 1 / 2m Piloted!
4	10	2	2.5	1-2	12 / 2m 6.5 / 3m
5	9-11	1	1.5	1	9 / 2m 3 / 3m
6	12-13	< 0.5	0.5	0.5	2 / 1m 0.5 / 2m
7	10	3	4	8-10	18 / 2.5m 12 / 4m 10 / 6m 6 / 9m
8a[3]	5-9	7	8	10-12	27 / 9m
8a	5	6	7	7-10	13 / 9m
8b	9-7	11	12	9-12	Flame > 9m
9	10	~4 (piloted)	-	1-2	-
10	10	~8	-	4-5	-
11	10	~15	-	-	-

[1] Continuous flame for more than 10 seconds.

[2] highest floating average over a ten second period. Very short peaks are thus ignored. The values within parenthesis are for PT partially engulfed in flames.

[3] This was a shorter test with higher pressure, which ended due to instrument malfunction.

The ease of ignition of the leaking methane was very different for the different tests. In short, for gas releases it was more difficult to ignite the leaking stream if the flow from the opening was very high. The flow often put out the pilot flame instead of being ignited by it. Introducing the pilot from below the methane stream was the most successful strategy. It was also easier to ignite the release if liquid was released from the opening compared to gas.

Even though the pressure for most of the tests was around 10 bar the released methane did not predominantly result in a jet flame direction according to the whole direction if the stainless steel braid was covering the opening. Instead the flame was just slightly offset from vertical and was just as influenced by the gentle wind as the opening direction. The flame was often divided into two streams opposite each other. The luminous flame started just at the pipe/hose with liquid methane dripping from the braid or ejected to the close area (< 1m).

However, for the tests without a covering braid a jet was produced. The first part of the release was not ignited but consisted of liquid phase methane or high concentration gas. Further down the stream the gas was ignited, continued as a jet and ended by deflecting upwards due to buoyancy and loss of horizontal momentum.

5 Discussion

In general it was easier to ignite the methane stream when liquid was released from the opening compared to the case with only gas. For small openings the gas release flow was often high such that the pilot flame was put out. A release that is not ignited could potentially be more hazardous if the release momentum is confined somehow so a small cloud with a flammable mixture is formed which is partially demonstrated in the first run of test 8a. These cases are however not studied here.

In all tests but 1a, 1b and test 5, the opening was oriented in an optimal position for maximum heat exposure to vertically oriented PT, all placed on the same height as the pipe/hose. Nevertheless, since buoyancy becomes dominant further away from the leak as the horizontal velocity in the flame reduces, the flames tend to rise. Therefore, the maximum heat exposure to a vertical surface would be at an elevated height from the leak. At what height the maximum exposure occurs is very difficult to determine and it will vary significantly between the different tests.

The two most important tests of this study is test 4 and 7, 1" and 2" hoses cut 1/3 of their circumference at a constant pressure of 10 bar. These tests represent the hoses from dispenser and truck, respectively. They are both damaged according to the design scenario and have realistic pressures. Additionally, the location of about 0.5 m above ground is relevant for the situations at a filling station. The results show that the inner hose did not open up more than the initial cut during the tests and the stainless steel braid was undamaged as well. The 15 kW/m^2 limit is reached within 2 m for the 1" hose and well within 4 m for the 2" hose. The 5 kW/m^2 limit is reached just over 3 m and 9 m for the 1" and 2" hoses, respectively. The maximum temperatures of the vertical PT are well below 300 °C at 2 m and 4 m distance for hoses of 1" and 2", respectively. These temperatures can be regarded as close to the upper limit of what a vertical surface can reach.

Comparisons with tests 1b and 2b, which represent similar openings as test 4 but without the braid shows that the effect of the flexible braid is considerable. It disables the formation of a jet flame, spreads the release of methane in different directions and thereby reduces the horizontal spread.

Summarizing table 4.1 in a figure we notice that for no test where the braid covered the opening, except the very large opening of test 8a, did the incident radiant heat flux exceed 15 kW/m^2 at a distance beyond 4 m. However, the first attempt of test 8a did generate an incident heat flux at 9 m of 27 kW/m^2.

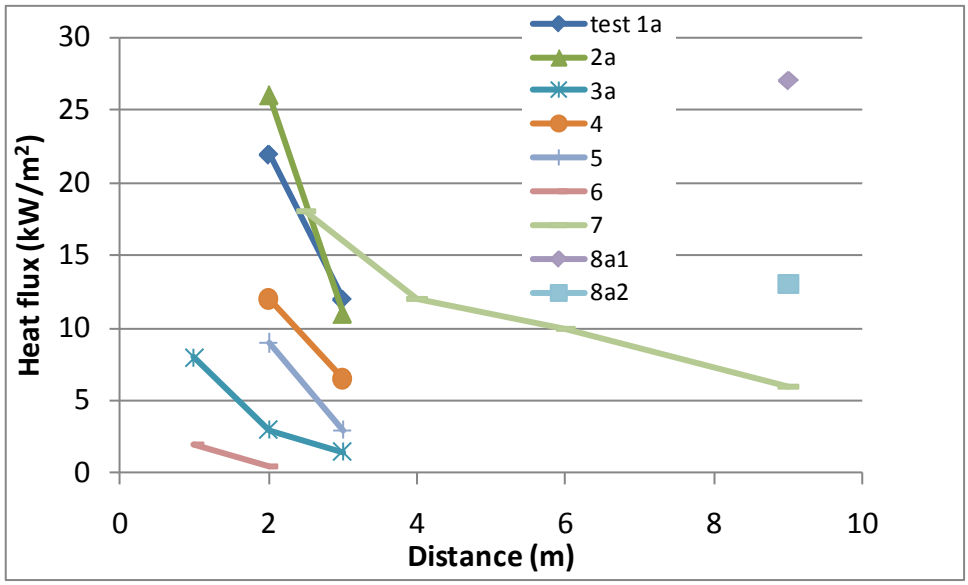

Figure 5.1. Summary of highest horizontal heat fluxes from the tests with a stainless steel braid covering the opening.

In general, very high temperatures are recorded within the flames but as soon as the object is outside the flame the temperatures are quite modest. For test 2b, where a jet flame is produced and directed straight against the vertical PT the temperatures just outside the flame (4 m) is well below 300 °C throughout the test with an incident radiant heat flux below 15 kW/m^2. The same behaviour is found for similar flames such as test 7 or 8a where the temperatures are also below 300-350 °C just outside the flame. Thus, the extension of the flame seems to be a very important factor for the thermal impact from these spills.

From the IR images the highest flame temperature are between 850 and 1000 °C. This is the temperature that is recorded by the IR cameras. However, this temperature is dependent on the emissivity of the flame. A flame with a very low emissivity exhibit a higher gas temperature . However, the flame emissivity depends on the flame thickness and optical depth coefficient, which is not known in these tests. Thus, a thinner flame has a lower emissivity and therefore radiates less than a thicker flame even if the actual gas temperature in the two cases are the same. Also, air entrainment in the flame reduces the emissivity.

The pressure dependence on the thermal impact on the surrounding differs between tests. In general, it can be noticed that the pressure correlated well with the incident heat flux for the cases where the opening was free, without the obstruction of the stainless steel braid. This is clearly noticed in test 2b, and 8b. For test 1b both the heat flux and pressure stayed rather constant throughout the test. The pressure had only minor effect for the incident heat flux in the tests where the braid covered the pipe or hose. Examples include tests 2a, 3a, 4 and 5. For some tests the dependence cannot be studied since both pressure and heat flux stayed constant. However, for the largest tests, such as 8a, a dependence on the pressure, even when using a braid, can again be noticed.

The smaller openings with a covering braid instead seemed to be controlled by other mechanisms. It can be noticed that many of the tests exhibited a stepwise increase of the incident heat flux. The first (and often largest) of these steps is associated with a decrease of temperature upstream of the opening. Thus, it is possible that the heat flux increases as the liquid methane reaches all the way to the opening. Both test 4 and 5 are examples of this. The additional steps can possibly originate in the liquid ejected from the opening finding a better path through the braid. This is indicated in the video recordings of many

of the tests. It can therefore be difficult to establish a “final” heat flux or flame length for a long time exposure. The tests without the braid can however be considered as an absolute maximum. However, the heat flux level in many tests actually indicated a stable level after the initial stepwise increases. In addition, the leakage from the 2" hoses are limited to a 5 minutes exposure since the flow from a tanker truck needs to be re-activated every 5^{th} minute.

From the IR images it can be noticed that no pockets of cold gas could be identified as long as the flame was active. Often LNG was dripping from the braid down to the ground but the pool (or often soaked insulation material) burned continuously and no evaporated cold methane could be seen moving away from the fire. However, for prolonged non-burning leaks clouds of methane could be formed and different clouds could separate from each other. Therefore, when ignition occurred not all methane needed to be ignited. However, the ignition of large assemblies of methane gas clouds is beyond the scope of this report.

6 Conclusions

This study describes a series of tests of leaking LNG pipes and hoses subject to a pilot flame. The leaks were of different sizes from 1 mm^2 holes to slots of 5 by 45 mm in 1" and 2" pipes/hoses. The tests mimic situations of leakage from hose from dispenser as well as from tanker truck providing LNG to the station. The damage scenario defined by the Swedish contingency agency is wear from the inside on the convoluted hose resulting in an opening with a length corresponding to 1/3 of the hose circumference and does not include other scenarios that potentially could be more hazardous.

The study shows that, for the pressure range studied here, ~10 bar, jet flames are not easily formed when a stainless steel braid was covering the opening. For the design scenarios of 1" and 2" hoses (test 4 and 7) the distance to an incident radiant heat flux of 15 kW/m^2 is 2 and 4 m, respectively. The equivalent distance to 5 kW/m^2 is 3 and 9 m, respectively. These levels are subject to a hose pressure of 10 bar. It is also shown that small changes in pressure have only minor effect on the thermal impact if an undamaged stainless steel braid is covering the opening. For scenarios without a braid pressure is a much more important factor for the spatial range of the thermal impact.

7 References

[1] SÄIFS 2000:4, Sprängämnesinspektionens föreskrifter (SÄIFS 2000:4) om cisterner, gasklockor, bergrum och rörledningar för brandfarlig gas, (2000) (in Swedish).

[2] Anvisningar för tankstationer, TSA 2010, Energigas Sverige, (2010) (in Swedish).

[3] Anvisningar för flytande naturgas, LNGA 2010, Energigas Sverige, (2010) (in Swedish).

[4] Raj P.K., Large LNG Fire Thermal Radiation – Modelling Issues & Hazard Criteria Revisited, Process Safety Progress, vol 24 (2005), no. 3, p 192-202.

[5] LNGFIREIII: A Thermal Radiation Model for LNG Fires. Gas Technology Institute, Des Plaines, USA (2004).

[6] Jo, Y.-D. and Ahn B.J. A simple model for the release rate of hazardous gas from a hole on high-pressure pipelines, Journal of Hazardous Materials A97 (2003) 31–46.

[7] Dong G. et al Evaluation of hazard range for the natural gas jet released from a high-pressure pipeline: A computational parametric study, Journal of Loss Prevention in the Process Industries 23 (2010) 522-530.

[8] Andersson B., Andersson P., Holmstedt G. and Särdqvist S., Naturgas, Säkerhetsnivå, Riskanalys, Lund (1994) (in Swedish).

[9] Phast, Det Norske Veritas, Hovik, Norway (2011).

[10] Brandlastberäkningar – Anvisningar för flytande metan på tankstationer. Study by Scandpower for Energigas Sverige (2012).

[11] Konsekvensutredning - för revidering (BFS 2011:26) av avsnitt 5 Brandskydd i Boverkets byggregler, BBR (BFS 2011:6) - för allmänt råd om analytisk dimensionering av byggnaders brandskydd (BFS 2011:27), Boverket (2011) (in Swedish).

[13] Drysdale D., An introduction to fire dynamics, Wiley (1985).

[13] Claesson A. Tolkning av begreppet betryggande i lagstiftning om brandfarliga och explosiva varor med fokus på betryggande avstånd, Lunds Tekniska Högskola (2011).

[14] Ingason H. and Wickström U., ”Measuring incident radiant heat flux using the plate thermometer” Fire Safety Journal (2007) vol. 42, pp. 161–166.

[15] Sjöström J. and Wickström U., ”Different types of plate thermometers for measuring incident radiant heat flux and adiabatic surface temperature” Proceedings of Interflam ’13 (2013) London.

[16] Sjöström J., Amon F., Appel G. and Persson H., “ETANKFIRE – Large scale burning behaviour of ethanol fuels”, (2013) SP report 2013:02.

8 Appendix – test results

8.1 Temperatures and pressures from all tests

Test 1a – 1”pipe with braid, 2*25mm hole, instrument setup 1

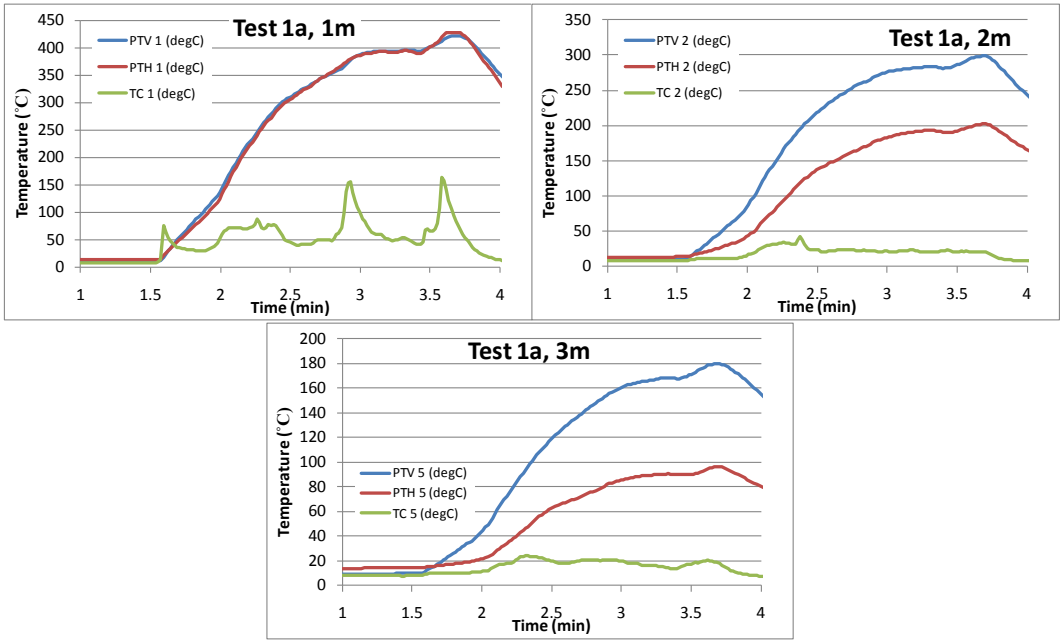

Figure 8.1. PT and TC temperatures along the main direction. V represents vertically oriented PT and H represents horizontally oriented PT.

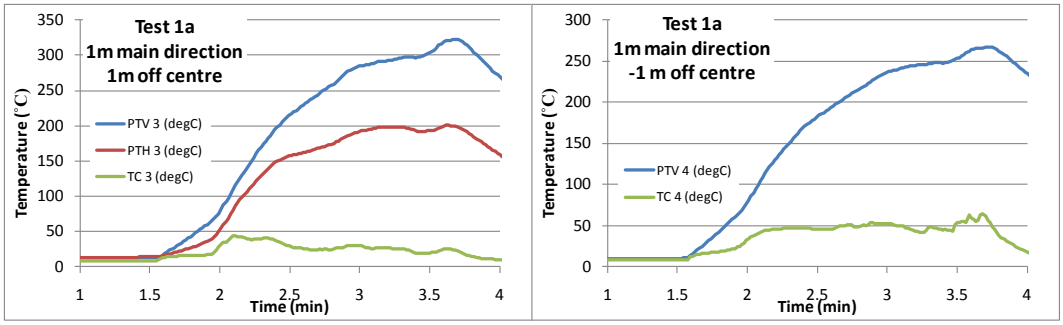

Figure 8.2. PT and TC temperatures in the off centre positions. (c.f. figure 3.2)

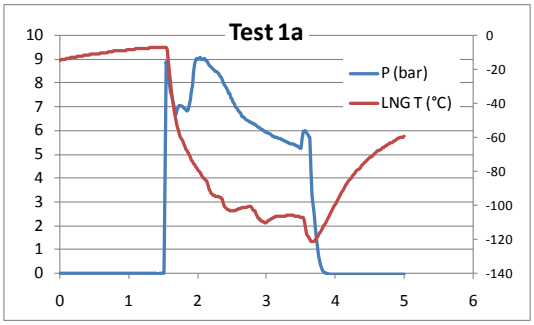

Figure 8.3. Pressure (left axis) and temperature (right axis) measurements in the pipe.

Test 1b - 1”pipe without braid, 2*25mm hole, instrument setup 2

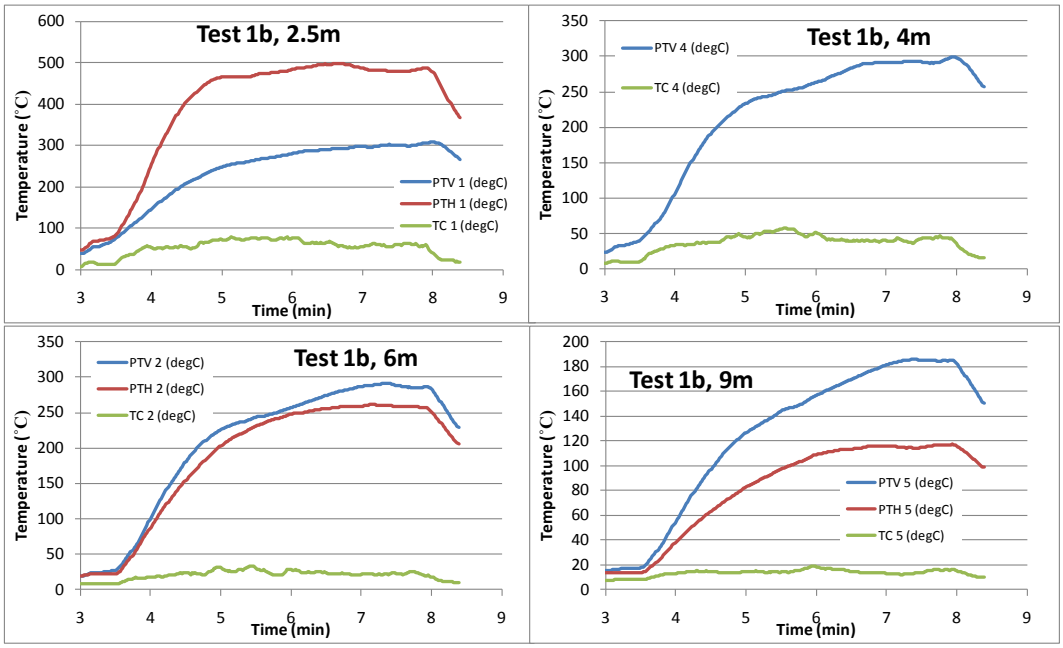

Figure 8.4. PT and TC temperatures along the main direction. V represents vertically oriented PT and H represents horizontally oriented PT.

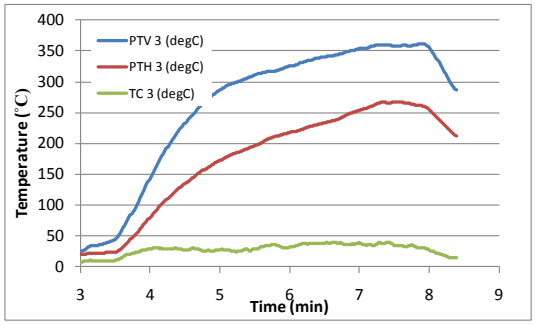

Figure 8.5. PT and TC temperatures in the off centre position. (c.f. figure 3.2)

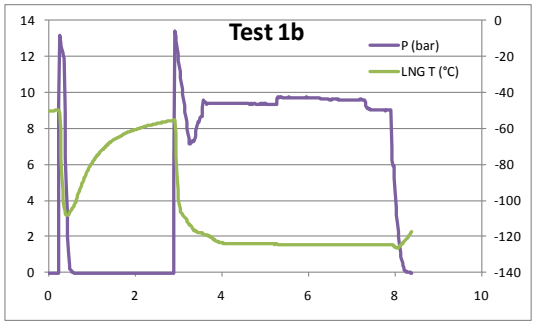

Figure 8.6. Pressure (left axis) and temperature (right axis) measurements in the pipe.

Test 2a – 1”pipe with braid, 1*10 mm hole, instrument setup 1

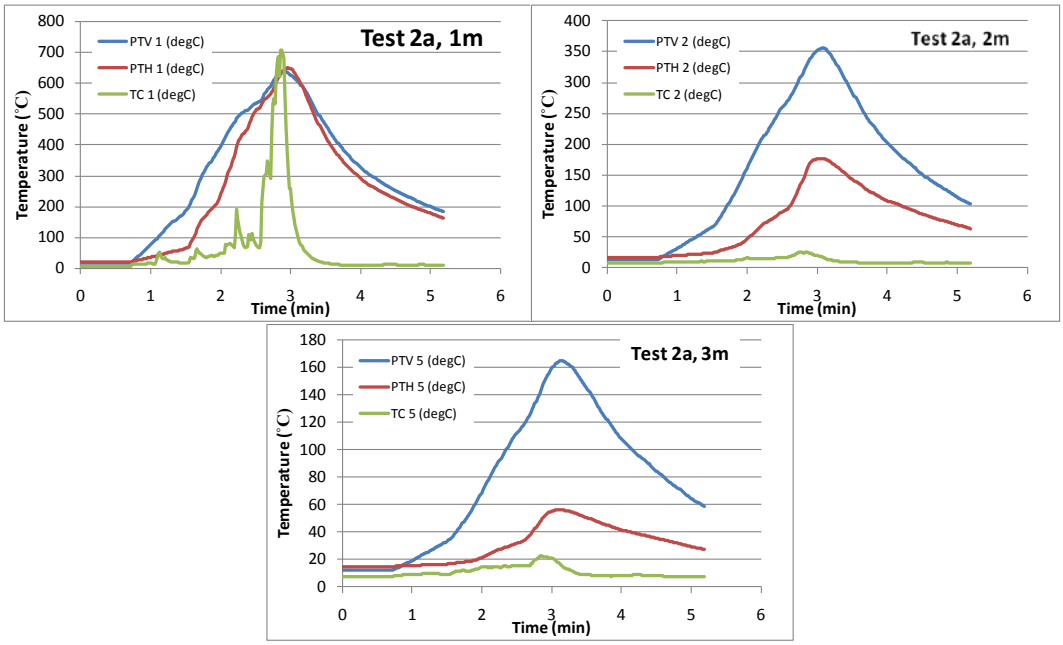

Figure 8.6. PT and TC temperatures along the main direction. V represents vertically oriented PT and H represents horizontally oriented PT.

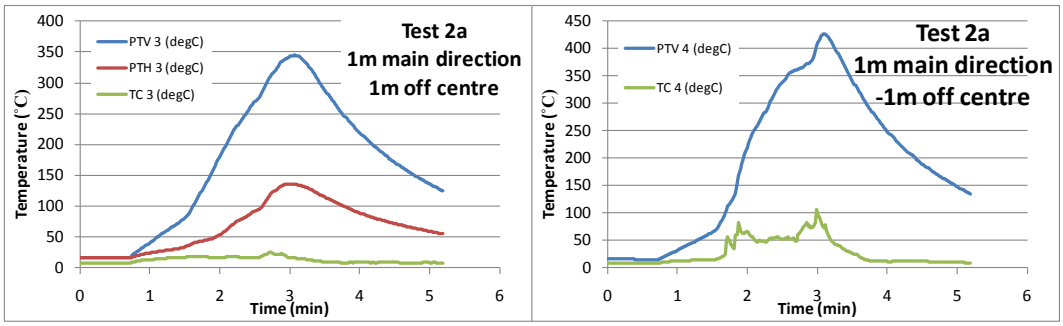

Figure 8.7. PT and TC temperatures in the off centre positions. (c.f. figure 3.2)

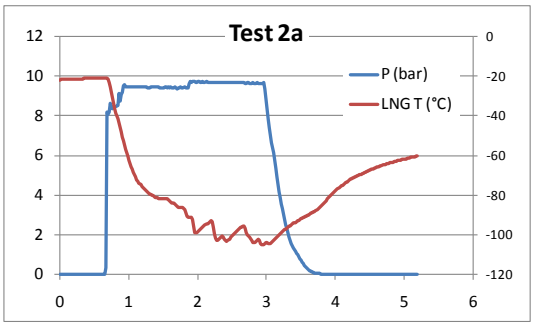

Figure 8.8. Pressure (left axis) and temperature (right axis) measurements in the pipe

Test 2b - 1”pipe without braid, 1*10 mm hole, instrument setup 2

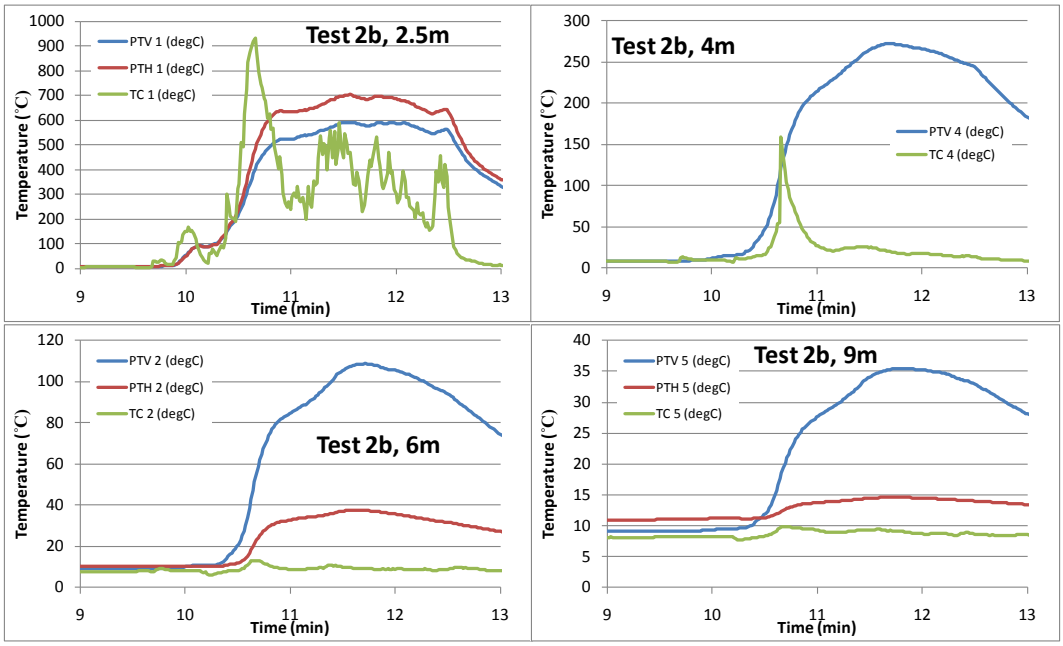

Figure 8.9. PT and TC temperatures along the main direction. V represents vertically oriented PT and H represents horizontally oriented PT.

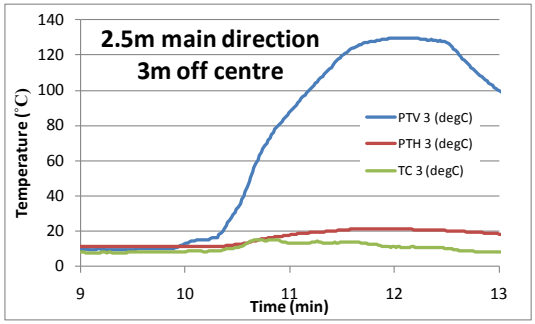

Figure 8.10. PT and TC temperatures in the off centre position. (c.f. figure 3.2)

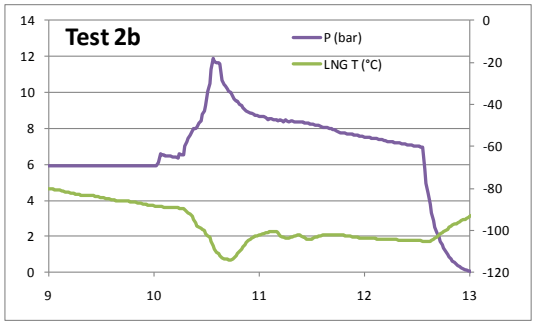

Figure 8.11. Pressure (left axis) and temperature (right axis) measurements in the pipe

Test 3a - 1”pipe with braid, 1*1 mm hole, instrument setup 1

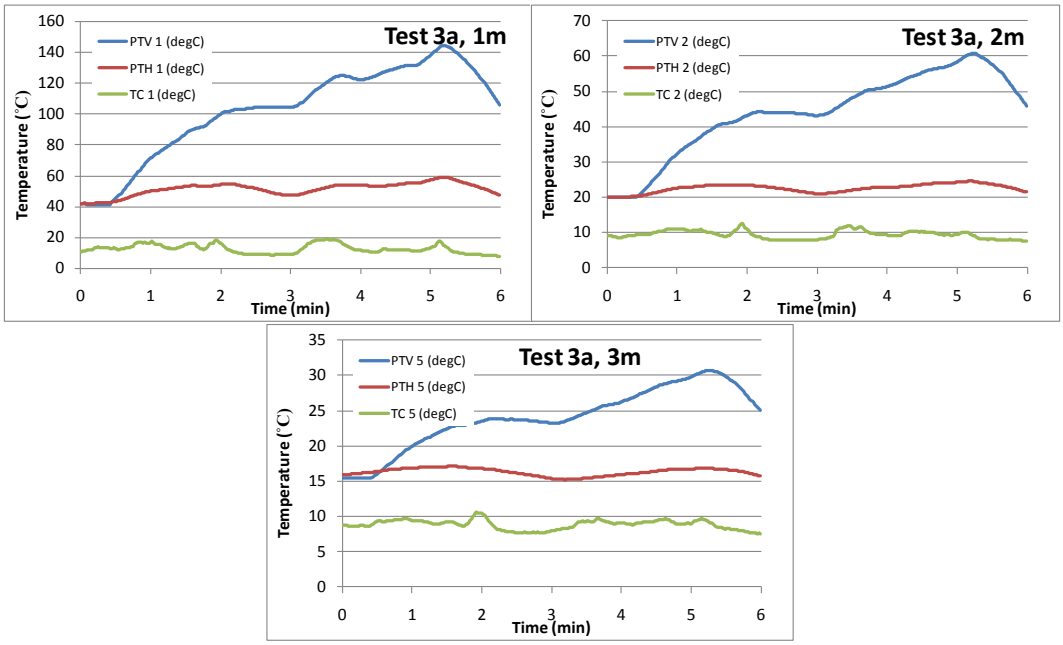

Figure 8.12. PT and TC temperatures along the main direction. V represents vertically oriented PT and H represents horizontally oriented PT

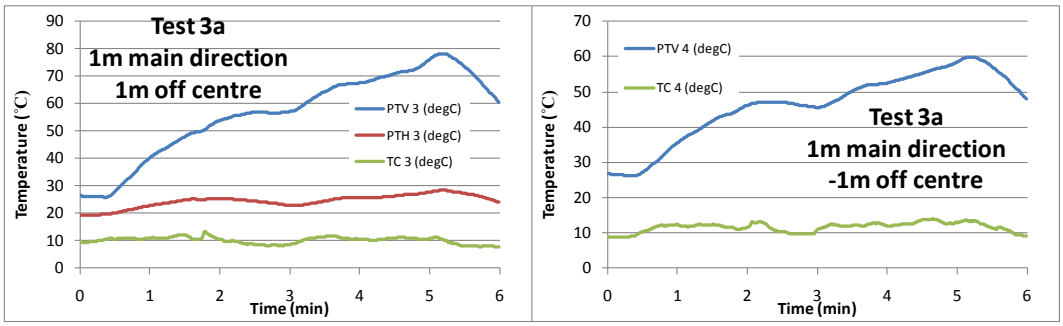

Figure 8.13. PT and TC temperatures in the off centre positions. (c.f. figure 3.2)

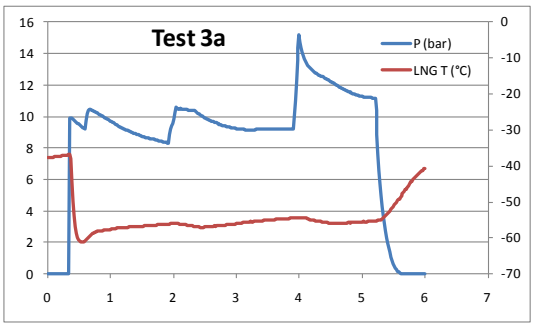

Figure 8.14. Pressure (left axis) and temperature (right axis) measurements in the pipe

Test 3b - 1”pipe without braid, 1*1 mm hole, instrument setup 1

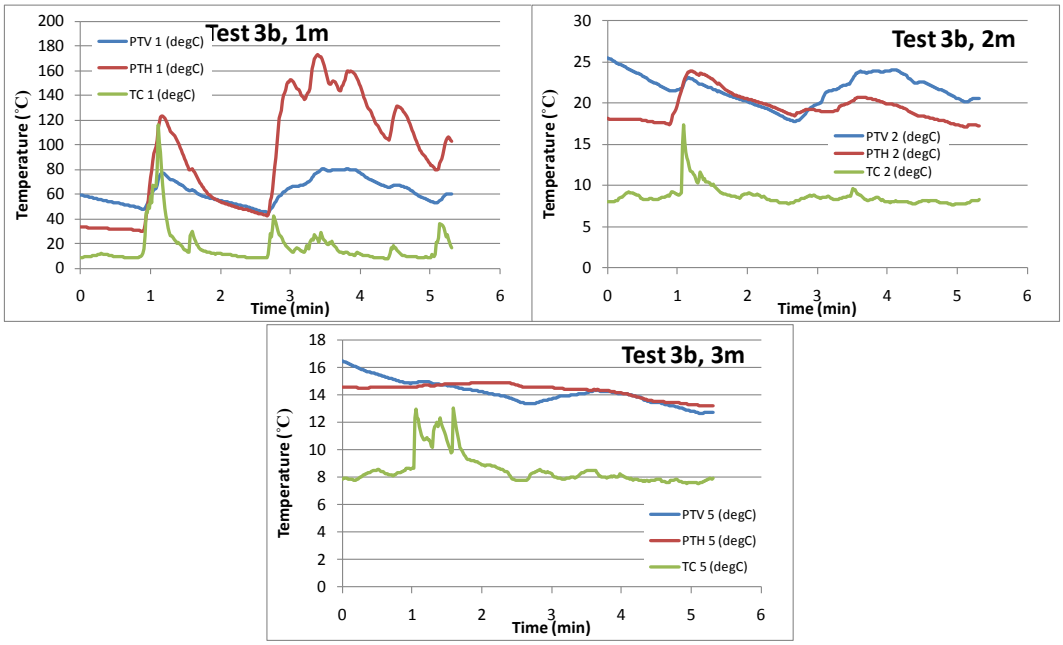

Figure 8.15.PT and TC temperatures along the main direction. V represents vertically oriented PT and H represents horizontally oriented PT

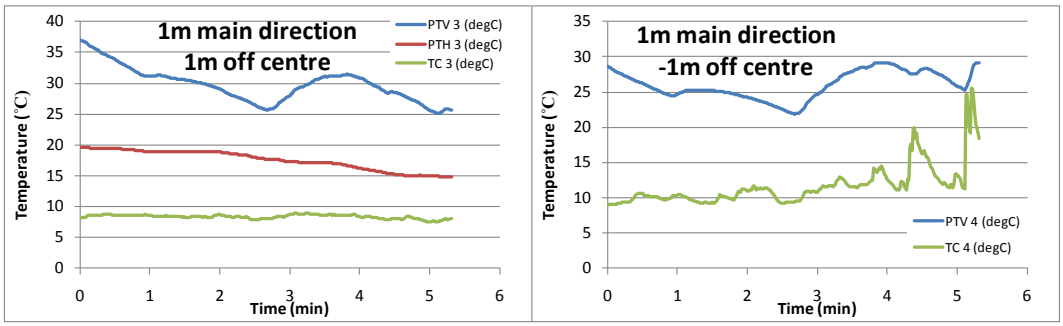

Figure 8.16. PT and TC temperatures in the off centre positions. (c.f. figure 3.2)

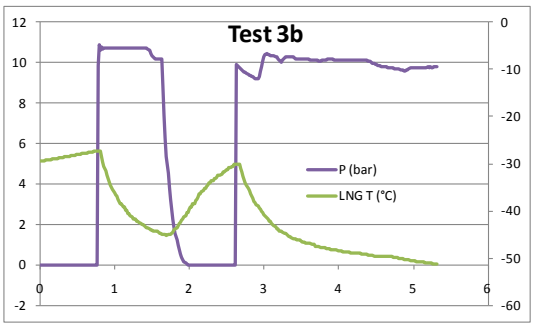

Figure 8.17. Pressure (left axis) and temperature (right axis) measurements in the pipe

Test 4 - 1”hose with braid, 1*mm hole 1/3 of circumference, instrument setup 1

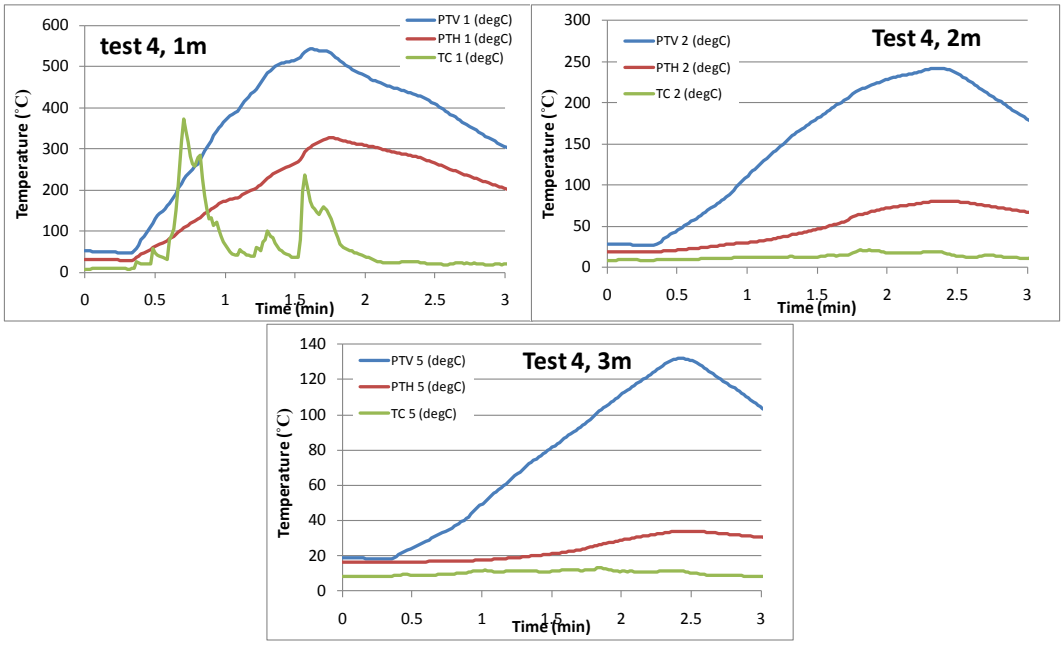

Figure 8.18. PT and TC temperatures along the main direction. V represents vertically oriented PT and H represents horizontally oriented PT

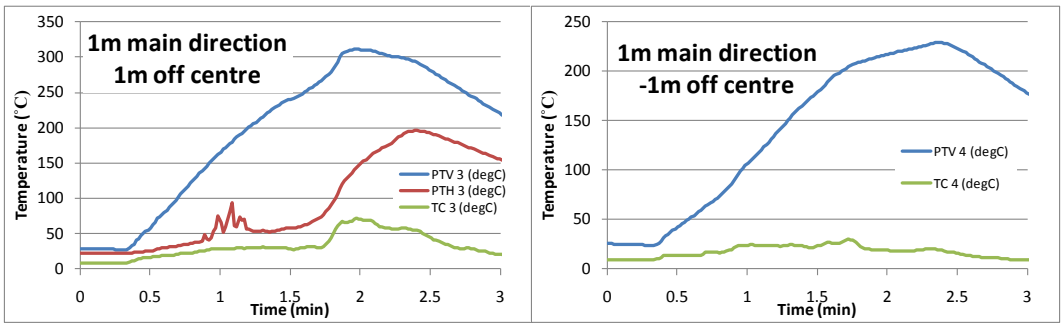

Figure 8.19. PT and TC temperatures in the off centre positions. (c.f. figure 3.2)

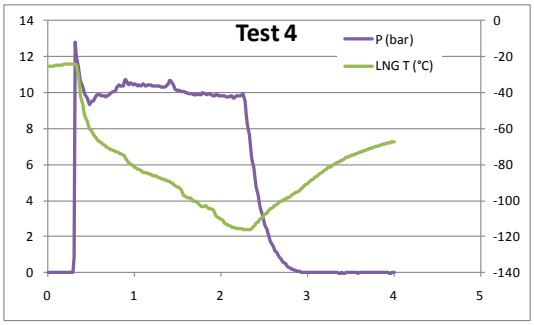

Figure 8.20. Pressure (left axis) and temperature (right axis) measurements in the pipe

Test 5 - 1”hose with braid, 1*5 mm hole, instrument setup 1

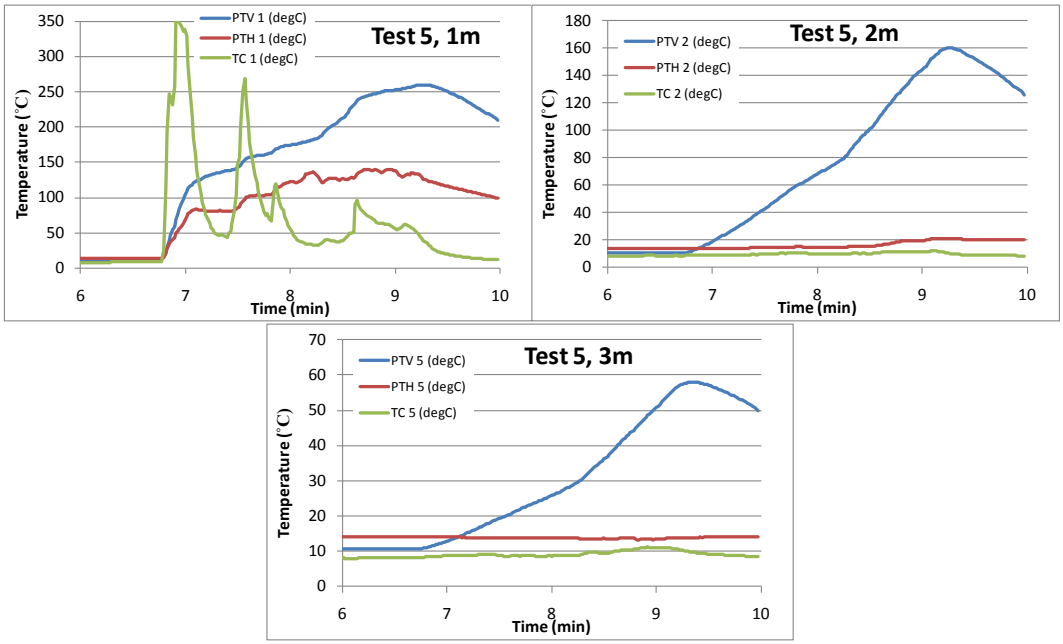

Figure 8.21. PT and TC temperatures along the main direction. V represents vertically oriented PT and H represents horizontally oriented PT

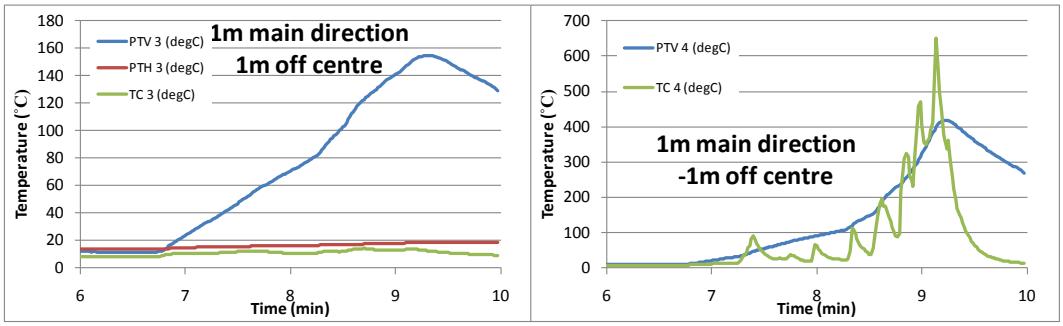

Figure 8.22. PT and TC temperatures in the off centre positions. (c.f. figure 3.2)

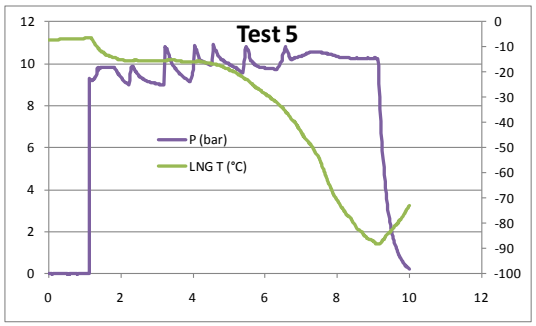

Figure 8.23. Pressure (left axis) and temperature (right axis) measurements in the pipe

Test 6 - 1”hose with braid, 1*1 mm hole, instrument setup 1

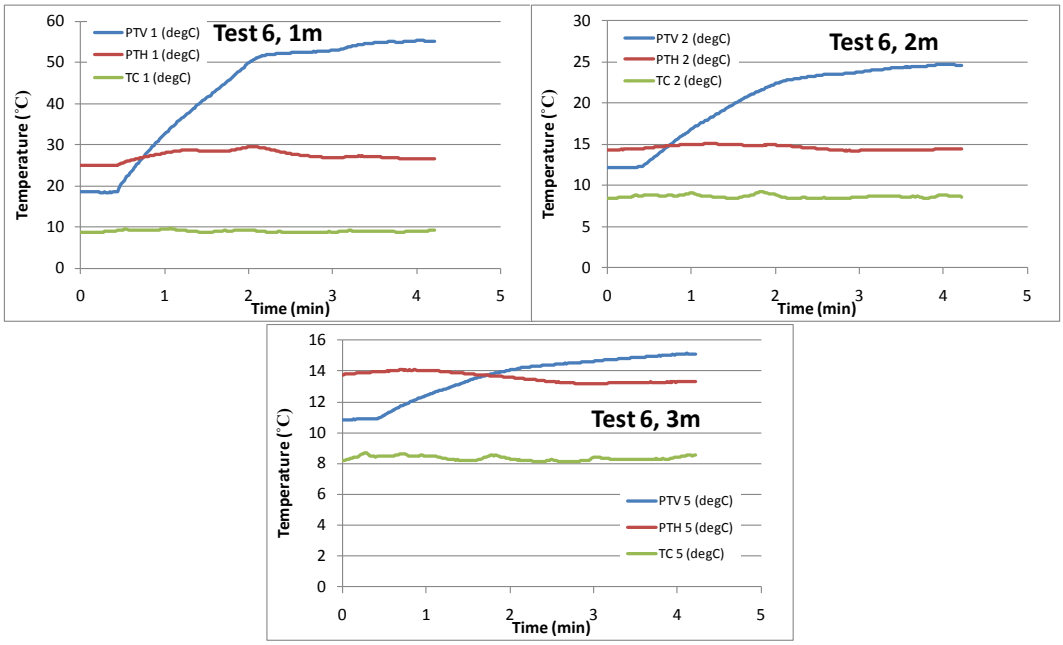

Figure 8.24. PT and TC temperatures along the main direction. V represents vertically oriented PT and H represents horizontally oriented PT

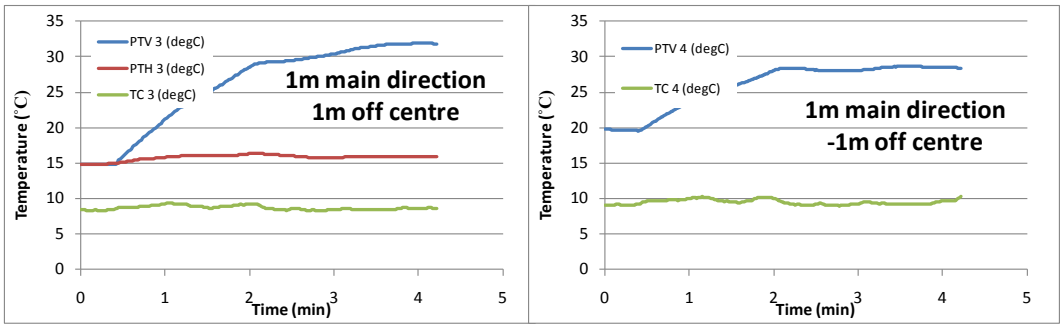

Figure 8.25. PT and TC temperatures in the off centre positions. (c.f. figure 3.2)

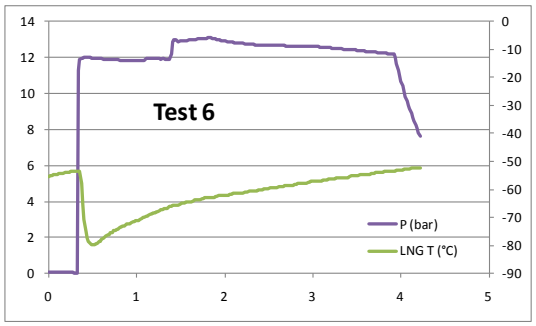

Figure 8.26. Pressure (left axis) and temperature (right axis) measurements in the pipe

Test 7 - 2”hose with braid, 1*mm hole 1/3 of circumference, instrument setup 2

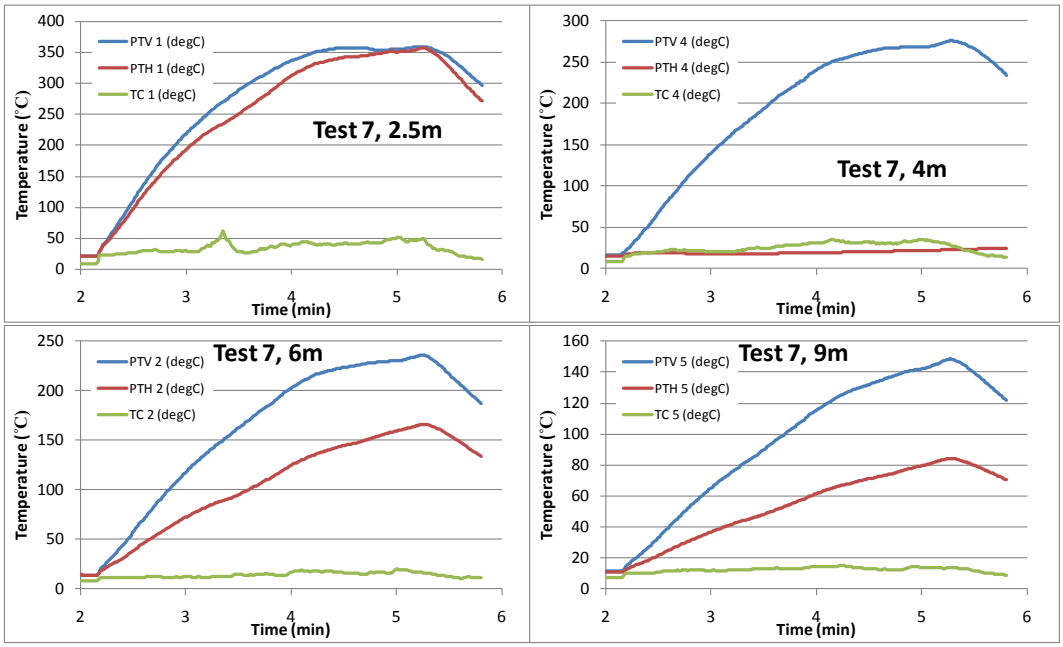

Figure 8.27. PT and TC temperatures along the main direction. V represents vertically oriented PT and H represents horizontally oriented PT

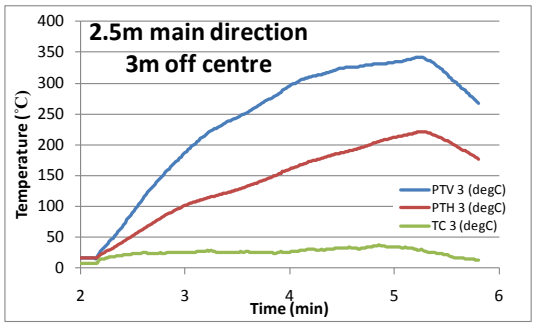

Figure 8.28. PT and TC temperatures in the off centre position. (c.f. figure 3.2)

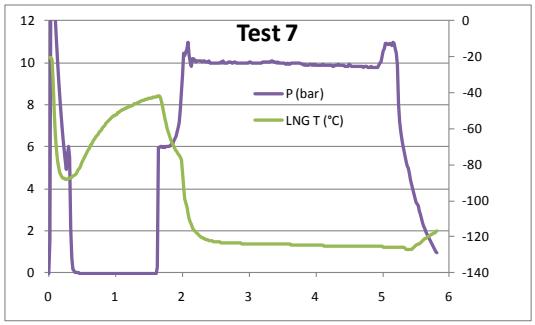

Figure 8.29. Pressure (left axis) and temperature (right axis) measurements in the pipe

Test 8a, first run (not immediately ignited) - 2”pipe with braid, 5*45 mm hole, instrument setup 2

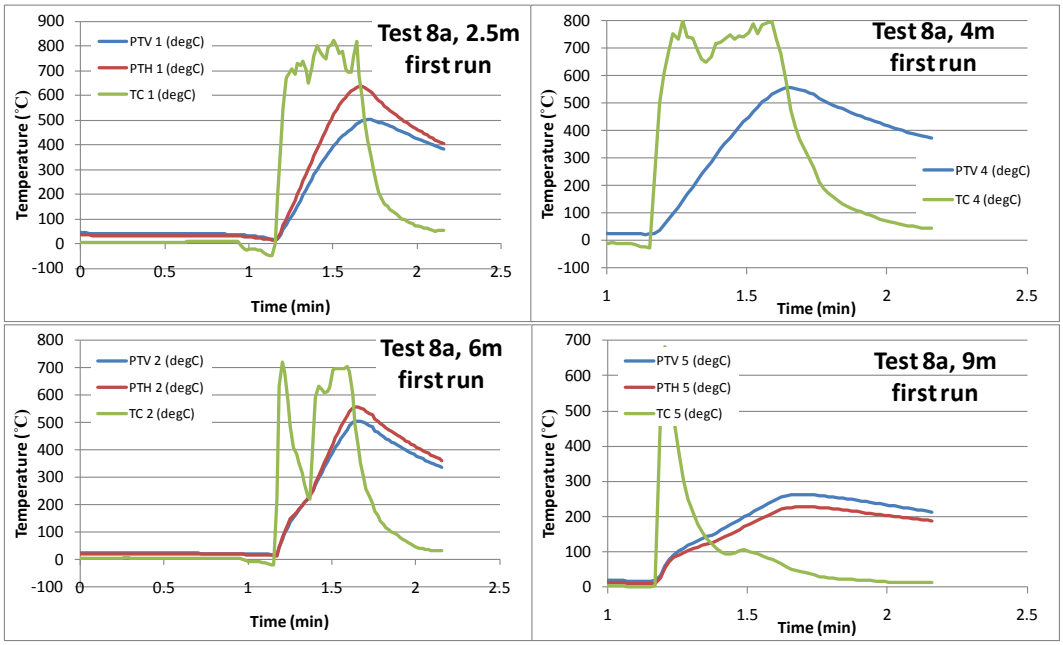

Figure 8.30. PT and TC temperatures along the main direction. V represents vertically oriented PT and H represents horizontally oriented PT

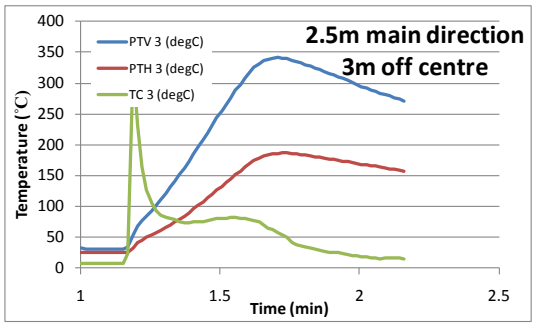

Figure 8.31. PT and TC temperatures in the off centre position. (c.f. figure 3.2)

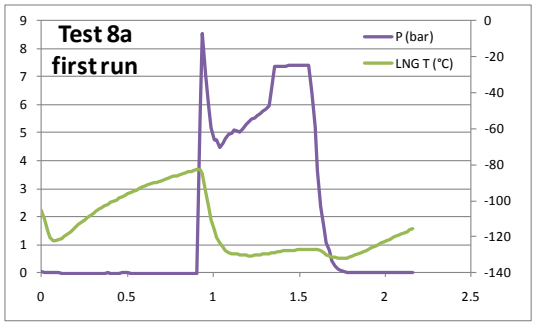

Figure 8.32. Pressure (left axis) and temperature (right axis) measurements in the pipe

Test 8a, second run (ignited immediately) - 2”pipe with braid, 5*45 mm hole, instrument setup 2

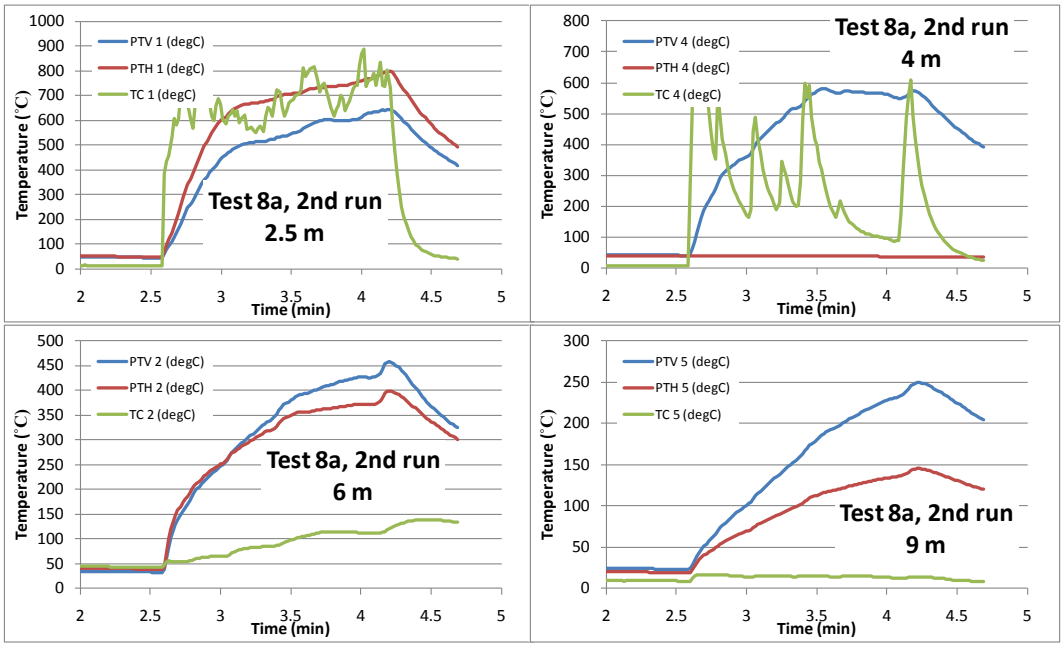

Figure 8.33. PT and TC temperatures along the main direction. V represents vertically oriented PT and H represents horizontally oriented PT.

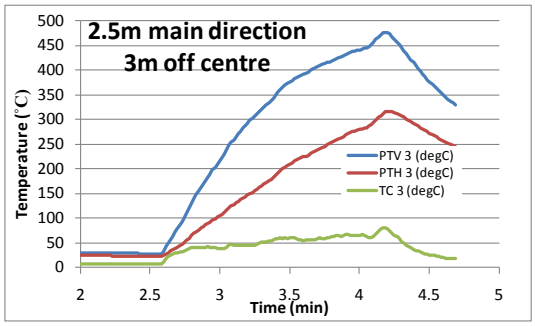

Figure 8.34. PT and TC temperatures in the off centre position. (c.f. figure 3.2).

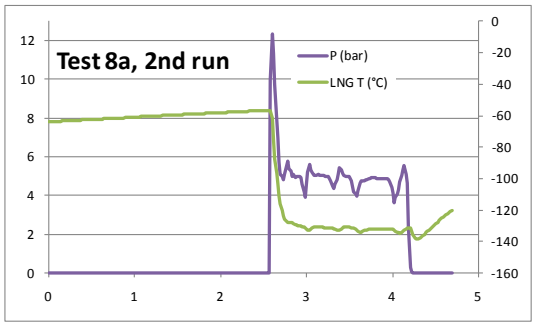

Figure 8.35. Pressure (left axis) and temperature (right axis) measurements in the pipe.

Test 8b - 2”pipe without braid, 5*45 mm hole, instrument setup 2

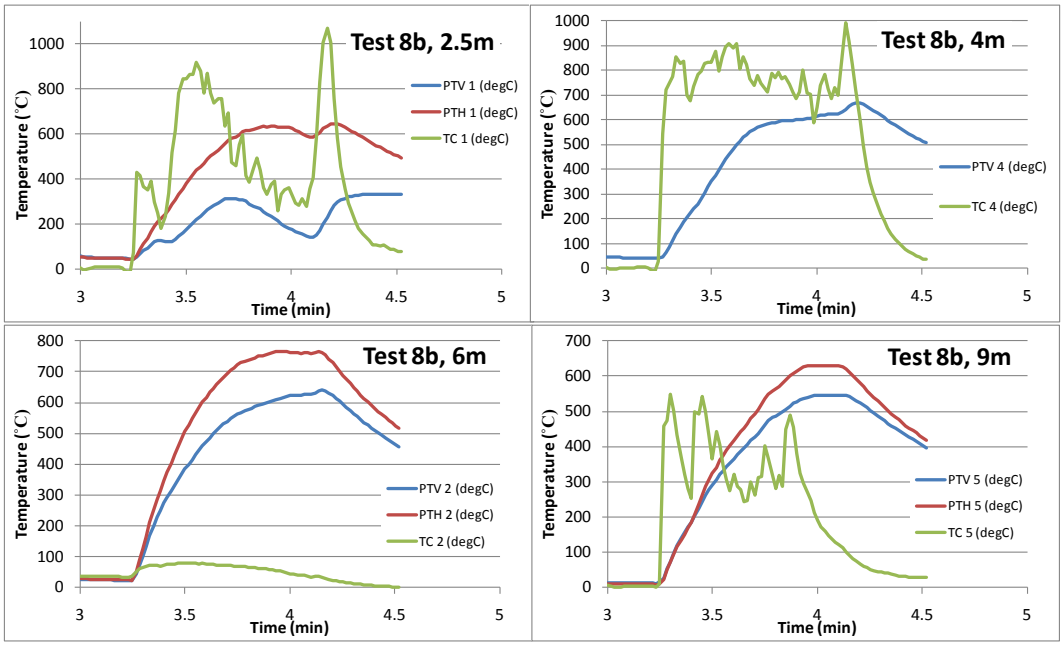

Figure 8.36. PT and TC temperatures along the main direction. V represents vertically oriented PT and H represents horizontally oriented PT.

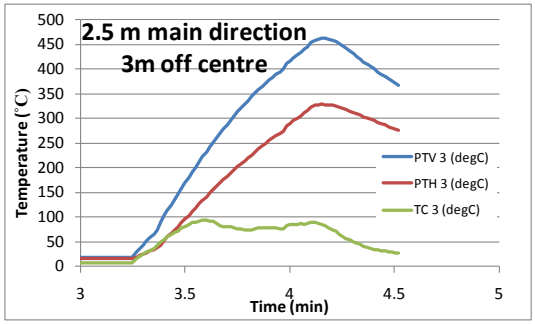

Figure 8.37. PT and TC temperatures in the off centre position. (c.f. figure 3.2).

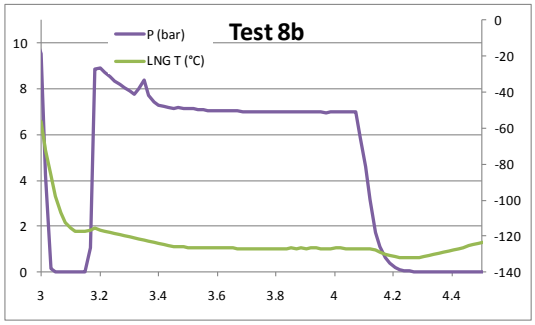

Figure 8.38. Pressure (left axis) and temperature (right axis) measurements in the pipe.

8.2 Calculated heat fluxes from all tests

The calculated heat fluxes to all PT are presented for all tests below. The fluxes are calculated using h = 15 kW/m^2 and the measured gas temperature behind each PT. Surface emissivity is set to 0.85. In each figure, qV and qH represent incident flux to the vertically and horizontally oriented PT, respectively.

Test 1a – 1"pipe with braid, 2*25mm hole, instrument setup 1

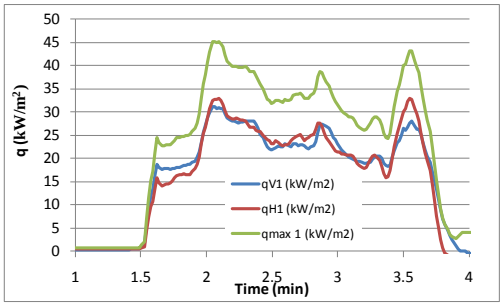

1 m along main direction

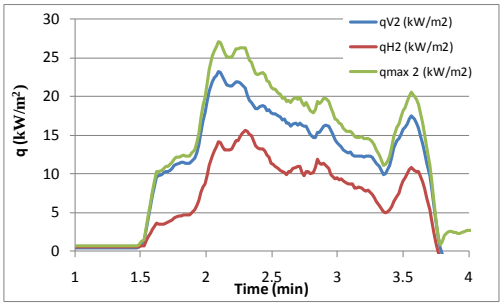

2 m along main direction

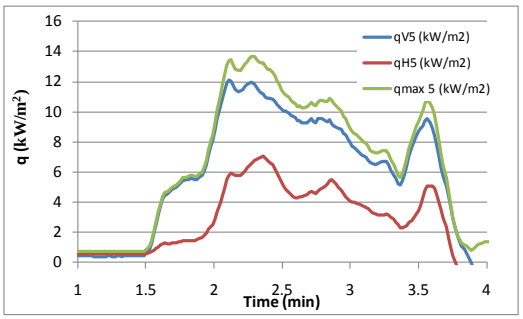

3 m along main direction

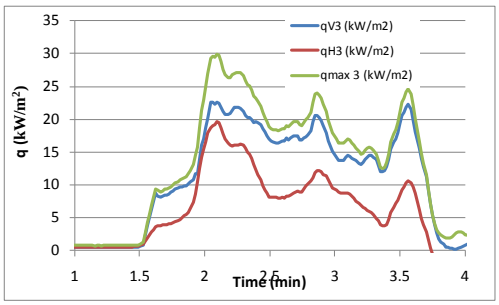

1 m along main direction, 1 m off centre.

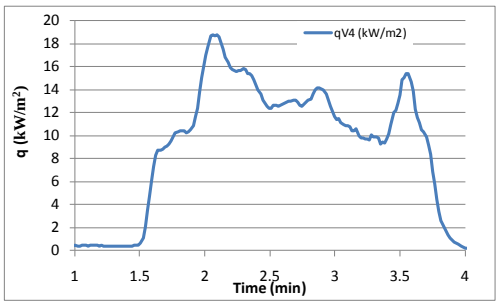

2 m along main direction,-1 m off centre.

Test 1b - 1”pipe without braid, 2*25mm hole, instrument setup 2

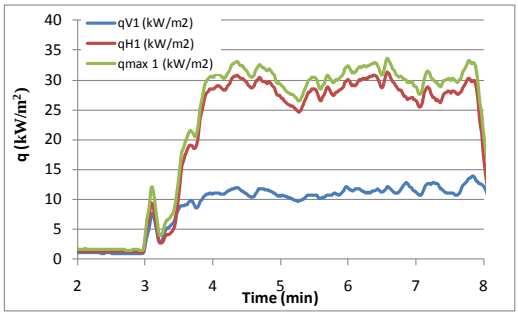

2.5 m along main direction

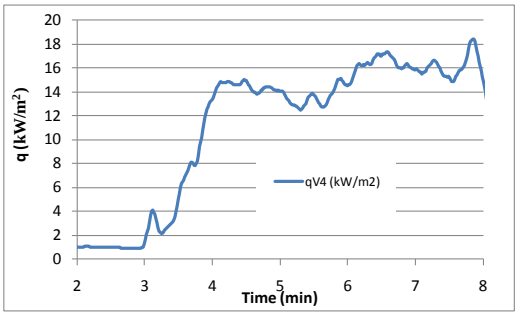

4 m along main direction

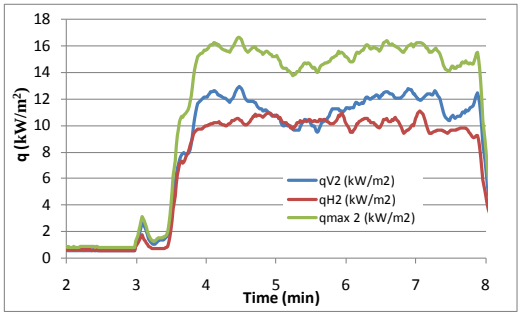

6 m along main direction

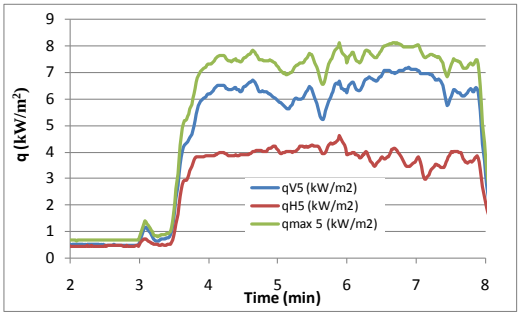

9 m along main direction

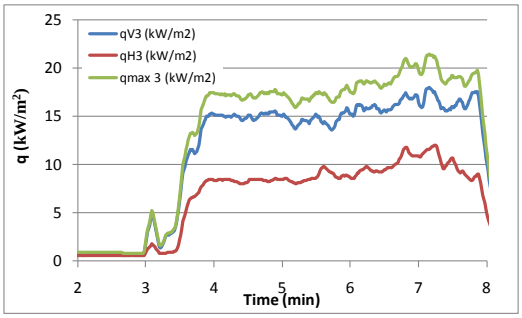

2.5 m along main direction, 3 m off centre.

Test 2a – 1”pipe with braid, 1*10 mm hole, instrument setup 1

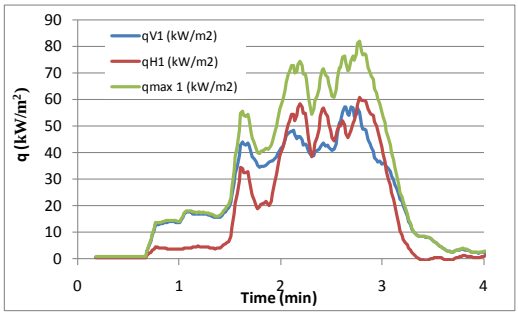

1 m along main direction

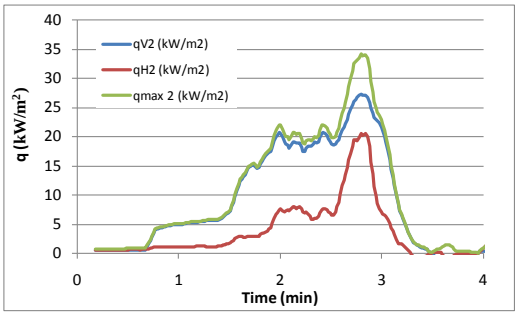

2 m along main direction

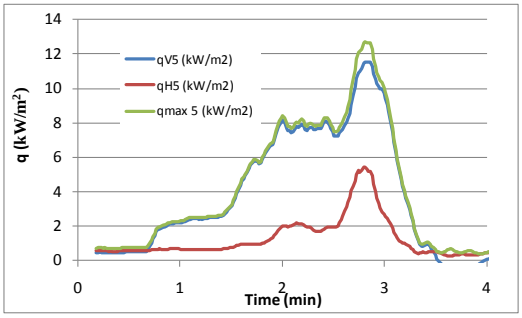

3 m along main direction

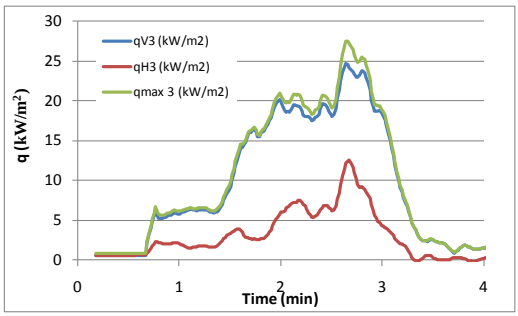

1 m along main direction, 1 m off centre.

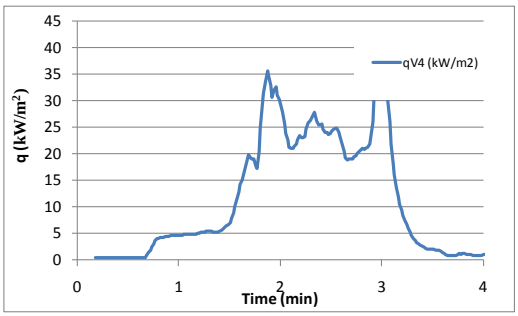

2 m along main direction,-1 m off centre.

Test 2b - 1”pipe without braid, 1*10 mm hole, instrument setup 2

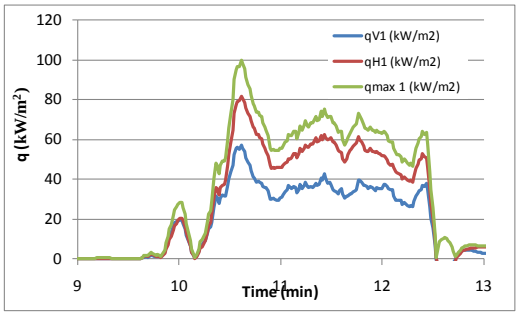

2.5 m along main direction

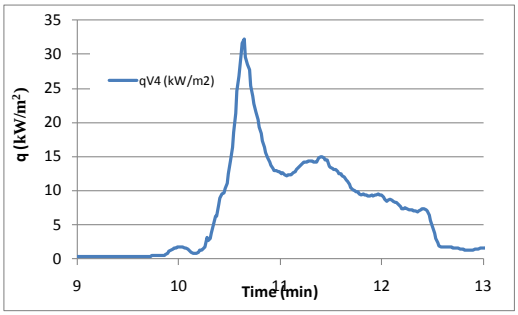

4 m along main direction

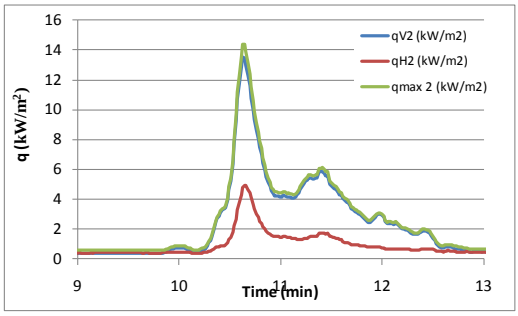

6 m along main direction

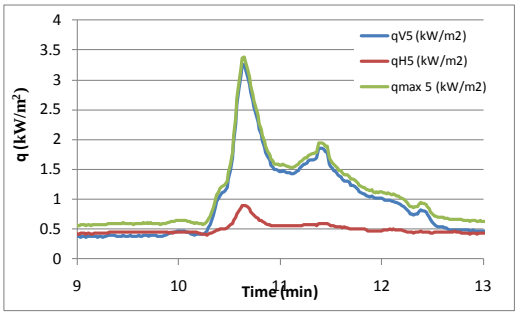

9 m along main direction

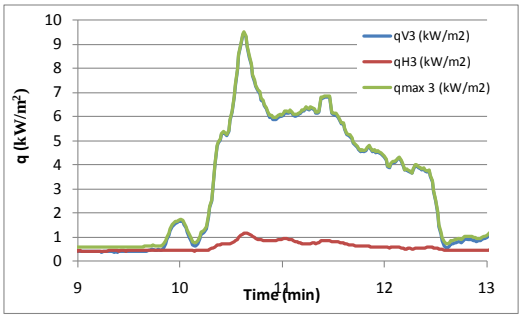

2.5 m along main direction, 3 m off centre.

Test 3a - 1”pipe with braid, 1*1 mm hole, instrument setup 1

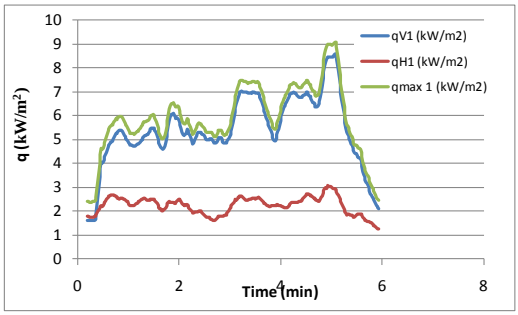

1 m along main direction

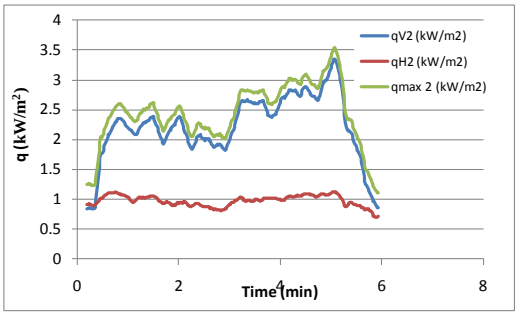

2 m along main direction

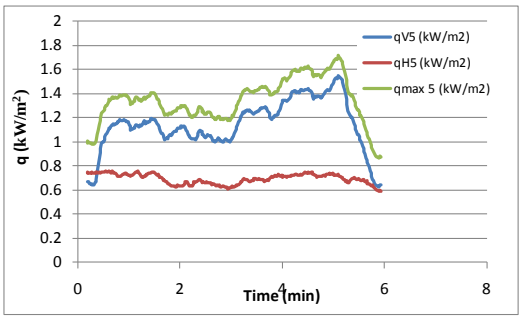

3 m along main direction

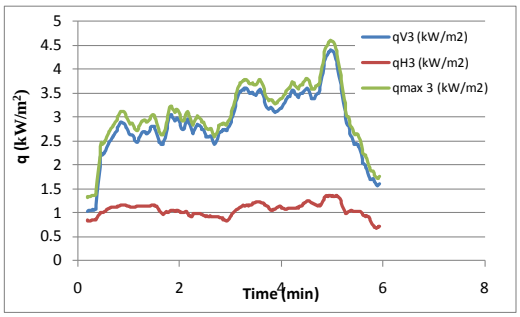

1 m along main direction, 1 m off centre.

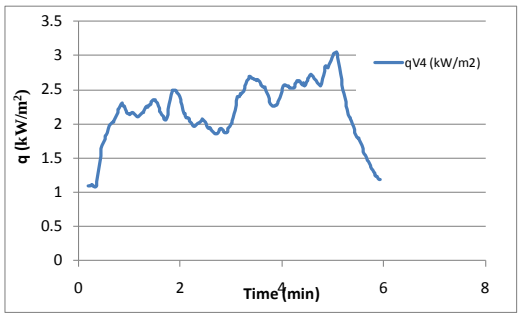

2 m along main direction,-1 m off centre.

Test 3b - 1”pipe without braid, 1*1 mm hole, instrument setup 1

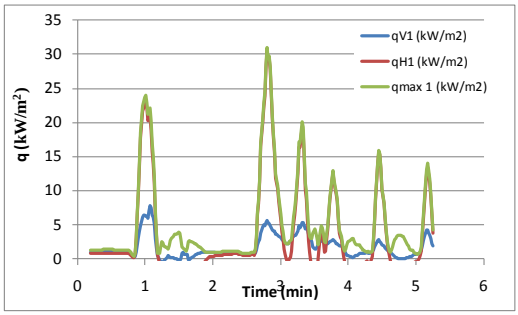

1 m along main direction

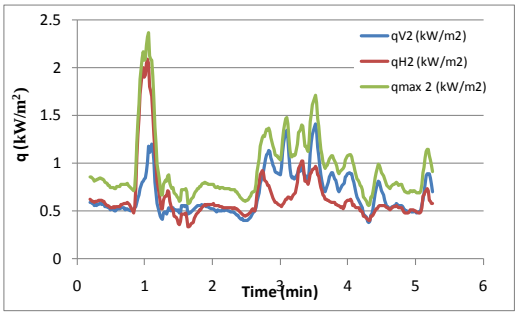

2 m along main direction

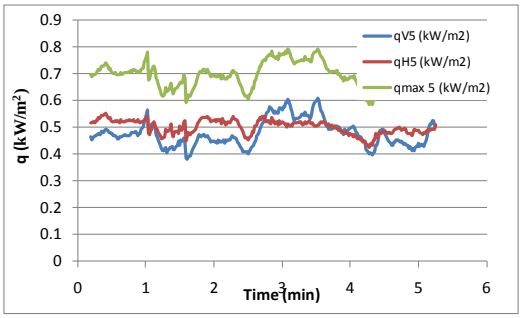

3 m along main direction

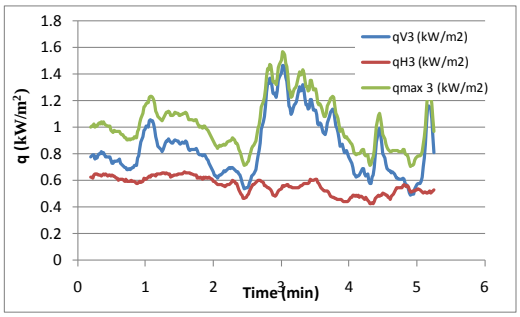

1 m along main direction, 1 m off centre.

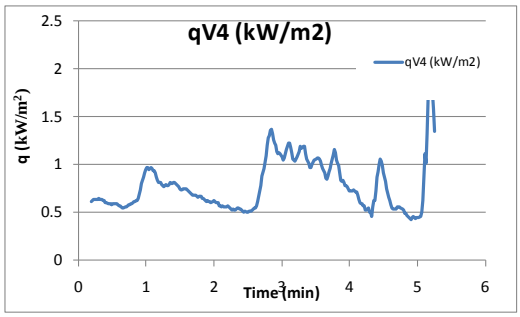

2 m along main direction,-1 m off centre.

Test 4 - 1”hose with braid, 1*mm hole 1/3 of circumference, instrument setup 1

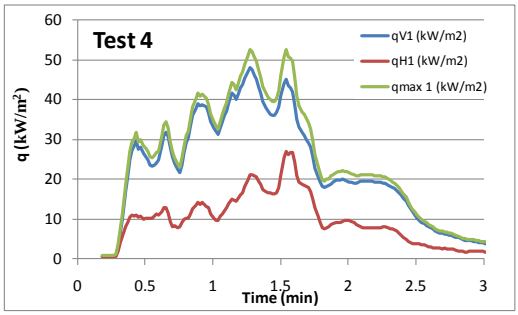

1 m along main direction

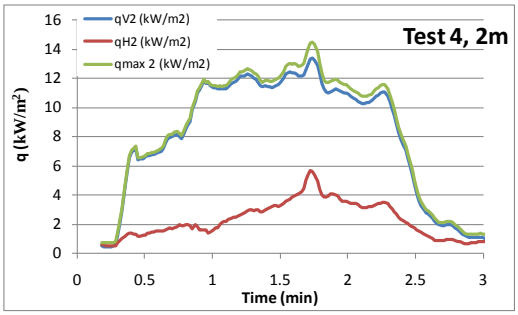

2 m along main direction

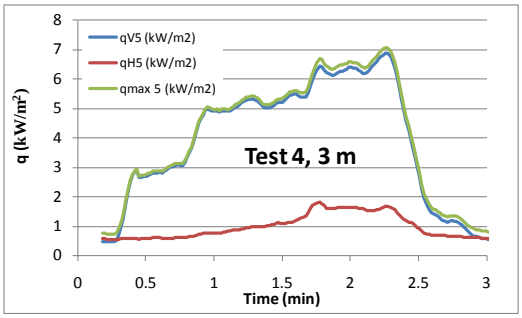

3 m along main direction

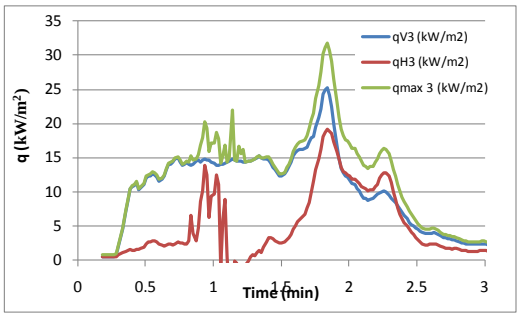

1 m along main direction, 1 m off centre.

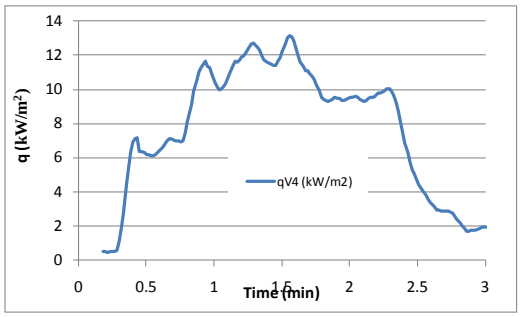

2 m along main direction,-1 m off centre.

Test 5 - 1”hose with braid, 1*5 mm hole, instrument setup 1

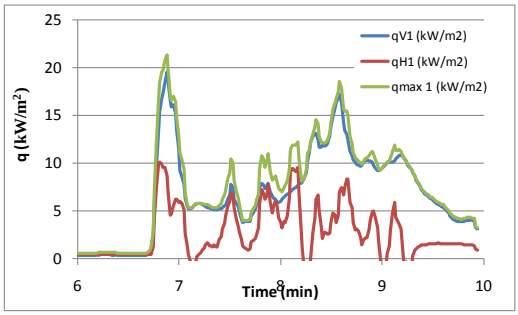

1 m along main direction

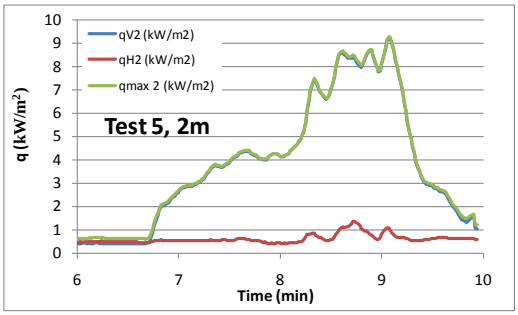

2 m along main direction

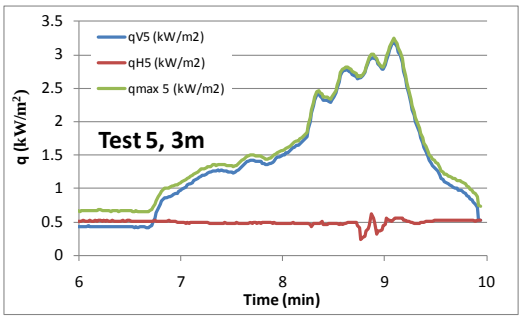

3 m along main direction

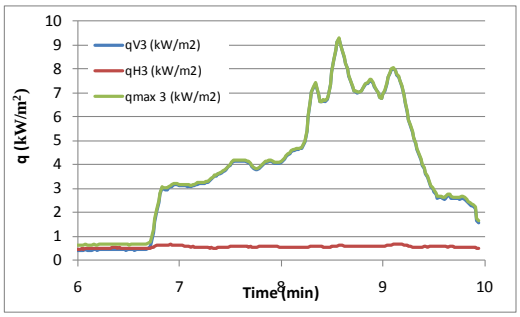

1 m along main direction, 1 m off centre.

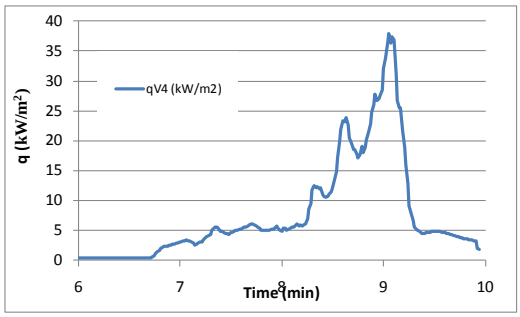

2 m along main direction,-1 m off centre.

Test 6 - 1”hose with braid, 1*1 mm hole, instrument setup 1

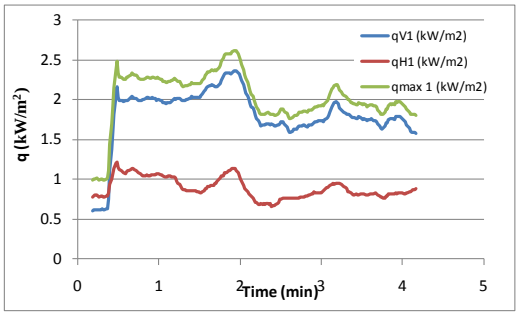

1 m along main direction

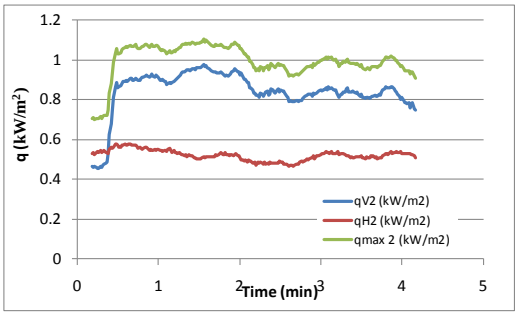

2 m along main direction

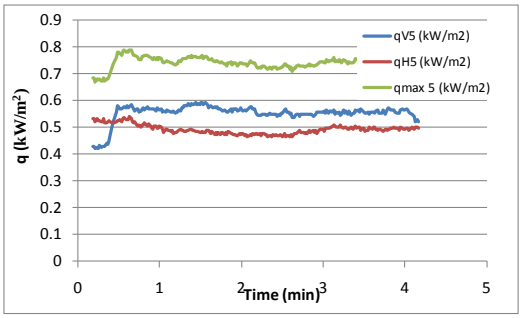

3 m along main direction

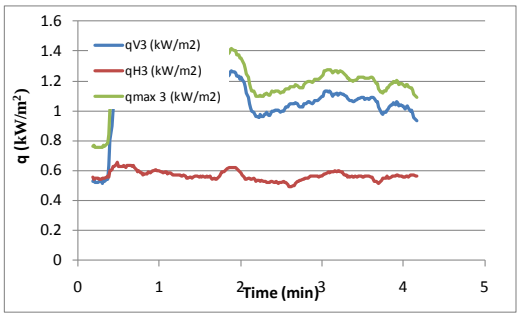

1 m along main direction, 1 m off centre.

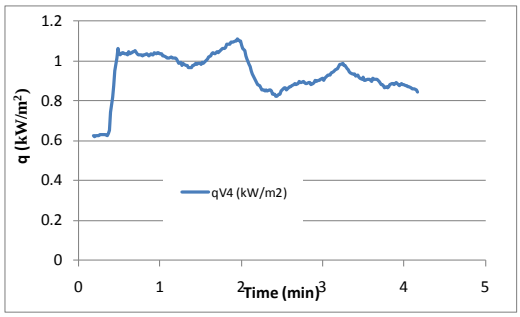

2 m along main direction,-1 m off centre.

Test 7 - 2”hose with braid, 1*mm hole 1/3 of circumference, instrument setup 2

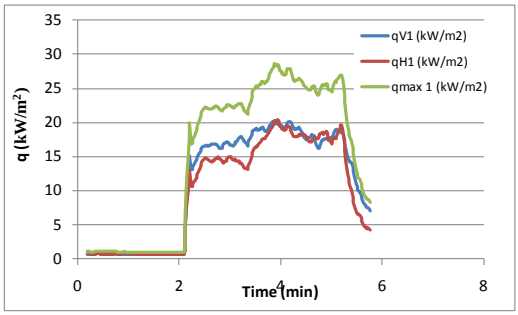

2.5 m along main direction

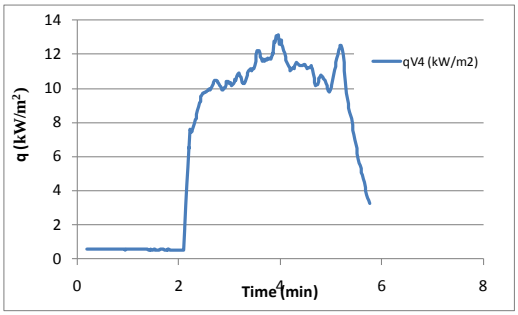

4 m along main direction

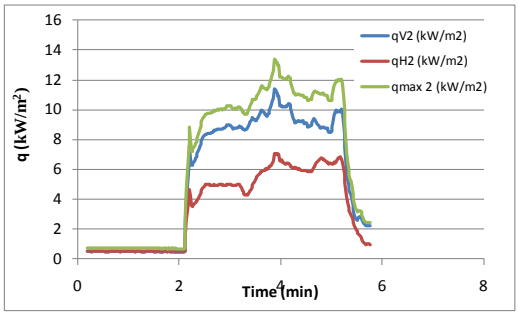

6 m along main direction

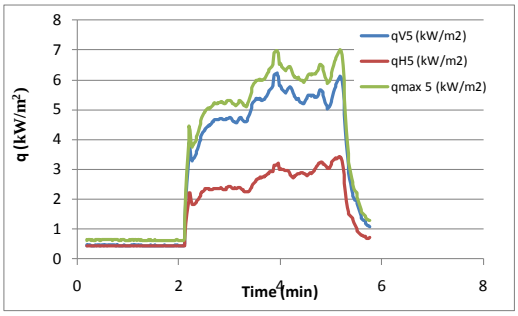

9 m along main direction

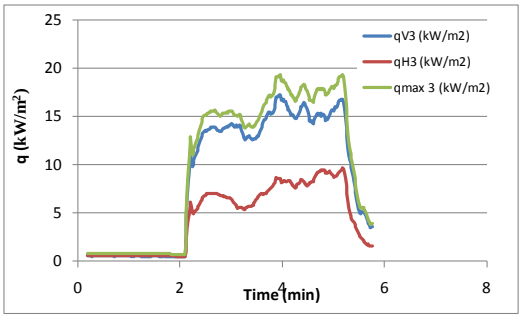

2.5 m along main direction, 3 m off centre.

Test 8a 2nd run - 2”pipe with braid, 5*45 mm hole, instrument setup 2

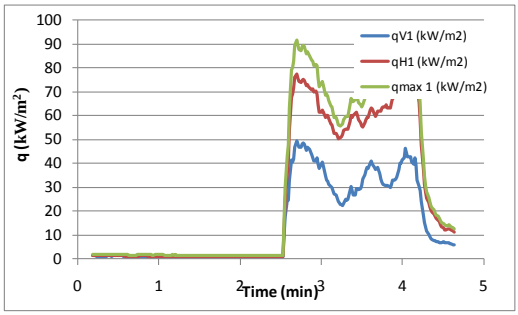

2.5 m along main direction

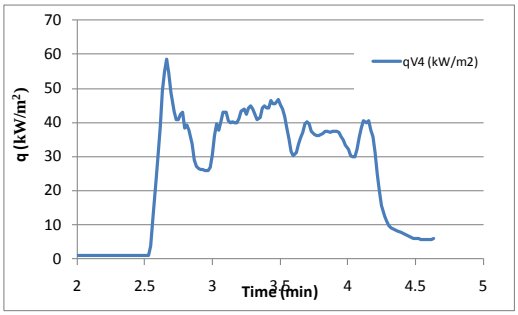

4 m along main direction

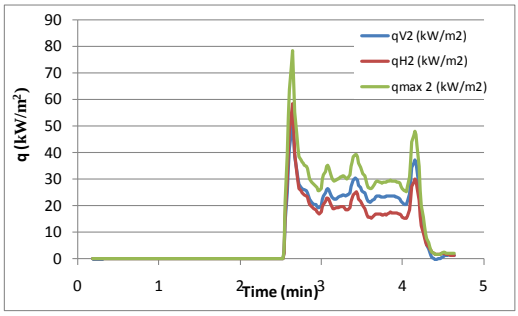

6 m along main direction

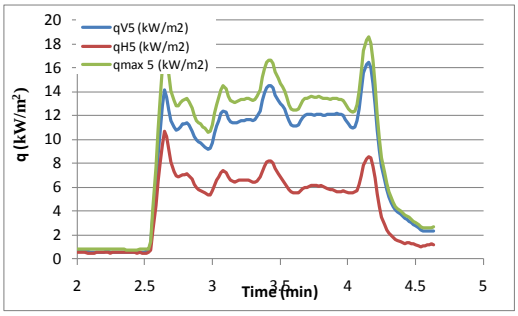

9 m along main direction

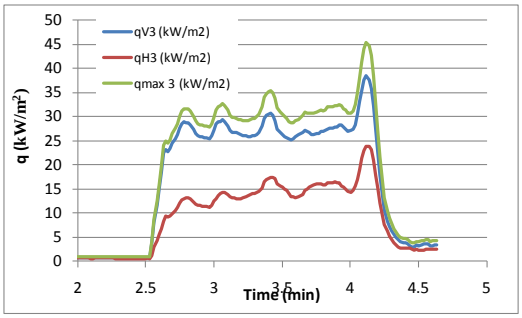

2.5 m along main direction, 3 m off centre.

Test 8b - 2”pipe without braid, 5*45 mm hole, instrument setup 2

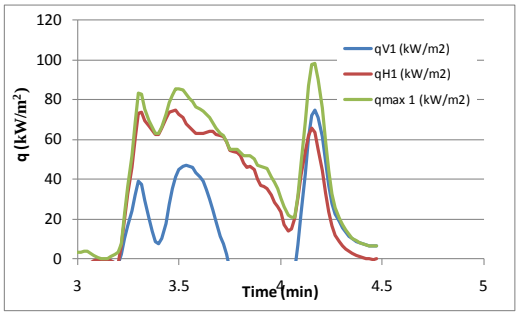

2.5 m along main direction

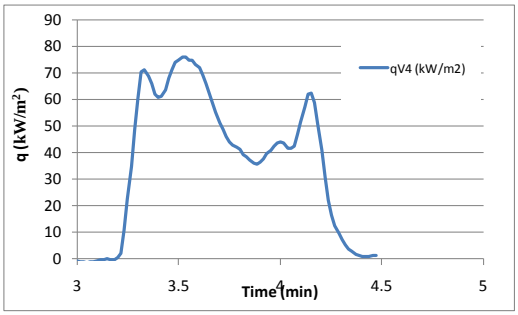

4 m along main direction

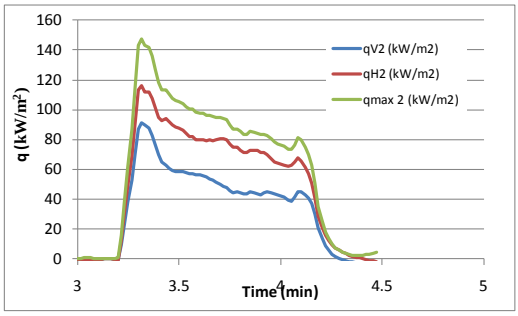

6 m along main direction

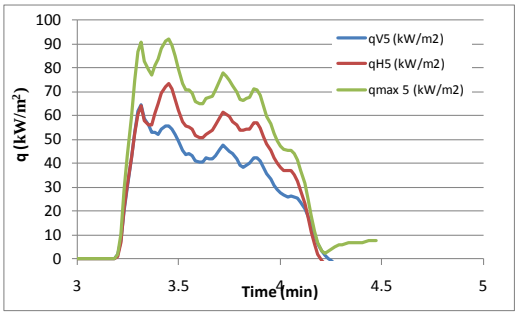

9 m along main direction

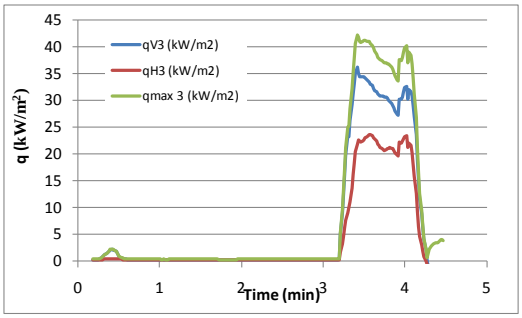

2.5 m along main direction, 3 m off centre.

8.3 Sensitivity study of calculated heat fluxes

The incident radiant heat flux calculated from the PT temperatures depends on a number of assumptions. These are, apart from the already calibrated correction parameters (Sjöström 2013) assumptions of the adjacent gas temperatures, the convective heat transfer coefficient and the surface emissivity of the PT. In this sensitivity assessment the vertical PT at 2 m from test 4 and 3 m from test 5 are used as case studies. These represent one high and one low radiant heat level. The parameters are varied beyond the plausible values for this study. In next section the PT calculations are compared with the HFM, which are widely recognised as a good measure of the incident radiant heat flux.

The adjacent gas temperature is in the calculations set to the value of the TC, placed just behind the PT. Since the TC is very small, it is highly influenced by the gas temperature and the placement behind the PT means that it is likely to be shaded from radiation originating from the flames. The difference between $\dot{q}''_{inc}$ calculated using the measured gas temperature a fixed gas temperature of 5 °C is shown below.

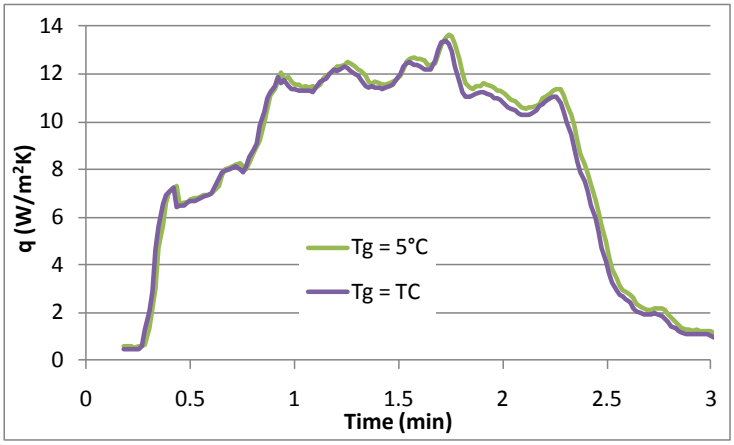

Difference in incident radiant heat flux for test 4, if gas temperature is taken to be the one measured by the TC or fixed to 5°C.

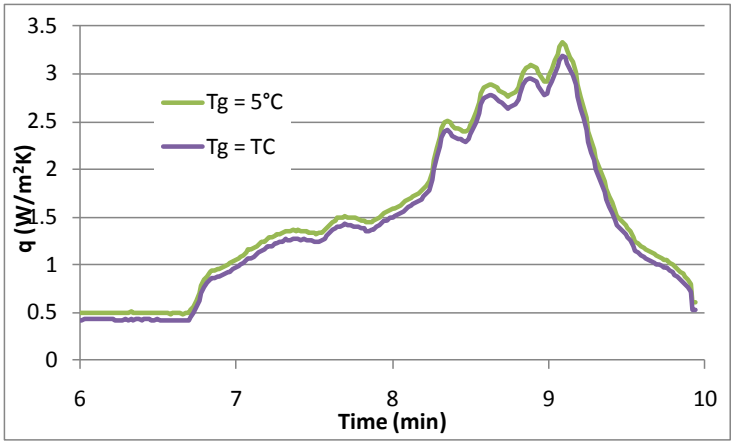

Difference in incident radiant heat flux for test 5, if gas temperature is taken to be the one measured by the TC or fixed to 5°C.

The convective heat transfer coefficient is set to 15 W/m^{2}K in all calculations. However, if the gas flows over the surface with a speed of 7 m/s the flow can be considered as

forced and the coefficient h = 30 W/m^{2}K. For no forced convection the coefficient h = 10 W/m^{2}K. The influence of this is shown below.

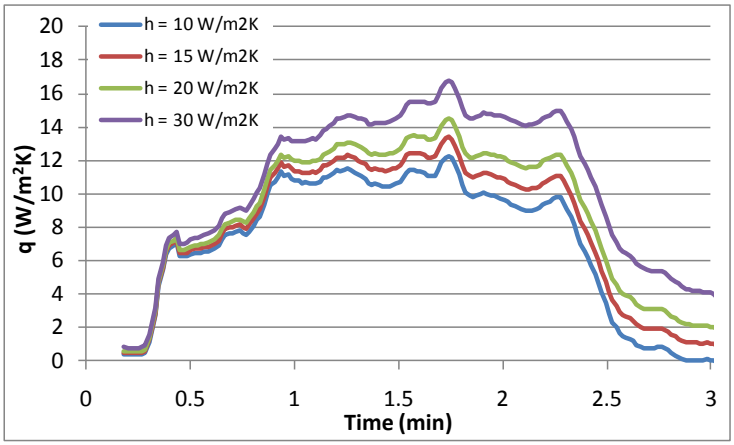

Difference in incident radiant heat flux for test 4, for different convective heat transfer coefficients.

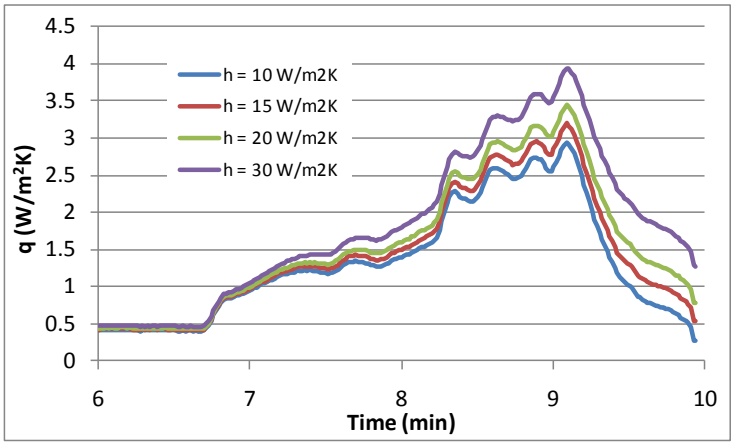

Difference in incident radiant heat flux for test 4, for different convective heat transfer coefficients

The surface emissivity is tested for a number of PT used in this study. The value is always between 0.8 and 0.85. However, to account for any differences from extreme values we vary the emissivity between 0.75 and 0.95. the impact is shown below.

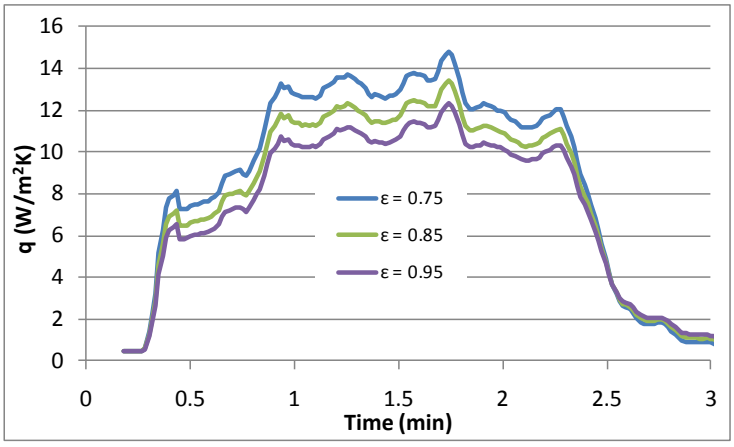

Difference in incident radiant heat flux for test 4, for different surface emissivity.

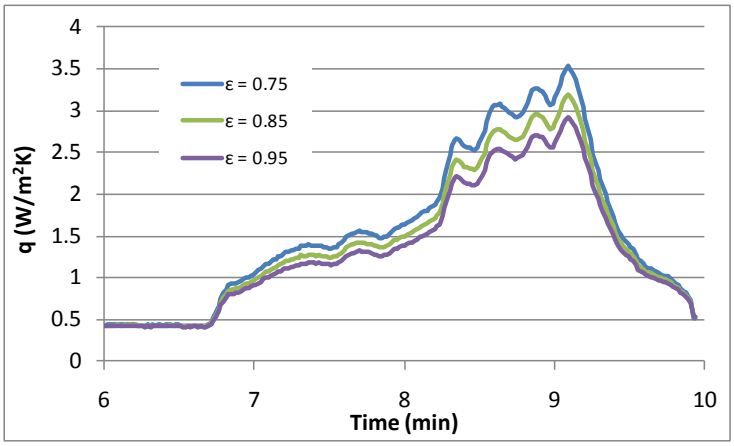

Difference in incident radiant heat flux for test 4, for different surface emissivity.

As seen in the figures above the impact on the incident heat flux radiation is limited when using these extreme values. The variation is in the order of ± 10%.

8.4 Comparing heat fluxes from PT and HFM.

The comparison between incident heat flux calculated by PT measurements and those obtained from HFM measurements are shown for all cases where the PT/HFM are not engulfed in the flame of experiencing an incident heat flux < 2.5 kW/m^2. As seen the agreement is very good between the two measurements.

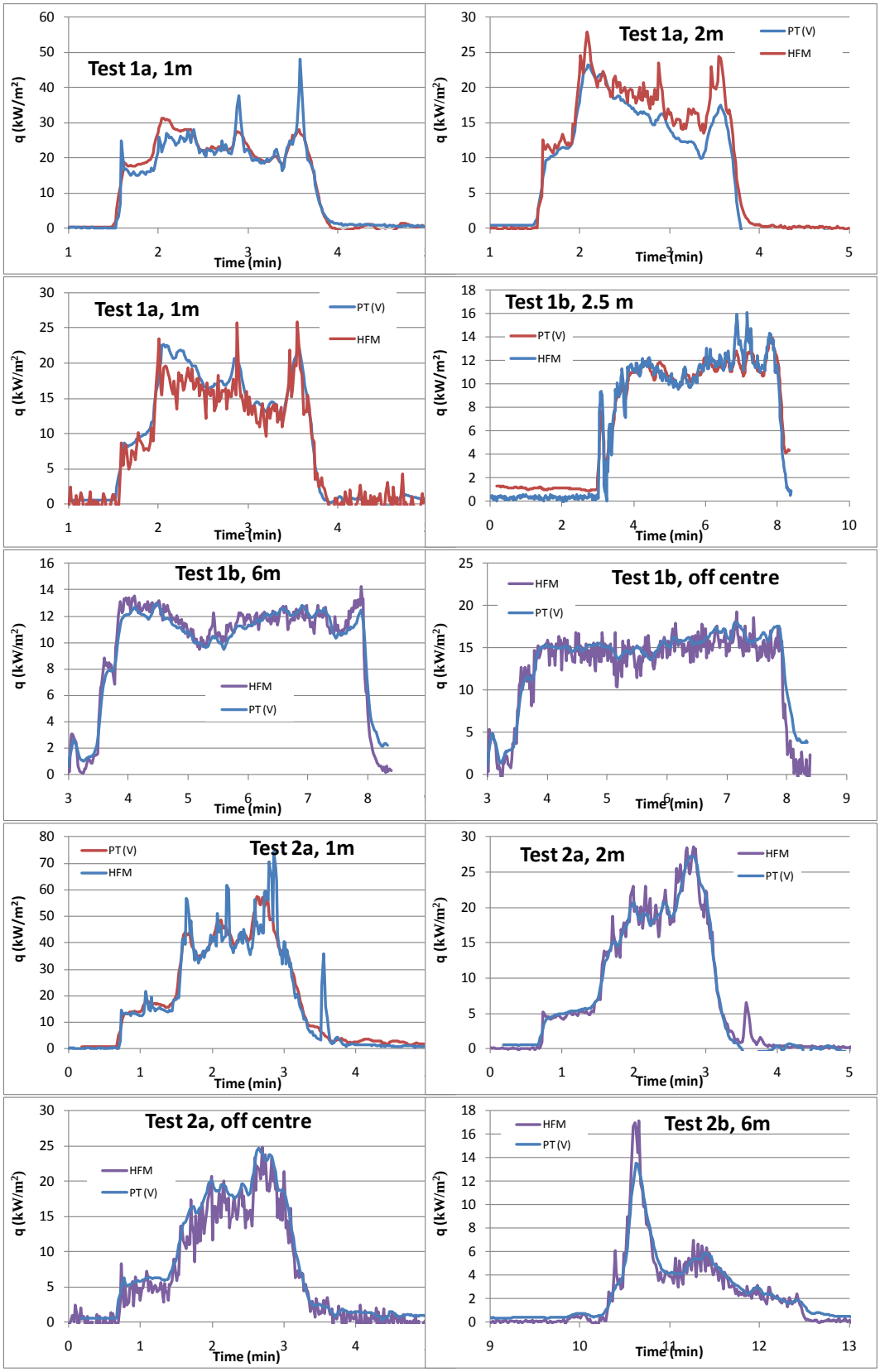

Incident radiant heat flux to a vertical surface for test 1a-2b.

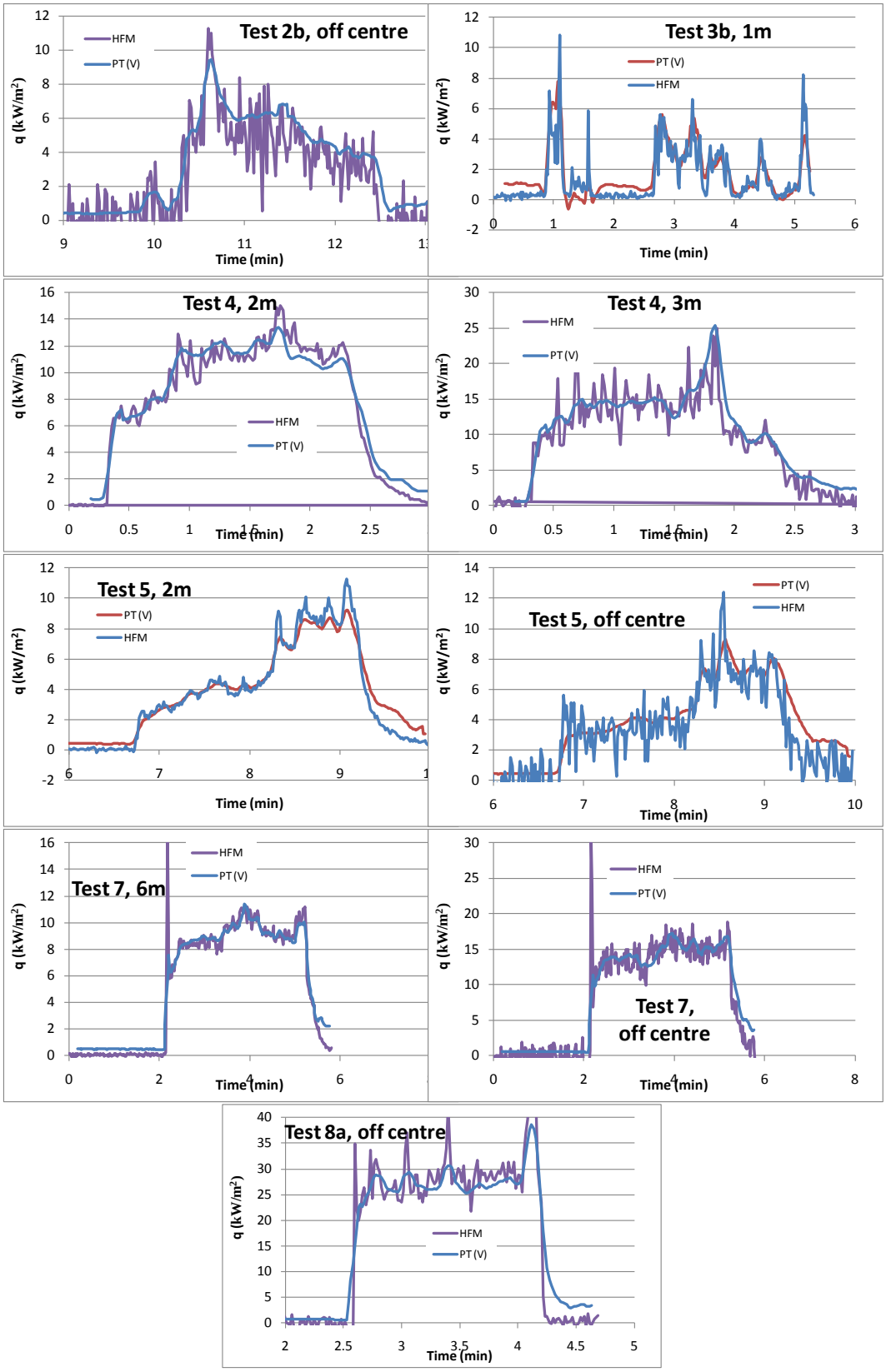

Indecent radiant heat flux to a vertical surface for test 2b-8a.

8.5 Additional photos from the tests

Test 4

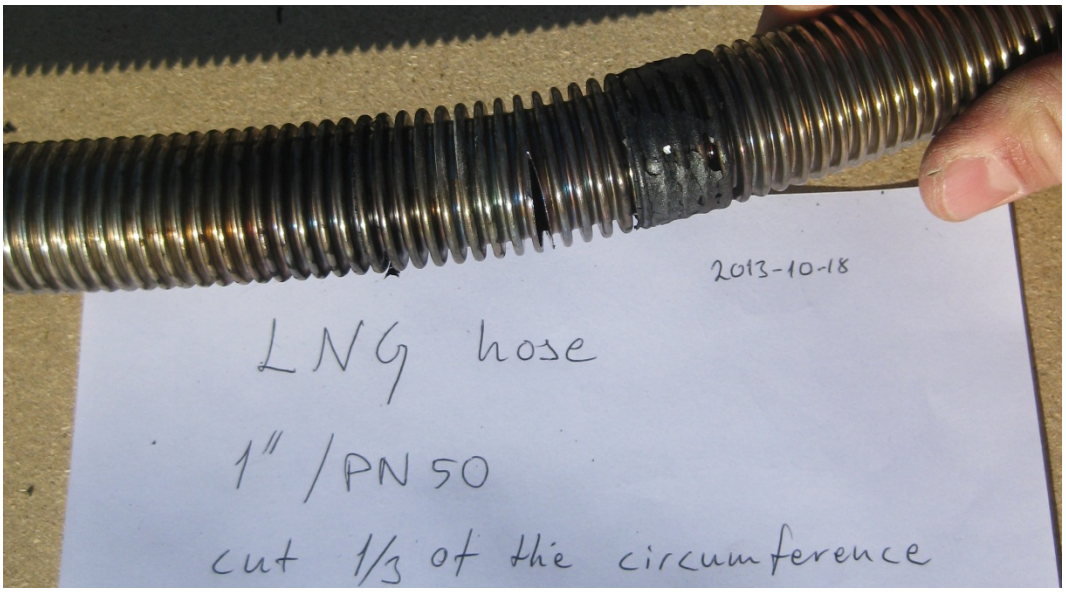

The 1" hose of test 4 after the test with the braid taken off.

Additional photos from test 4.

Test 5

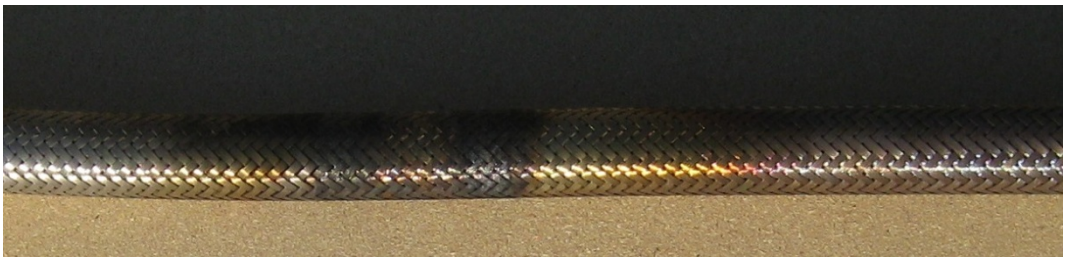

The 1" hose of test 5 (cut 5 mm) after the test with the braid still on.

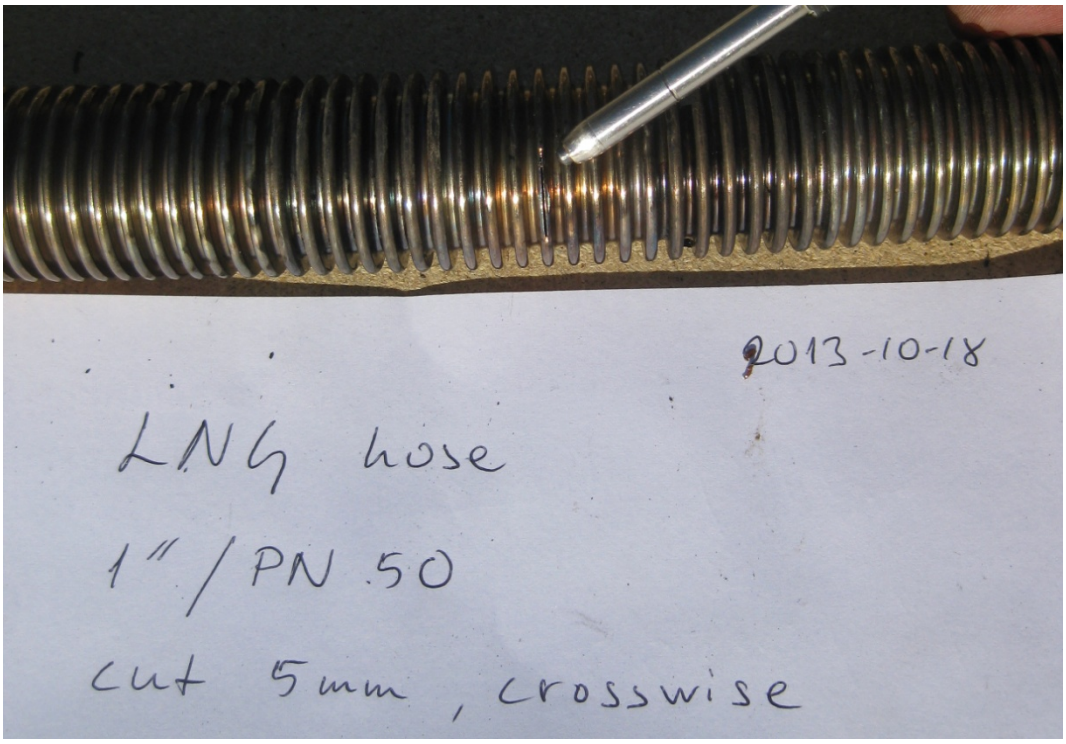

The 1" hose of test 5 (cut 5 mm) after the test with the braid taken off.

Test 6

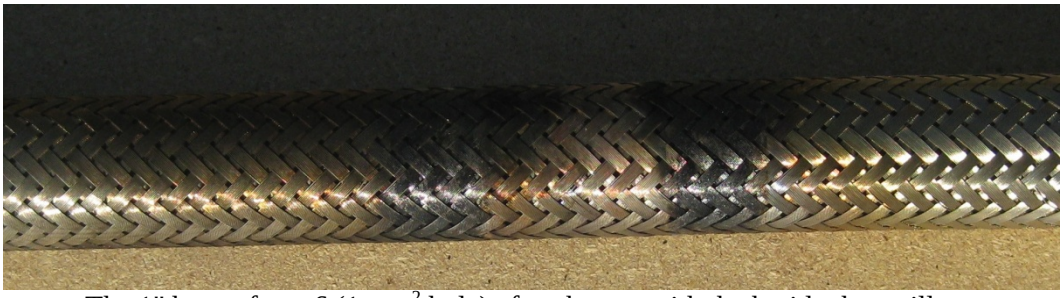

The 1" hose of test 6 (1 mm^2 hole) after the test with the braid taken still on.

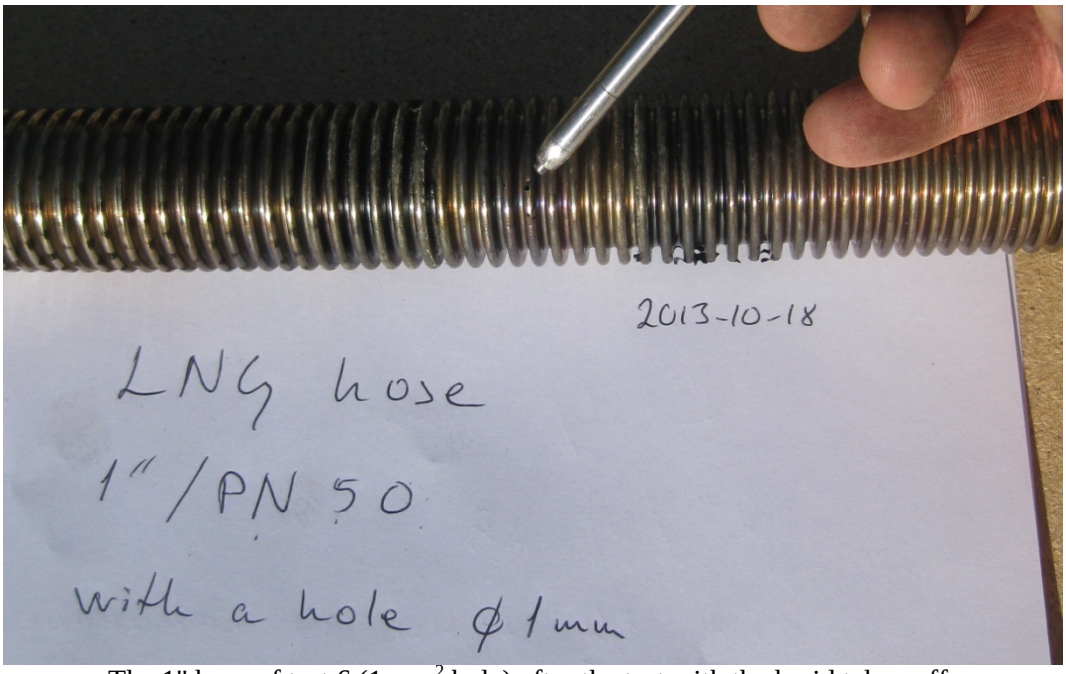

The 1" hose of test 6 (1 mm^2 hole) after the test with the braid taken off.

Test 7

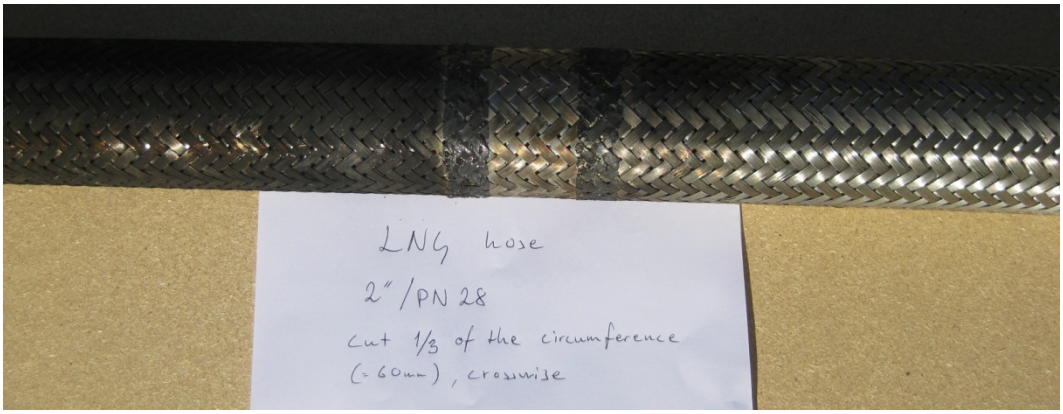

The 2" hose of test 7 after the test with the braid still on.

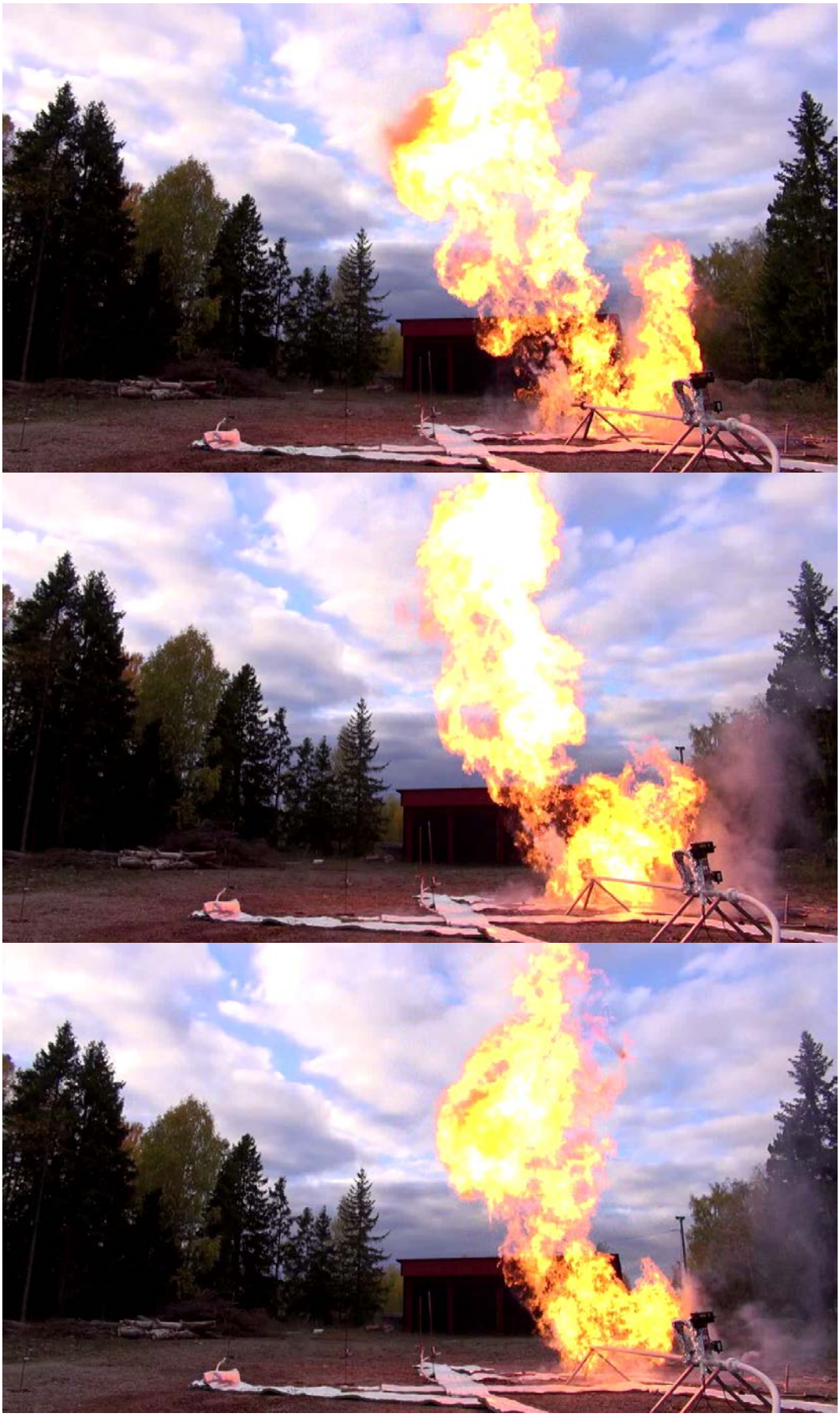

Additional photos from test 7.

The 2" hose of test 7 after the test with the braid taken off. Note that the slot is still 1/3 of the circumference.

SP Technical Research Institute of Sweden

Our work is concentrated on innovation and the development of value-adding technology. Using Sweden's most extensive and advanced resources for technical evaluation, measurement technology, research and development, we make an important contribution to the competitiveness and sustainable development of industry. Research is carried out in close conjunction with universities and institutes of technology, to the benefit of a customer base of about 10000 organisations, ranging from start-up companies developing new technologies or new ideas to international groups.

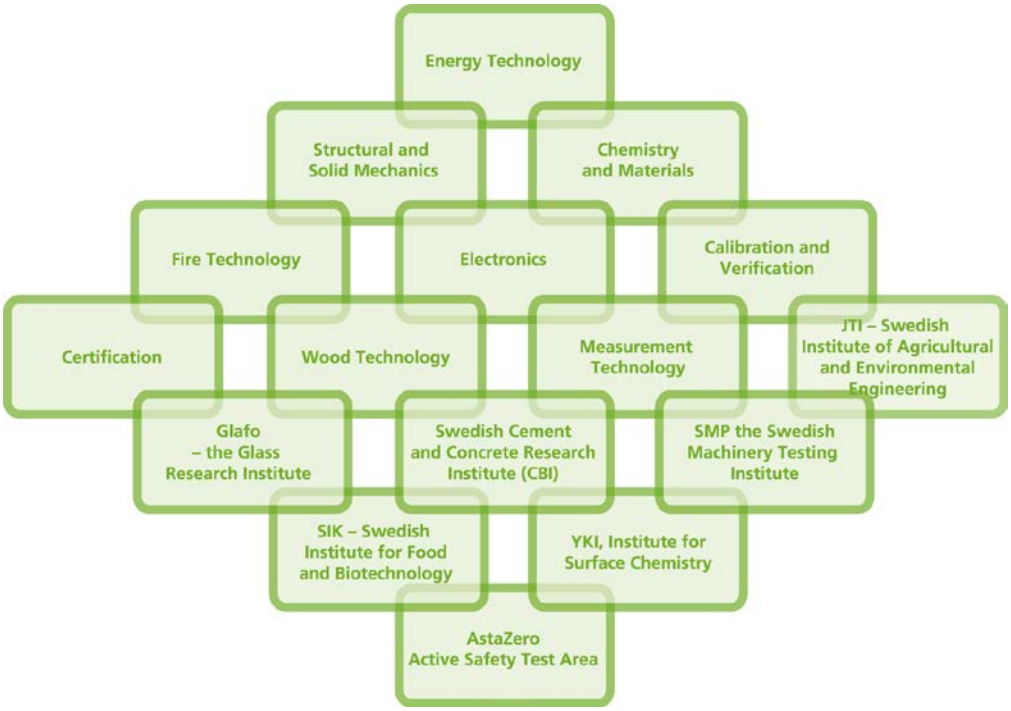

SP Technical Research Institute of Sweden
Box 857, SE-501 15 BORÅS, SWEDEN
Telephone: +46 10 516 50 00, Telefax: +46 33 13 55 02
E-mail: info@sp.se, Internet: www.sp.se
www.sp.se

Fire Technology
SP Report 2013:61
ISBN 978-91-87461-47-7
ISSN 0284-5172

More information about publications published by SP: **www.sp.se/publ**